PURDUE UNIVERSITY
GRADUATE SCHOOL
Thesis/Dissertation Acceptance

This is to certify that the thesis/dissertation prepared

By Megan Elizabeth Carter

Entitled
Blood on FTA™ Paper: Does Punch Location Affect the Quality of a Forensic DNA Profile?

For the degree of   Master of Science

Is approved by the final examining committee:

Christine Picard
_____
Chair

Stephen Randall

Jay Siegel

To the best of my knowledge and as understood by the student in the *Research Integrity and Copyright Disclaimer (Graduate School Form 20)*, this thesis/dissertation adheres to the provisions of Purdue University's "Policy on Integrity in Research" and the use of copyrighted material.

Approved by Major Professor(s): Christine Picard
_____

Approved by: Christine Picard   05/09/2012
_____
Head of the Graduate Program   Date

PURDUE UNIVERSITY
GRADUATE SCHOOL

Research Integrity and Copyright Disclaimer

Title of Thesis/Dissertation:

Blood on FTA™ Paper: Does Punch Location Affect the Quality of a Forensic DNA Profile?

For the degree of _____Master of Science_____

I certify that in the preparation of this thesis, I have observed the provisions of *Purdue University Executive Memorandum No. C-22,* September 6, 1991, *Policy on Integrity in Research.**

Further, I certify that this work is free of plagiarism and all materials appearing in this thesis/dissertation have been properly quoted and attributed.

I certify that all copyrighted material incorporated into this thesis/dissertation is in compliance with the United States' copyright law and that I have received written permission from the copyright owners for my use of their work, which is beyond the scope of the law. I agree to indemnify and save harmless Purdue University from any and all claims that may be asserted or that may arise from any copyright violation.

Megan Elizabeth Carter
_____
Printed Name and Signature of Candidate

05/09/2012
_____
Date (month/day/year)

BLOOD ON FTA™ PAPER: DOES PUNCH LOCATION AFFECT
THE QUALITY OF A FORENSIC DNA PROFILE?

A Thesis

Submitted to the Faculty

of

Purdue University

by

Megan Elizabeth Carter

In Partial Fulfillment of the

Requirements for the Degree

of

Master of Science

August 2012

Purdue University

Indianapolis, Indiana

ACKNOWLEDGMENTS

TABLE OF CONTENTS

LIST OF TABLES

LIST OF FIGURES

LIST OF ABBREVIATIONS

°	degree
µL	microliter
-A	minus A
+A	plus A
ABI	Applied Biosystems
ANOVA	analysis of variance
bp	base pairs
BSA	bovine serum albumin
C	Celsius
CE	capillary electrophoresis
CODIS	combined DNA index system
DNA	deoxyribonucleic acid
EDTA	ethylenediaminetetraacetic acid
FTA™	fast technology for analysis of nucleic acids
IUPUI	Indiana University-Purdue University Indianapolis
min.	minute(s)
mm	millimeter
ηg	nanograms
PCR	polymerase chain reaction
pg	picograms
RFLP	restriction fragment length polymorphism
RFU	relative fluorescence unit
RMP	random match probability
sec.	second(s)

STR	short tandem repeat
SWGDAM	Scientific Working Group on DNA Analysis Methods
UV	ultraviolet
VNTR	variable number of tandem repeats

ABSTRACT

Carter, Megan Elizabeth. M.S., Purdue University, August 2012. Blood on FTA™ Paper: Does Punch Location Affect the Quality of a Forensic DNA Profile? Major Professor: Christine Picard.

Forensic DNA profiling is widely used as an identification tool for associating an individual with evidence of a crime. Analysis of a DNA sample involves observation of data in the form of an electropherogram, and subsequently annotating a DNA "profile" from an individual or from the evidence. The profile obtained from the evidence can be compared to reference profiles deposited in a national DNA database, which may include the potential contributor. Following a match, a random match probability is calculated to determine how common that genotype is in the population. This is the probability of obtaining that same DNA profile by sampling from a pool of unrelated individuals. Each state has adopted various laws requiring suspects and/or offenders to submit a DNA sample for the national database (such as California's law that all who are arrested must provide a DNA sample). These profiles can then be associated with past unsolved crimes, and remain in the database to be searched in the event of future crimes. In the case of database samples, a physical sample of the offender's DNA must be kept on file in the laboratory indefinitely so that in the event of a database hit, the sample is able to be retested.

Current methods are to collect a buccal swab or blood sample, and store the DNA extracts under strict preservation conditions, i.e. cold storage, typically -20° C. With continually increasing number of samples submitted, a burden is placed on crime labs to store these DNA extracts. A solution was required to help control the costs of properly storing the samples. FTA™ paper was created to fulfill the need for inexpensive, low

maintenance, long term storage of biological samples, which makes it ideal for use with convicted offender DNA samples. FTA™ paper is a commercially produced, chemically treated paper that allows DNA to be stored at room temperature for years with no costly storage facilities or conditions. Once a sample is required for DNA testing, a small disc is removed and is to be used directly in a PCR reaction. A high quality profile is important for comparing suspect profiles to unknown or database profiles. A single difference between a suspect and evidentiary sample can lead to exclusion. Unfortunately, the DNA profile results yielded from the direct addition have been unfavorable. Thus, most crime laboratories will extract the DNA from the disc, leading to additional time and cost to analyze a reference sample. Many of the profiles from the direct addition of an FTA™ disc result in poor quality profiles, likely due to an increase in PCR inhibitors and high concentrations of DNA.

Currently, standardized protocols regarding the recommended locations for removal of a sample disc from a bloodspot on an FTA™ card does not exist. This study aims to validate the optimal location by comparing DNA profiles obtained from discs removed from the center, halfway, and edge locations of a bloodspot from 50 anonymous donors. Optimal punch location was first scored on the number of failed, partial or discordant profiles. Then, profile quality was determined based on peak characteristics of the resulting DNA profiles. The results for all three disc locations were 5.3% failed amplifications, 4.2% partial amplifications, and one case of a discordant profile. Profile quality for the majority of the samples showed a high incidence of stutter and the absence of non-template adenylation. Of the three disc locations, the edge of the blood stain was ideal, due to a presumably lower concentration of DNA and likely more dilute amount of the PCR inhibitor heme. Therefore, based on the results of this study, there is a greater probability of success using a sample from the edge of a blood stain spotted in FTA™ paper than any other location of the FTA™ card.

CHAPTER 1. INTRODUCTION

1.1   Introduction to Forensic DNA Analysis

Forensic DNA identification technology is widely used as a tool for associating an individual with evidence of a crime. Analysis of a sample involves developing an individual's "profile" by analyzing a biological sample which contains DNA. The profile obtained from an evidentiary sample can be compared to the profile obtained from a suspect or a database. Following a match, statistical analysis is performed to determine the random match probability (RMP) of the profile, which is of finding an identical profile in a given ethnic population (if known). For example, in the case of a sexual assault, biological material such as semen left on the victim or at the crime scene is collected and a DNA profile of is obtained. If there is a suspect associated with the case, this evidentiary profile is then compared to a suspect's profile to determine whether there is a match. If no suspect is associated with a case, the unknown profile may be searched against a national DNA database called CODIS (Combined DNA Index System). Depending on the state, any person is convicted of a crime is required to have his or her profile entered into a searchable database and this profile can then be associated with evidence from past unsolved crimes, and possibly assist in the event of future crimes. Therefore, it is crucial to upload a reliable profile in order to make a comparison between a suspect and the evidence.

1.2   History of Forensic Biology

Prior to DNA profiling, blood type analysis was used, albeit primarily for exclusion purposes, and with only four blood types plus Rhesus factors, little discrimination was possible [1, 2]. For example, 42% of the population has type A blood and 42% has type O blood, and 85% of the population is positive for Rhesus factor [2]. The probability of discrimination for ABO blood typing is approximately 0.40, which means there is a 40 percent chance that two randomly selected people would have the same blood type [2]. Following blood typing, protein-specific antibody tests based on polymorphic proteins associated with the immune system were used. Although these methods were more discriminating than the blood typing system, with a power of 0.19, about one in every five people [2]. More modern techniques of the analysis of biological materials include the analysis of DNA (deoxyribonucleic acid). Every nucleated cell contains 23 pairs of chromosomes, one inherited maternally and one paternally. Interspersed among genes and regulatory elements are repetitive sequences of DNA which are used to develop a DNA profile.

DNA profiling, or simply genotyping, was first utilized in a forensic context by Sir Alec Jeffreys in 1985 [3]. It was based on counting the number of repeats of a specific DNA sequence at known locations (loci) in the human genome [3]. Jeffreys's original genotyping method, referred to as restriction fragment length polymorphism (RFLP) analysis, used restriction enzymes to digest DNA at enzyme specific sequences [3]. The fragments, known as alleles, would be electrophoretically separated based on their size, and one or two alleles would appear, depending on whether the person was homozygous (meaning the same number of repeats for both alleles) or heterozygous (meaning a different number of repeats, resulting in differently sized fragments). These sequence repeat regions are known as variable number tandem repeats (VNTRs), and are forensically useful because the number of repeats is variable, or polymorphic, within the human population [3, 4]. VNTRs have a core repeat length of approximately ten to 100 bases, resulting in fragments that could be thousands of base pairs long [3, 4]. Though VNTRs are discriminatory, they require a large amount of template DNA that is of high quality, and unfortunately this is not a likely scenario with most forensic samples.

An alternative to VNTR genotyping is short tandem repeat (STR) genotyping. This method that takes advantage of PCR (polymerase chain reaction), which reduces the need for large concentrations of DNA [5-7]. STRs are similar to VNTRs, but with a shorter core repeat length of approximately two to six bases, resulting in overall shorter lengths of polymorphic fragments [8]. The shorter lengths of STRs as compared to VNTRs are useful because degraded samples are common in forensic samples, and shorter sequences are less likely to become degraded than longer sequences, thereby reducing the need for high quality DNA.

The steps, in order, of the current standard DNA analysis are as follows: collection, extraction, quantitation, STR amplification, separation and detection, and data analysis [9]. Collection involves the initial recovery of a DNA sample, either from a crime scene or from a reference sample. This step is crucial in preventing contamination, and followed by proper storage to minimize degradation. Following collection, extraction is then performed to isolate and purify the DNA from the remaining cellular material and halt any further enzymatic degradation. Next, and importantly to the specific downstream applications, the quantity of DNA must be determined. This step is important because commercial PCR amplification reactions call for narrow concentration ranges of DNA [9]. If too much DNA is added, profiles will have split or off-scale peaks. If too little DNA is added, profiles are susceptible to stochastic fluctuations in PCR amplifications, which can lead to partial profiles or false homozygosity [9-11].

The process of PCR was invented by Kary Mullis in 1985 [12]. PCR takes a DNA region of interest and makes many copies of that specific sequence, a process is known as amplification [12]. PCR is a series of heating and cooling cycles during which sequence-specific primers anneal to single stranded template DNA. These primers are then extended by a polymerase adding bases complementary to the template DNA sequence, creating new copies of the DNA of interest [12]. After each cycle, the number of template DNA molecules doubles [12]. This exponential growth in the number of specific regions of DNA, known as amplicons, leads to millions or billions of copies after 25 to 35 cycles [12]. This amplified DNA containing only the loci of interest is then separated and detected either using gel or capillary electrophoresis (CE). The fragments

are separated by size, with smaller fragments traveling through the matrix more quickly than larger fragments [6]. In modern forensic DNA practices, this is performed using CE. In a CE instrument, a laser is used to excite the fluorescently labeled primers that were added to the DNA fragments during PCR amplification. These laser-excited fragments are then detected as they travel through the instrument past a detection window [6]. The use of fluorescently labeled primers also allows for multiplexing of amplifications, allowing for the detection of up to 20 STR loci in a single PCR reaction [5, 6, 8, 9].

This information is then analyzed with genotyping software, such as GeneMapper® (Applied Biosystems, Foster City, CA) or GeneMarker® (Softgenetics, State College, PA). An internal size standard is run through the CE instrument in conjunction with all STR amplification products in order to properly size all fragments [6]. The size standard is a set of DNA fragments of known sizes that is used to create a standard curve (Figure 1).
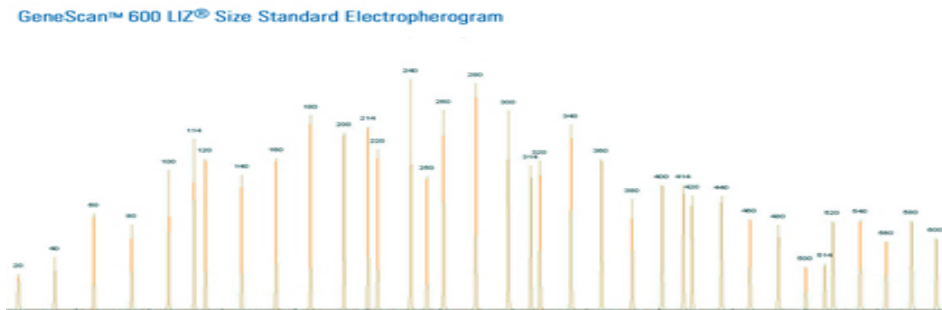
Figure 1 An electropherogram of the GeneScan™ 600 LIZ® Size Standard showing the different sizes of the fragments. Copyright © 2011 Life Technologies Corporation. Used under permission.

The sizes are recorded as peaks in an electropherogram. A standard curve is created to correlate the size of the fragments with the time of travel from injection to the detection window.
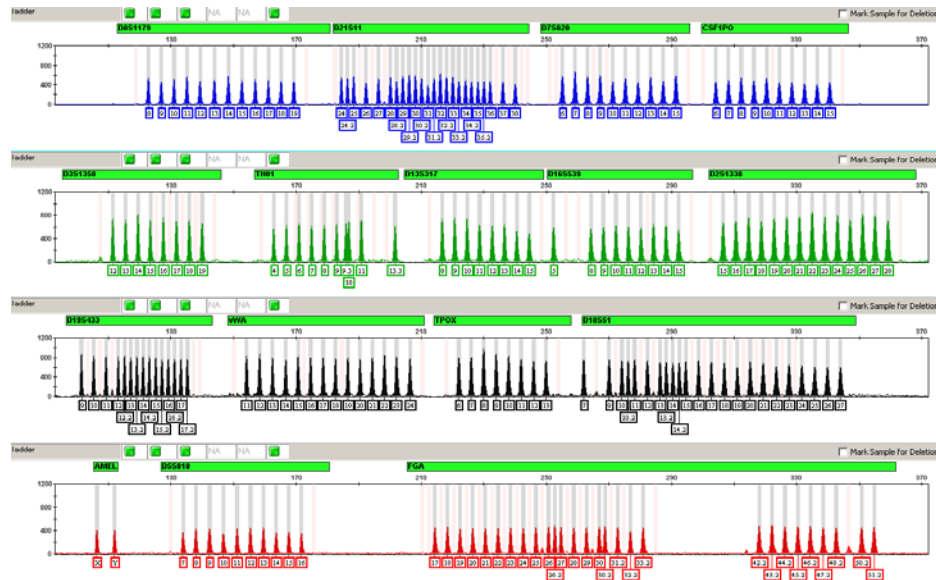
Figure 2 The allelic ladder from the Identifiler® Plus PCR amplification kit [9]. It contains the most common alleles at each locus in the kit. The STR amplification product is compared to this ladder and allele calls are made. Copyright © 2011 Life Technologies Corporation. Used under permission.

This is then used to calculate the sizes of the fragments in an allelic ladder. An allelic ladder (Figure 2) is a DNA sample that contains all of the common alleles at each locus included in the kit [6].

An allelic ladder must be included with each run of the genetic analyzer. The sized STR fragments are then genotyped based on the ladder allele calls. The numbers represent the number of repeats of the STR sequence present at each locus. For example, if a person inherited 17 repeats from their mother and 18 repeats from their father at one locus, their heterozygous genotype at that locus is 17, 18. A person can also inherit the same number of repeats from both parents, for example 18, 18, which is considered homozygous.

STR loci are chosen based on certain characteristics which make them beneficial for forensic analysis. For CODIS, there are 13 core STR loci [9]. These selected STR loci are polymorphic, which means there is large variation in the different possible numbers of repeats present within the human population, and therefore they are capable

of individualizing identifications [5, 8]. Because STRs are so polymorphic, multiplexing them to analyze several loci at once results in a high power of discrimination between individuals [8]. The statistical calculations performed on DNA profiles are known as random match probability (RMP). The RMP is the chance that a person randomly selected from a population would have the same DNA profile. RMPs are calculated by multiplying the allele frequencies from all loci using the product rule because each locus is independent, and then dividing one by that number. Due to the polymorphic nature of each locus, statistical calculations give a RMP of more than one in a trillion when all 13 core CODIS loci are tested [13].

An important issue that can arise with forensic casework samples is the presence of PCR inhibitors. These samples are found in dirty locations where samples have been exposed to substances that can interfere with the genotyping process. An example is PCR inhibitors [5, 14]. Items such as soil, plants, leather, clothing dyes such as indigo, and even heme in blood are known inhibitors [15-17]. Inhibitors prevent cell lysis (extraction of DNA from a cell), degrade samples, and prevent the polymerase from binding and annealing to the template, all of which lead to failed amplifications [9, 14]. Possible solutions to reduce the effects of PCR inhibitors are sample dilutions, the addition of excess polymerase, the addition of BSA or further purification with silica columns all reduce the effects of inhibitors [17, 18].

Forensic DNA samples are also degraded by environmental factors such as UV light, heat, moisture, bacterial growth, therefore biological samples must be stored carefully to avoid further damaging or contaminating the samples. When collecting biological samples, they must be dried and carefully packaged to avoid coming into contact with other evidence. In addition, the samples are stored cold to prevent any further degradation. In the case of database samples, a physical sample of the offender's DNA must be kept in the laboratory indefinitely in case a database hit ever occurs and the sample must be retested. Due to the large number of these samples, a solution was required to help control the costs of properly storing the samples while also minimizing the risk of contaminating the evidence. FTA™ paper was created to fulfill the need for

inexpensive, low maintenance, long term storage of biological samples, which makes it ideal for use with convicted offender samples.

1.3   Introduction to FTA™ Paper

FTA™ paper is a special cellulose-based paper developed in the late 1980s by Leigh Burgoyne [19] and commercialized by Whatman™ (Florham Park, NJ, a division of GE Healthcare). FTA™ paper is used to store any biological sample that can be applied to the filter paper, typically consisting of blood and buccal samples [10, 20-22]. In terms of forensic samples, FTA™ paper is commonly used for the long-term storage of reference and convicted offender samples. FTA™ paper is treated with a mixture of a base, a chelating agent, an anionic surfactant, and uric acid [10, 22, 23]. These chemicals help capture and protect the DNA from degradation by nuclease activity, UV, bacteria and other detrimental conditions [5, 20, 22, 24, 25]. Upon contact with denaturants, the cells are lysed, and the DNA becomes entangled within the paper's matrix (Figure 3) [5, 10, 20, 22, 25, 26].
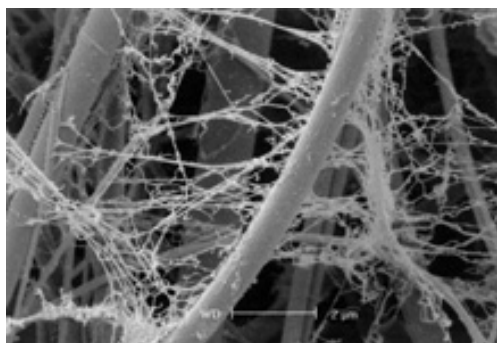
Figure 3 DNA entangled in Whatman FTA™ Paper matrix [23]. Copyright © 2011 GE Healthcare Corporation. Used under permission.

This type of treatment allows for DNA to be stored on FTA™ paper for years at room temperature [5, 10, 20-26]. These properties of FTA™ paper helps eliminate the requirement of refrigerated storage for biological samples, which is expensive and requires large, specialized areas for storage [21-24, 26]. Also, use of FTA™ paper

prevents cross contamination between samples, even if they come in contact with each other [20]. This means that large amounts of samples can be stored together without the requirement for specialized storage equipment; one study even suggests using an ordinary filing cabinet [20]. In addition, FTA™ cards are small in size at only three and a half inches by five inches in size [10].

When using FTA™ paper for blood sample collection and storage, the liquid blood is spotted directly on the card's sample collection area and allowed to dry [20, 22]. When an analyst is ready to for analysis, a small disc (1.2 mm in diameter) is removed from the bloodstain using a micro-punching tool, such as the Harris Uni-Core™ punch. Following the removal of the disc, three to five washes are performed using a specialized reagent remove inhibitors and contaminants [5, 21]. Potent PCR inhibitors are present in blood samples (including heme and the anticoagulant EDTA), and they must be removed prior to PCR amplification [15, 26]. Removal of heme can be visually observed with FTA™ paper, as its red color also washes away [27]. If the washes are effective, they should leave a colorless paper disc containing the purified DNA and little or no remaining heme to inhibit amplification.

The purification reagent is then washed away with water, and the disc is then dried. The manufacturer's protocol then states that the disc is ready to be added directly to a PCR amplification reaction [9, 21, 22]. A benefit of the direct addition of FTA™ paper discs to the amplification reaction is that it reduces the amount of handling by an analyst, thereby reducing the potential for contamination [27]. However, no quantification is performed, a deviation from the normal PCR amplification procedures outlined by the manufacturers of STR amplification kits. These kits have been optimized to use a narrow range of DNA amounts (i.e. 0.5-1 ηg DNA), and anything more or less may result in a poor quality profile [9, 27]. The absence of this quantitation step is both a benefit and a drawback of using FTA™ paper. Bypassing the quantification step saves time and reduces the amount of sample used; however, this also introduces uncertainty in the quality of profile to be generated [9, 27]. If the amplification procedure fails, then a second amplification has to be done, and that comes with added cost and time. According to the PCR amplification kit components manufacturer, no quantification is

necessary for successful amplification and analysis of FTA™ samples [9]. Their literature states that a 1.2-mm disc contains between 5 and 20 ηg of DNA, and will give reliable results [9].

Previous studies suggested that the quantity of DNA present at the center and edge of a blood sample spotted on FTA™ paper is uniform [26]. Therefore, it has been postulated that DNA is distributed evenly throughout a blood sample as it diffuses through the FTA™ paper's matrix [26]. Also, the study demonstrated that the speed of delivery of the blood sample onto the FTA™ paper had no effect on uniformity of DNA concentration [26]. Additionally, the study showed that there was no difference in uniformity of DNA whether there is one point of application or multiple points, and with no effect from different people making the applications [26]. However, Dr. Christine Picard has found on average, using blood spotted FTA™ cards, that amplification reactions either failed or yielded poor quality profiles in greater than 25% amplifications in a study of 100 individuals [28].

1.4   Evaluating Profile Quality

The purpose of this study was to determine whether there was a difference in the quality of DNA profile obtained from different punch locations from a blood spot on FTA™ paper. The purpose of this was to demonstrate to current DNA laboratories the optimal disc locations for the greatest probability of amplification success, therefore enabling them to use the technology as it was intended. The number of failed reactions, partial profiles, and concordance between individual genotypes was examined at each locus, for all three punch locations. Furthermore, peak characteristics such as presence and amount of minus A (-A) and stutter, average peak height in relative fluorescence units (RFUs), heterozygote ratios, and allelic dropout were examined.

1.4.1   Peak Characteristics

When observing an electropherogram, good quality peaks should be sharp, symmetric and well-defined, and easily distinguished from background noise [29]. They should not be split, rounded, or otherwise misshapen [6, 29]. Sometimes normal peaks may have associated biological artifacts such as –A and stutter peaks, as will be discussed below [6, 9, 29]. Problems with the size, shape, and associated products of peaks can lead to issues with obtaining a correct DNA genotype.

1.4.2   Concordance

Concordance failures are defined as unexpected differences in genotype at any locus for a single individual's FTA™ card blood sample. This is likely due to extra peaks, missing peaks, or other abnormalities. Unusual peak characteristics, including high percentages of –A [9], and the presence of high stutter percentages can result in allelic drop-in, where these alleles are amplified over a predetermined threshold or are even preferentially amplified over the true allele. In addition, heterozygote imbalance and allelic dropout can also lead to different genotypes for the same individuals [6, 9, 29]. These issues will be discussed in detail in the following sections.

A failed amplification reaction occurs when the electropherogram does not show peaks that can be reliably distinguished from background noise [29]. A failed reaction may occur if insufficient DNA is present, which may have occurred if the DNA from the punch was not correctly extracted into the PCR mixture. High concentrations of inhibitors can also cause the amplification step to fail [14, 29]. Additionally, it is possible that the DNA sample may have become too degraded to produce a profile; however this is unlikely with the use of FTA™ paper under proper storage conditions.

Larger loci, such as D18S51 and FGA, are more susceptible to small changes in the PCR conditions. For example, if the DNA sample has been degraded or has a high concentration of inhibitors, amplification of these loci may fail while the smaller loci are correctly amplified [9, 29]. Amplification failure of one or more loci results in a partial

profile, which is still forensically useful, but its power of discrimination is reduced with each additional failed locus [29].

During the PCR amplification process, the polymerase adds an extra base, adenosine, to the 3'-end of the newly synthesized strand [30, 31]. Addition of this adenosine occurs during the final extension step of PCR amplification, in order to ensure all PCR products are adenylated [9, 10, 30]. This extra adenosine results in a new strand that is one base pair longer than the original DNA sequence [10, 30, 31]. This addition is referred to as adenylation, and the resulting adenylated strand is known as the '+A' form [9, 30, 31]. If the adenylation does not occur, the non-adenylated strand is known as the '-A' form [30, 31]. In forensic DNA typing, it is important that all PCR products generated from the same template strand are of the same size to be resolved, either all +A or all –A, therefore the thermalcycling conditions for each STR amplification kit add an extra 15 to 60 minute extension step to ensure all PCR products have been adenylated. On an electropherogram, -A peaks will appear one base pair less than the true alleles and the alleles represented by the allelic ladder, which are always in the +A form, and this will lead to the appearance of split peaks, or peak broadening [9, 10]. Higher concentrations of DNA than are recommended in kit protocols will result in incomplete adenylation [9, 10]. Therefore, it is important to determine the quantity of DNA present in a sample prior to PCR [9].

Stutter, a result of strand slippage during DNA replication [5, 32], is a common occurrence during PCR amplification of STR products [9, 32]. Strand slippage means that one of the two DNA strands being amplified forms a non-base-paired loop during primer extension, resulting in a product that is either one (or more) repeat unit longer, or more typically one (or more) repeat shorter in length than the original sequence [5, 10, 32]. If a stutter product is amplified in an early cycle during PCR, a resulting peak can be called as an allele [32]. This is especially problematic if mixtures are being amplified [9], and is not a likely scenario with reference samples; however, if a stutter peak is called as a true allele in a reference sample and then uploaded to a DNA database, then potential crime scene samples would result in a false negative. Analysts calculate the percentage of stutter present by dividing the height of the stutter peak by the height of the

corresponding allele peak [9, 10]. Stutter has been characterized for each allele by the kit manufacturers, and this data is used in the calling and interpretation of alleles within the confines of the software [9]. If a peak falls above this threshold, then the allele is called. Generally, longer alleles exhibit a greater stutter percentage than smaller alleles [5, 9, 10]. Expected stutter peak heights should be less than 15 percent of true peak heights for all 13 core CODIS loci under standard conditions [9].

Peak heights on electropherograms are measured along the y-axis in relative fluorescence units, or RFUs. When examining peaks, peak heights are useful in distinguishing between true peaks, stutter, potential contamination or some other technological issues [6]. When analyzing data, the analyst will set a threshold minimum RFU value, below which no peaks are called [6]. This threshold minimum should be standardized laboratory-wide and determined through validation studies [10, 29]. The minimum RFU limit should be at a level that is high enough to consistently show differentiation between true allele peaks and background peaks [10, 29]. RFU levels generally correlate to the amount of DNA present in a sample; high RFUs correlate to a high concentration of DNA, while low RFUs correlate to a low concentration of DNA. In cases of high concentrations of DNA, sometimes a phenomenon known as 'pull up' can occur, where the capillary electrophoresis instrument's detector becomes overloaded with fluorescence and the signal "bleeds" over to another color, resulting in false peaks appearing where they would not otherwise be present [6]. Low concentrations of DNA can lead to peak heights that are not much higher than the baseline peaks, which can make it difficult or impossible to determine which peaks are the true allele peaks.

Heterozygote ratio refers to the difference in peak heights between the two heterozygous alleles at a single locus [29]. The ratio is calculated by dividing the peak height in RFUs of the shorter allele by the peak height of the taller allele [9, 27, 29]. The ratio between heterozygote allele peaks is expected to be 0.60-0.70 or more for a single-source sample under standard conditions [10, 29, 33]. When the ratio is below this threshold, this is typically an indicator of a mixture [9, 10]. Normal heterozygote peak imbalance at a locus occurs because of unequal amplification of the two alleles during the PCR process [10, 11]. During the early rounds of amplification, one allele may be

preferentially amplified, which leads to unequal proportions of the two alleles [10, 11]. This effect is referred to as stochastic fluctuation [11]. Stochastic effects are especially seen where there is a low concentration of DNA template [9-11]. Greater than normal heterozygote peak imbalance can lead to issues in interpretation of electropherograms by making it difficult to tell if an unusually small peak is a true peak, especially if the shorter peak happens to be in the stutter position [6, 9]. This is a serious issue when it comes to comparison of reference or convicted offender samples to evidentiary samples, because the difference of one allele between suspect and evidence can be enough to lead to a false negative where the suspect is wrongly excluded.

Allelic dropout is an extreme form of heterozygote imbalance, where one of the two alleles of a heterozygote is preferentially amplified to the near exclusion of the other [11]. This can lead to false homozygosity, where only one of the two allele peaks is called [11]. Allelic dropout can be caused by low concentrations of DNA or degraded DNA [9-11, 29]. If the amount of DNA is less than 100 picograms, which is found in approximately 17 diploid copies of genomic DNA, then allelic dropout has been demonstrated to occur more frequently [34]. Allelic dropout can also occur if there is a sequence polymorphism in the primer binding site [7, 9, 10]. If the polymorphism is located in the primer binding region of the DNA template strand, the primer may fail to anneal to the single-stranded template DNA, resulting in a null allele, or the failure of amplification of the allele [7, 10, 11]. This would mean that the sequence actually does exist, but due to primer binding problems, would appear not to exist [7, 10, 11].

1.5   Purpose of the Study

The validation of the profile quality associated with punch locations was evaluated herein. Blood samples were collected from fifty anonymous volunteers according to the Scientific Working Group on DNA Analysis Methods (SWGDAM) guidelines for developing a validation study [35], and pipetted onto FTA™ cards. Once dry, discs were removed from the bloodspots at three locations: center, halfway, and edge

(Figure 4). These discs were then processed according to previously established protocols [9, 20, 27], and the DNA was analyzed.
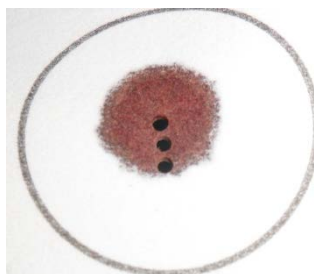
Figure 4 An example of the three disc locations taken from a bloodspot on FTA™ paper: center, halfway, and edge [photo, Megan Carter]. Average bloodspot size was found to be 9.74 mm in diameter, distance from center to edge was an average 4.87 mm, and distance from halfway to edge was an average 2.44 mm.

The implications of this study are important for crime laboratories in their use of FTA™ paper as a means for storage of DNA samples in cases such as convicted offender samples. Studies have been previously performed to validate the use of FTA™ paper for long-term storage [23], as well as the success of different extraction methods [27, 36]. A difference in concentration of DNA present in the disc can also have drastic implications in the amplification step of DNA analysis, as mentioned earlier [26]. By comparing the DNA profiles obtained from all three punch locations, we can see when there are problems that would otherwise not have been detected if only one sample was used. For example, by comparing all three punch locations at each allele, it can easily be seen if there is any false homozygosity that would otherwise go undetected and any other problems that may lead to incorrect allele calls or issues with obtaining the correct DNA profile information. This study's results may help develop or refine standard operating procedures and protocols used by crime laboratories that utilize FTA™ paper.

CHAPTER 2. MATERIALS AND METHODS

2.1   Sample Collection Protocol

FTA™ Mini and Micro cards (Fisher Scientific, Pittsburgh, PA) were spotted with finger prick blood from 50 anonymous subjects. Thirty-three previously collected finger prick blood samples spotted on FTA™ cards from Dr. Christine Picard's previous study at West Virginia University (WVU approved human use protocol #16279) were used [27]. Seventeen additional finger prick blood samples were collected from healthy students at IUPUI (IUPUI IRB approved human use protocol #1108006603). The same collection process was followed as was previously done in Dr. Picard's study [27]. From each finger prick, blood was pooled onto a piece of Parafilm, and 50 µL of this liquid blood was immediately pipetted onto the FTA™ card from a height of approximately one to two inches onto the middle of the sample collection circle area. Cards were allowed to dry at room temperature overnight.

2.2   FTA™ Card Protocol

A 1.2 mm Harris Uni-Core punch (Fisher Scientific) was used to remove discs from each FTA™ card at three different locations: center, halfway, and edge of the bloodstain (Figure 4). Each disc was then individually placed into an appropriately labeled 1.5 mL tube. The punch tool was cleaned in between each use with bleach and sterile water, dried with a KimWipe, and then three clean punches were made to eliminate any cross contamination [20, 27, 37]. To each tube, 500 µL of FTA™ reagent (Fisher Scientific) was added. The tubes were vortexed occasionally over five minutes at

room temperature, after which all liquid was removed. The FTA™ reagent wash and vortexing were repeated twice more, and all liquid was removed after each. Then 500 µL of sterile PCR water was added. The tubes were again vortexed occasionally over five minutes at room temperature, after which all liquid was again removed. The tubes were then left open in a PCR Workstation (Fisher Scientific) in order to dry the discs at room temperature for at least two hours.

2.3   STR Amplification Protocol

Amplification was performed using a 25 µL reaction of the AmpFlSTR® Identifiler® Plus PCR Amplification kit (Applied Biosystems). This kit contains all thirteen core CODIS loci, the sex-determining locus amelogenin, as well as two additional loci, D2S1338 and D19S433 [9]. Amplification was performed using the following protocol per reaction: 10 µL PCR mastermix, 5 µL primers, 10 µL PCR water, and the direct addition of the previously washed and dried disc as the DNA source. The kit components and discs were added to appropriately labeled PCR tubes and place on the Mastercycler® pro Thermal Cycler (Eppendorf North America, Hauppauge, NY). The thermal cycler conditions used were as follows: 95° C enzyme activation for 11 minutes; then twenty-seven cycles of 94° C denaturation for 20 seconds, 59° C annealing for three minutes, 72° C extension for one minute; then 60° C extension for 10 minutes; followed by an indefinite hold at 4° C. The amplified products were then stored at 4° C until they were run on the genetic analyzer.

2.4   Fragment Analysis Protocol

After completion of PCR amplification, 1 µL of each PCR product was added to 9 µL of a HiDi® Formamide/LIZ® size standard solution (0.3 µL of GeneScan® 600 LIZ® size standard and 8.7 µL deionized HiDi® Formamide; Applied Biosystems), heat denatured on the thermal cycler at 95° C for three minutes, and snap cooled at 4° C. The

PCR product was then separated and detected on an ABI 3500 Genetic Analyzer
(Applied Biosystems), using default parameters.

2.5   Data Analysis

A total of 150 punches were initially analyzed: one punch from each of the three
locations (center, halfway, edge) from 50 FTA™ cards with blood samples from 50
different anonymous donors. Electrophoretic data was imported into the GeneMarker®
HID software package (Softgenetics, State College, PA). Peak detection thresholds were
set at 500 RFUs (minimum intensity) and 30,000 RFUs (maximum intensity). Allele
evaluation of peak score was set as follows: reject at less than 0.0, check at less than 0.3,
and pass at greater than 0.3. Ladder selection was set to auto select best ladder.

Genotypes for all 50 individuals from all three punch locations were then
imported into Excel (Microsoft, Redmond, WA) and further analyzed. At each location,
the following was examined: number of failed reactions, any discordance issues between
individual genotypes at all three punch locations, partial profiles, and peak characteristics
such as -A and stutter percentages, average peak height (RFUs), deviations from expected
heterozygote ratios, and allelic dropout.

A sample was considered a failed amplification when the electropherogram did
not show peaks that could be definitively distinguished from background noise [29]. All
failed amplifications were re-injected a second time in the genetic analyzer to rule out the
possibility of an issue with the electrophoresis. A discordance problem was defined as
any unexpected or unexplainable differences between DNA profiles within an individual
at the three punch locations. A partial profile was called when one or more loci failed to
amplify any peaks that could reliably be distinguished from background noise in an
otherwise normal sample. The number of partial profiles was recorded and the
percentage of total profiles at each punch location that contained any locus failures was
recorded.

Peak characteristics were recorded if they met any of the conditions described
below. Peaks were called as –A when they were present at a position one base pair in

length shorter than the associated true allele, and greater than 20 percent of the height of the associated allele peak [29]. The number of loci with –A present in each sample was recorded, and the average number of loci with –A was compared across all punch locations. Peaks were called as stutter when an unexpected peak was present at a location four base pairs, or one repeat in length, shorter than the true allele [29]. Since all AmpFlSTR® Identifiler® Plus amplicons except Amelogenin have tetranucleotide (four base pair) repeat units, this means stutter peaks should be at the n-4 bp position [9]. The amount of stutter present was calculated by dividing the height of the stutter peak by the height of the associated true allele peak. The stutter filter, or minimum height percentage to be called as stutter, was pre-set at each locus by the GeneMarker® HID software for the Identifiler® kit (Table 1).

Table 1 Stutter filter percentages (GeneMarker® HID). Only peaks above the listed percentages (below) were called or flagged by the software.

Loci	Stutter filter (% of associated allele peak height)
TH01, TPOX	5
D5S818	7
D7S820, D13S317, D8S1179	8
D21S11, CSF1PO	9
D16S539, Amelogenin	10
D3S1358, D2S1338	11
D19S433, vWA	13
FGA	15
D18S51	17

The number of samples with stutter was recorded, as well as the peak height ratios of the stutter peaks relative to their associated allele peaks. The average stutter ratios were also recorded for each punch location. The average peak height at each punch location was calculated by averaging the peak heights in RFUs of all called true alleles

across all loci from all samples at each punch location. The minimum intensity baseline was set at 500 RFUs, and maximum intensity was set at 30,000 RFUs. The threshold of 500 RFUs was chosen based on previous studies showing high sensitivity of the instrument being used for separation and detection (3500 Genetic Analyzer, Applied Biosystems), because it is more sensitive and has a higher RFU scale [9, 38].

The average heterozygote peak height ratios were calculated by taking the average of all called true alleles across all loci from all samples at each peak location. Peaks were called as having peak height imbalance when the ratio was less than the expected ratio for a normal heterozygote allele pair. The most conservative ratio found in the literature, an expected ratio of greater than or equal to 0.70 in a normal sample, was used for this analysis [10, 33]. Heterozygote peak height ratios were calculated by dividing the height of the smaller peak of a heterozygous individual by the height of the larger peak [9, 29]. The number of samples with imbalanced peak height ratios was recorded, as well as the peak height ratios of the imbalanced smaller peaks relative to their larger associated peaks. Allelic dropout was called when there was discordance between the three punch locations when one of the expected alleles of a heterozygote was missing, also known as false homozygosity. The number of samples with allelic dropout and percentage of samples with allelic dropout was recorded for each punch location.

Samples which were found to contain allelic drop-in and allelic dropout were identified, and punches were taken from locations adjacent to the original punches to replicate the original sample as closely as possible. These new punches were amplified and analyzed in the same fashion as the previous samples, and examined for the presence of allelic drop-in or dropout as was previously seen, to determine whether these phenomena were reproducible. Additionally, 15 more edge punches were removed and analyzed following analysis of the original 150 punches: five punches each from the edge locations of three randomly chosen FTA™ cards taken from the original pool of 50 cards. The purpose of this was to remove the punch location variable in the study in order to compare edge punch quality within an individual and determine whether differences in profile quality were truly due to punch location or to variations in profile quality between all punches.

Statistical analysis of the results of average peak height, peak height ratios, imbalanced peak height ratios, and –A was performed using one-way fixed-effect analysis of variance (ANOVA) tests performed on SPSS statistical software (IBM, New York, NY). *Post hoc* pair-wise comparisons among the three groups were evaluated with Dunnett's T3, which conducts multiple pairwise contrasts while controlling for family-wise error rate. A *p*-value of less than or equal to 0.05 was used to determine whether the results were significant.

CHAPTER 3. RESULTS

A total of 150 STR DNA profiles were initially analyzed: one punch from each of the three locations (center, halfway, edge) from 50 FTA™ cards with blood samples from 50 anonymous donors. Additionally, 15 more profiles were subsequently analyzed: five punches each from the edge punch locations of three randomly chosen FTA™ cards. The average diameter of the bloodspots on the 50 FTA™ cards was calculated and found to be 9.74 mm, the average distance from center to edge was calculated and found to be 4.87 mm, and the average distance from halfway to edge was calculated and found to be 2.44 mm.

3.1   Failed Reactions

Eight reactions out of the 150 initial reactions failed (5.3%). Two failed reactions occurred at the center punch location (25%), four failed locations occurred at the halfway punch location (50%), and two failed reactions occurred at the edge punch location (25%, Table 2). Out of all the reactions at each punch location, 4% of the center punch and edge punch location reactions failed and 8% of the halfway punch location reactions failed. The halfway punch location showed the highest percentage of failed reactions. The success rates of each punch location were therefore 96% at the center and edge punch locations and 92% at the halfway punch location.

Table 2 Results from the comparison of failed reactions at each punch location. The halfway punch location had the most failed reactions.

Punch location	Number observed	Percentage failed at each location (Out of 50)	Success rate
Center	2	4%	96%
Halfway	4	8%	92%
Edge	2	4%	96%

3.2 Partial Profiles

Six reactions out of the remaining 142 successful reactions were called as partial profiles, which is an overall rate of 4.2%. Three partial profiles occurred at the center punch location (50%), one partial profile occurred at the halfway punch location (17%), and two partial profiles occurred at the edge punch location (33%, Table 3). Out of all the successful reactions at each punch location, 6.3% of the total successful reactions at the center punch location were partial profiles, 2.2% of the total successful reactions at the halfway punch location were partial profiles, and 4.2% of the total successful reactions at the edge punch location were partial profiles. The center punch location had the highest percentage of partial profiles.
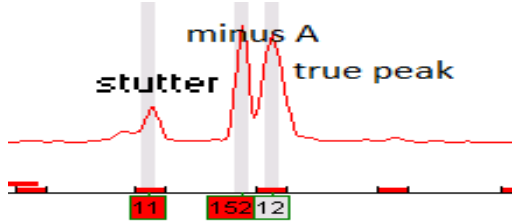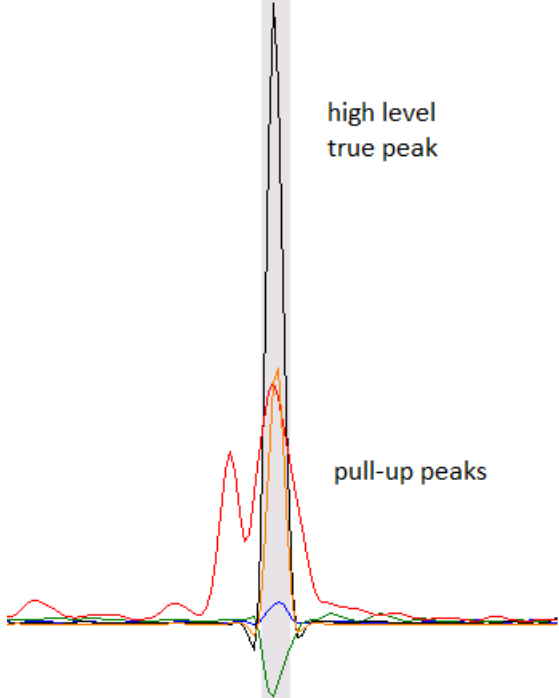
Table 3 Results from the comparison of partial profiles at each punch location. The center punch location had the highest number of partial profiles.

Punch location	Number of partial profiles observed	Percentage of total reactions
Center	3	6.3%
Halfway	1	2.2%
Edge	2	4.2%

3.3   Concordance

Upon initial analysis, several problems with concordance within individuals were observed. However, upon further investigation, all but one of the concordance problems were able to be explained by the following conditions: high amounts of -A causing widened or split peaks that were called incorrectly, pull-up because of high RFU peaks at other loci causing extra peaks, missing peaks due to allelic dropout, and high level stutter incorrectly called as peaks. Table 4 describes the criteria used to distinguish between true peaks and other extra peaks that were observed as a result of these biological or technological issues.

Table 4 Description of criteria used to distinguish true peaks from extra peaks caused by other technological or biological artifacts. Decisions were made based on the position of the peak, size of peak, and presence of peaks of the same size in multiple different colors. All examples were observed within samples collected in this experiment.

Condition	Description	Example
-A	In the -1 bp position to the true peak	
Stutter	Usually in the -4 bp position to the true peak, significantly smaller than the true peak	
Pull-up	Smaller peak(s) present beneath larger peak of a different color, caused by bleeding-over due to oversaturation	

Only one extraneous peak was observed that would be considered an issue with concordance that could not be explained by any of the previously mentioned conditions, and this was determined to be due to allelic drop-in (Figure 5). Allelic drop-in is the presence of an extra allele with an unknown origin where contamination has been ruled [39]. Contamination could be ruled out in this case because there were no other loci with

abnormalities within the sample, specifically no unexplained extra peaks that would have suggested the presence of a mixture.

Allelic drop-in can occur as a result of a PCR aberration where a smaller product, similar to stutter, is produced early on in the amplification process and then preferentially amplified to the point that it is similar in size to a true peak [39]. Allelic drop-in is not reproducible [39]. The observed extraneous peak occurred at the D19S433 locus at the center punch location of sample 565 of the study. The peak height ratio of the extraneous peak was eventually determined to be too high to be called as stutter (72%), although it was located at the stutter position to the true allele peak, leading to the determination of allelic drop-in. Allelic drop-in generally occurs with low level template DNA, however, so it is not clear why allelic drop-in occurred in this situation [39]. Upon repeat amplification of an adjacent punch to the center punch in sample 565, allelic drop-in was not observed a second time.
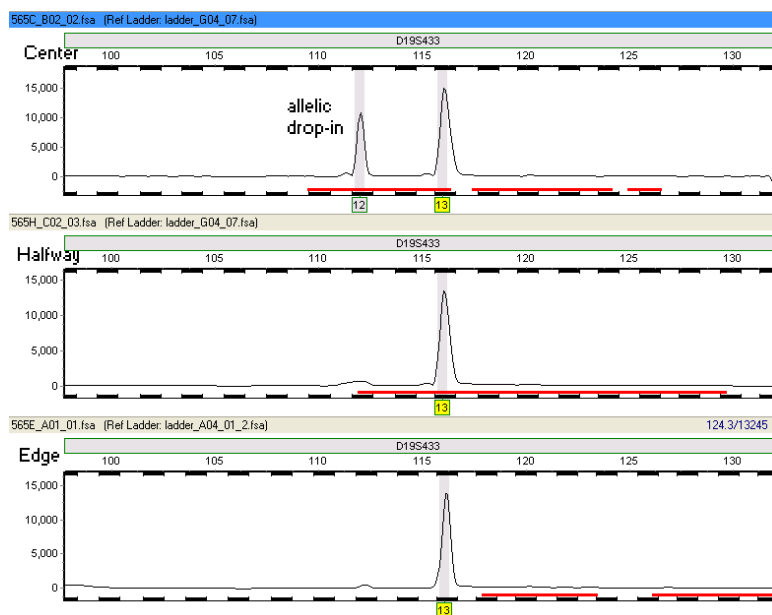
Figure 5 An example of allelic drop-in seen at the center punch location of sample 565 of the study. The extra peak was only observed in one of the three profiles at the D19S433 locus. This extra peak was determined to be the result of allelic drop-in and not the result of a mixture, contamination, or any other technological artifacts. The peak did not reoccur when an adjacent sample was amplified.

3.4   Peak Characteristics

3.4.1   Minus A

Overall, high levels of –A were present in most samples regardless of punch location. In fact, in some samples, the peak height of the –A peak was higher than the true allele peaks (Figure 6). This is likely due to adding an excess of DNA to the amplification reaction because no quantitation was performed, resulting in split peaks and incomplete adenylation. Out of all 16 loci tested, the average number of loci with –A present was found to be 5.94 (±0.50 standard error) for the center punch location, 5.72 (±0.56 standard error) for the halfway punch location, and 5.65 (±0.50 standard error) at the edge punch location (Figure 7). ANOVA testing showed that there was no significant difference found in the number of loci with the presence of -A across the three punch locations (Table 5).
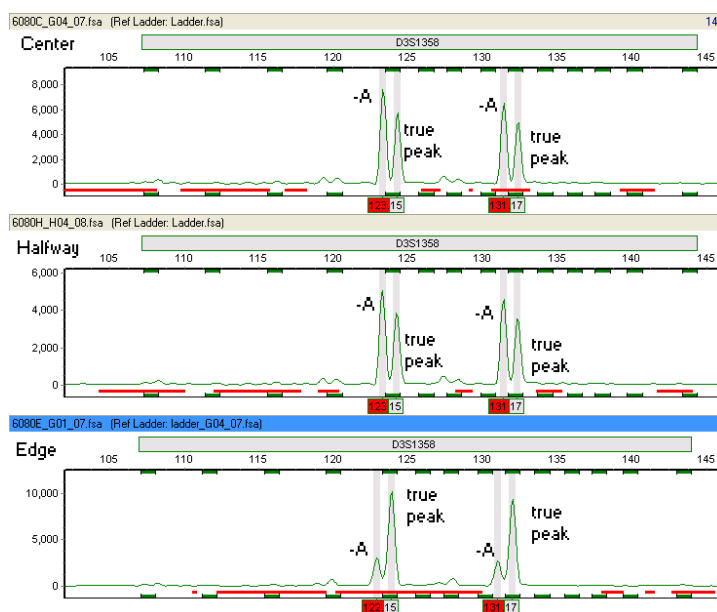
Figure 6 An example of –A peaks that surpassed the threshold amount and were flagged by the software at all three punch locations in sample 6080 of the study. The amount of – A is higher than the true peaks at the center and halfway punch locations.
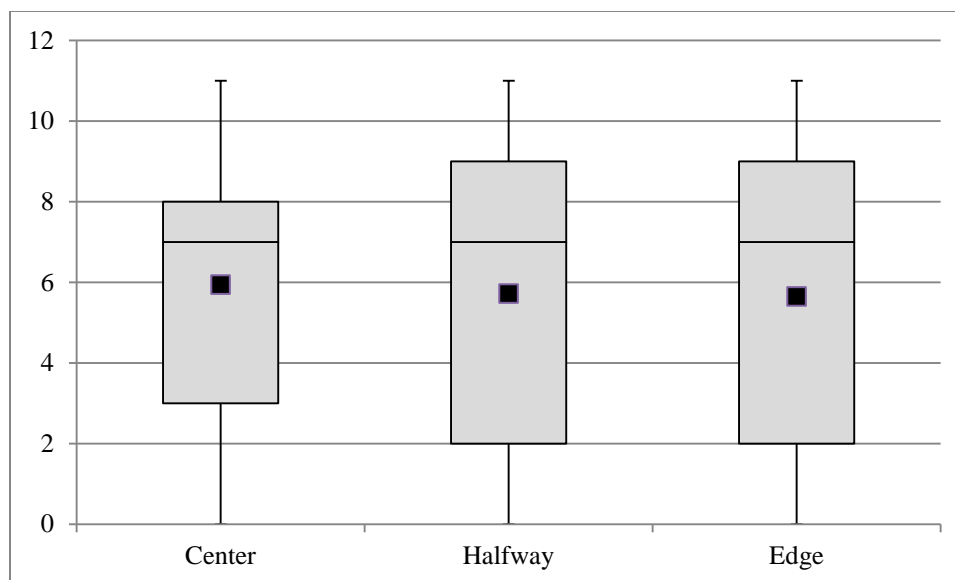
Figure 7 Box and whisker plot of the –A data. The dark square represents the location of the average number of loci with –A for each punch location.

Table 5 The ANOVA results for the –A examination shows that there is not a significant difference in the number of loci with –A between the three punch locations (significance >0.05).

ANOVA

Source of Variation	Sum of Squares	Degrees of Freedom	Mean Square	F	P-value
Between Punch Locations	2.213232	2	1.106616	0.085879	0.917754
Within Punch Locations	1791.118	139	12.88574		
Total	1793.331	141			

3.4.2   Stutter

Stutter was observed at two loci within all 142 successful reactions: once at the halfway punch location (50%) and once at the edge punch location (50%) (Figure 8, Table 6). The percentages of each stutter peak were found to be 15% at the halfway

punch location and 21% at the edge punch location. Out of all the successful reactions at each punch location, none of the center punch location contained stutter, 2.2% of the total successful reactions at the halfway punch location contained stutter, and 2.1% of the total successful reactions at the edge punch location contained stutter.
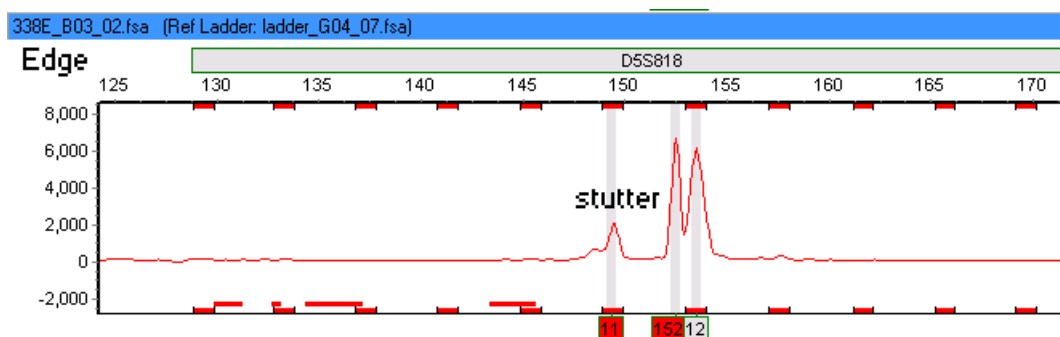
Figure 8 An example of a stutter peak (allele 11) at the edge punch location of sample 338 of the study. Minus A is also present one base pair shorter than the true allele (allele 12).

Table 6 Results from analysis of stutter. The halfway and edge punch locations had one stutter peak each as compared to zero stutter peaks observed at the center punch location.

Punch location	Number of stutter peaks observed	Percentage of total reactions	Stutter peak height percentage
Center	0	n/a	n/a
Halfway	1	2.2%	15%
Edge	1	2.1%	21%

3.4.3   Peak Heights

Average peak height in RFUs was calculated at each punch location for all true alleles across all loci. The average peak height at the center punch location was found to be 8776 RFUs (±108 standard error), at the halfway punch location was found to be 8827 RFUs (±109 standard error), and at the edge punch location was found to be 8763 RFUs

(±107 standard error) (Figure 9). ANOVA testing showed that there was no significant difference found in the peak heights across the three punch locations (Table 7).
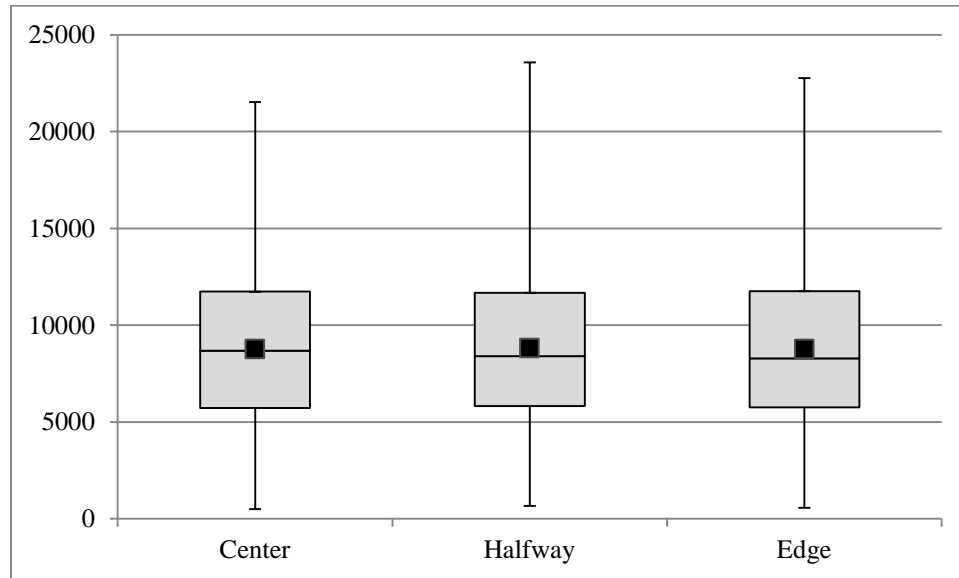
Figure 9 Box and whisker plot of the peak height data. The dark square represents the location of the average peak height for each punch location.

Table 7 The ANOVA results for average peak height shows that there is not a significant difference in the average peak height between the three punch locations (significance >0.05).

ANOVA

Source of Variation	Sum of Squares	Degrees of Freedom	Mean Square	F	P-value
Between Punch Locations	2981547	2	1490773	0.096259	0.908231
Within Punch Locations	6.17E+10	3984	15487164		
Total	6.17E+10	3986			

3.4.4 Heterozygote Peak Height Ratios

Average heterozygote ratios were calculated at all three punch locations and found to be 0.90 (<0.01 standard error) at the center location, 0.89 (<0.01 standard error) at the halfway punch location, and 0.91 (<0.01 standard error) at the edge punch location (Figure 10). A one-way ANOVA analysis indicated a statistically significant difference in peak height ratios between the three groups (Table 8). *Post hoc* pair-wise comparisons among the three groups were evaluated. Pair-wise comparisons among the three punch locations indicated that halfway had a significantly lower peak height ratio than the center and the edge, as indicated by Dunnett's T3 analysis (Table 9).
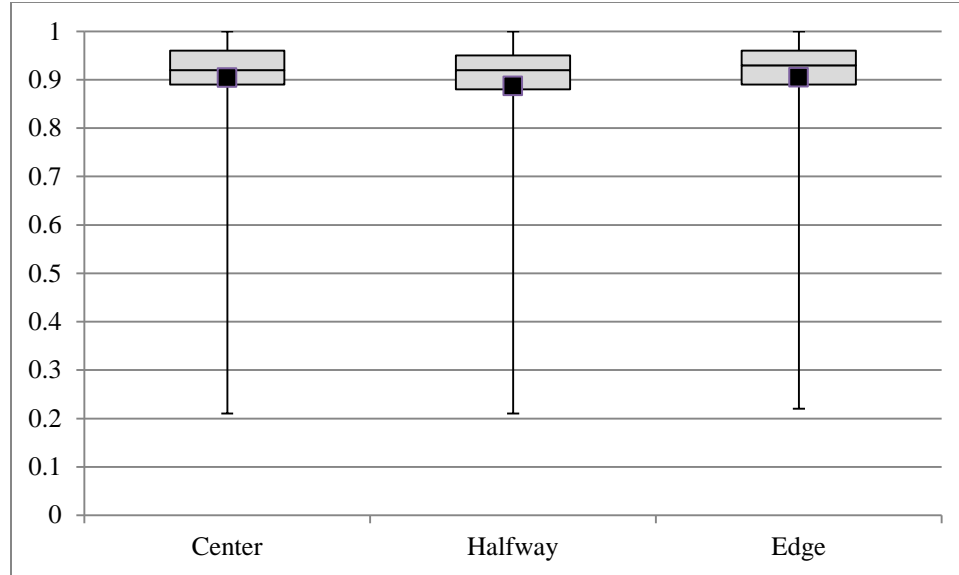
Figure 10 Box and whisker plot of the peak height ratio data. The dark square represents the location of the average peak height ratio for each punch location.

Table 8 The ANOVA results for the average peak height ratios shows that there is a significant difference in the average peak height ratios between the three punch locations (significance <0.05).

ANOVA

Source of Variation	*Sum of Squares*	*Degrees of Freedom*	*Mean Square*	*F*	*P-value*
Between Punch Locations	0.125	2	0.063	5.042	0.007
Within Punch Locations	22.141	1782	0.012		
Total	22267	1784			

Table 9 The results of *post hoc* Dunnett's T3 pair-wise comparisons of average peak height ratios showed that there is a significant difference in the peak height ratios between the center and halfway and edge and halfway punch locations but not between the center and edge punch locations (significance <0.05). Significant relationships are highlighted in bold.

(i) group	(j) group	Mean Difference (i-j)	Std. Error	Sig.	Lower Bound	Upper Bound
Center	**Halfway**	0.01745	0.00678	**0.030**	0.0013	0.0337
	Edge	-0.00067	0.00580	0.999	-0.0145	0.0132
Halfway	**Center**	-0.01745	0.00678	**0.030**	-0.0337	-0.0013
	Edge	-0.01813	0.00679	**0.023**	-0.0344	-0.0019
Edge	Center	0.00067	0.00580	0.999	-0.0132	0.0145
	Halfway	0.01813	0.00679	**0.023**	0.0019	0.0344

Imbalanced heterozygote peak ratio (ratio of less than or equal to 0.7, example Figure 11) was observed 68 times within all 142 successful amplifications; it was observed 16 times at the center punch location, 34 times the halfway punch location, and 18 times at the edge punch location. The average heterozygote imbalance ratio, calculated using only ratios less than 0.70 for each punch location was 0.45 (±0.04 standard error) for the center punch location, 0.43 (±0.03 standard error) for the halfway punch location, and 0.47 (±0.05 standard error) for the edge punch location (Figure 12). ANOVA testing showed there was no significant difference found in the average imbalanced peak height ratios across the three punch locations (Table 10).
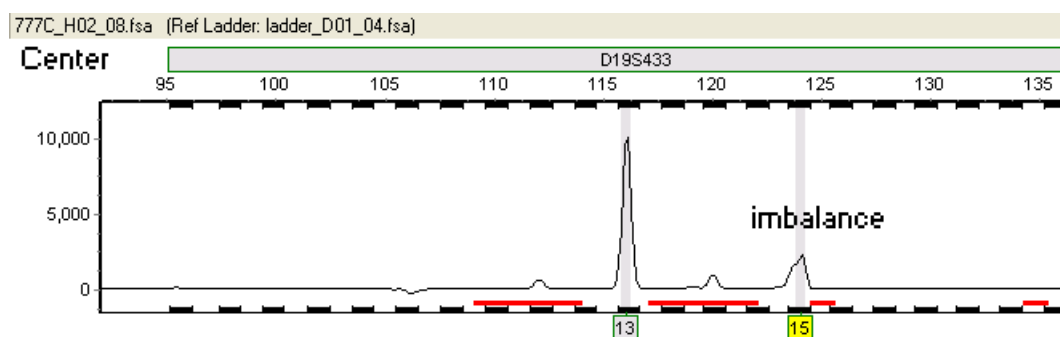
Figure 11 An example of peak height imbalance at the center punch location from sample 777 of the study. The peak at allele 15 is much shorter than the peak at allele 13, resulting in an imbalanced ratio.
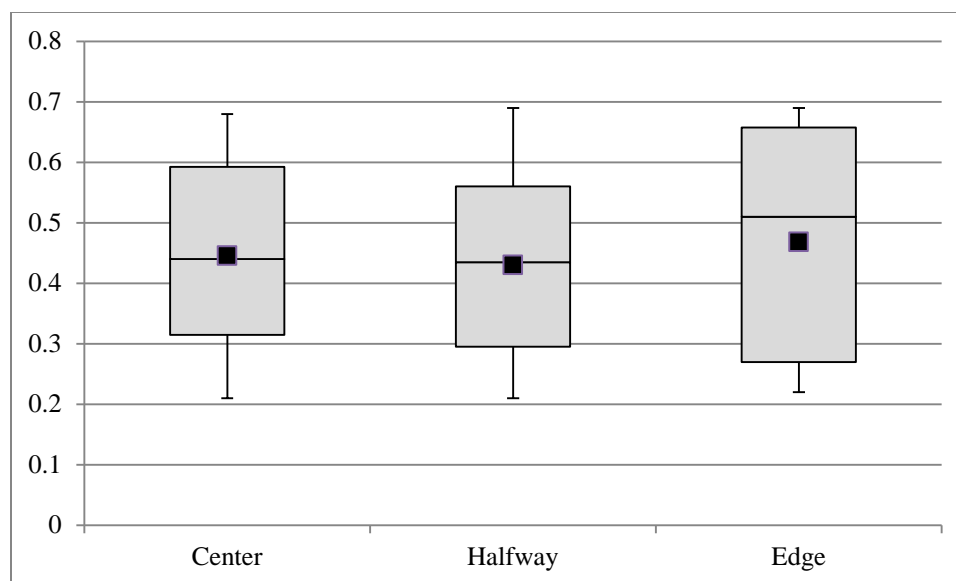
Figure 12 Box and whisker plot of the peak height imbalance data. The square represents the location of the average imbalance ratio for each punch location.

Table 10 The ANOVA results for the average peak height imbalance shows that there is not a significant difference in the average peak height imbalance between the three punch locations (significance >0.05).

ANOVA

Source of Variation	Sum of Squares	Degrees of Freedom	Mean Square	F	P-value
Between Punch Locations	0.016815	2	0.008408	0.30516	0.738056
Within Punch Locations	1.790832	65	0.027551		
Total	1.807647	67			

3.4.5 Allelic Dropout

Allelic dropout (Figure 13) was observed at seven loci within all 142 successful reactions, 3 times (43%) at the center punch location (including twice in one profile at two different loci), 2 times (29%) at the halfway punch location and 2 times (29%) at the edge punch location (Table 11). Out of all the successful reactions at each punch location, 6.3% of the total successful reactions at the center punch location contained allelic dropout, 4.3% of the total successful reactions at the halfway punch location contained allelic dropout, and 4.2% of the total successful reactions at the edge punch location contained allelic dropout. The center punch location showed the highest percentage of allelic dropout. Adjacent punches were taken for all samples that showed allelic dropout and a new amplification was performed. In the amplification of these new samples, allelic drop out did not reoccur in any of the samples which had previously displayed false homozygosity.
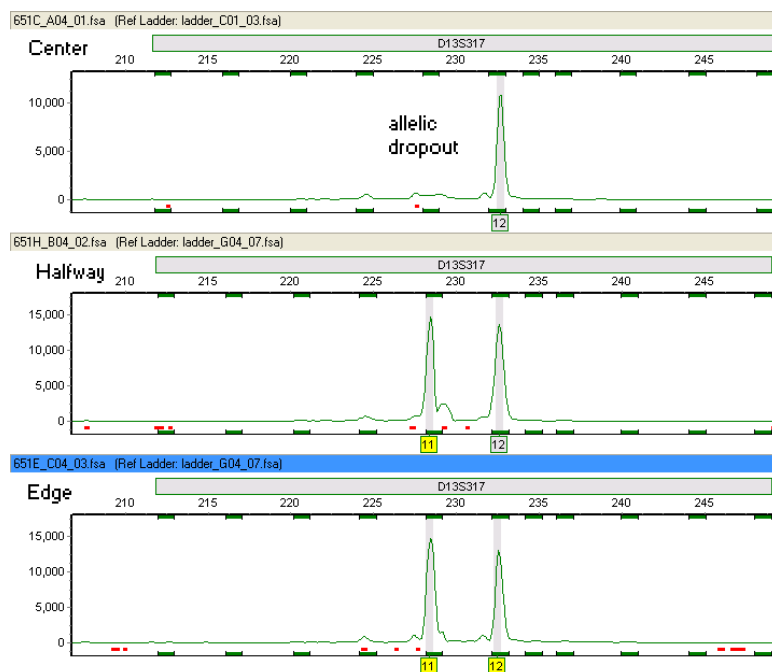
Figure 13 An example of allelic dropout of one allele (11) in a heterozygote (11, 12) resulting in false homozygosity at the center punch location of sample 651 of the study.

Table 11 Results from the analysis of allelic dropout. The center punch location had the highest number of profiles with allelic dropout present.

Punch location	Number of profiles with allelic dropout	Percentage of total reactions
Center	3	6.3%
Halfway	2	4.3%
Edge	2	4.2%

3.5   Edge Punch Comparison

Five samples each from the edge of three randomly selected FTA™ cards were removed and analyzed to compare profile quality between different punches from the same punch location within one individual's sample. In these 15 edge punch profiles, there were no failed reactions, giving a success rate of 100%. There were no partial profiles and no concordance issues observed, including no stutter and no allelic dropout.

3.5.1   Minus A

For each of the 15 edge punches, the number of loci with –A present was recorded (Table 12). The number of loci with –A present within each individual is similar: the variance in sample 3701 is less than nine percent, variance in sample 6233 is less than seven percent, and sample 7572 is less than 18%.

Table 12 A comparison of the number of loci with -A present in each of the edge punches at five different locations in three randomly selected FTA™ cards. The number of loci with -A within each individual is similar: the variance in sample 3701 is less than nine percent, variance in sample 6233 is less than seven percent, and sample 7572 is less than 18%.

Sample	Loci w/-A	Sample	Loci w/-A	Sample	Loci w/-A
3701 A	8	6233 A	9	7572 A	7
B	9	B	10	B	8
C	9	C	9	C	7
D	9	D	10	D	6
E	9	E	9	E	6

3.5.2   Peak Heights

Average peak height in RFUs and standard error was calculated for all true alleles across all loci for each of the 15 edge profiles (Table 13). Figure 14 shows box and whisker plots for peak height for each of the five punches from each of the three samples. Nested ANOVA testing showed that there was no significant difference found in the peak heights within each individual's five punches, or across all fifteen punches (Table 14).

Table 13 Results from the peak height comparison for the fifteen edge punches. Average peak height and standard error for each sample is given.

3701	Avg. Peak Height	Std. Error	6233	Avg. Peak Height	Std. Error	7572	Avg. Peak Height	Std. Error
A	5675	±465	A	8152	±589	A	8483	±587
B	5941	±507	B	5298	±494	B	7843	±492
C	7893	±567	C	8009	±605	C	7372	±536
D	5127	±453	D	8888	±565	D	8210	±548
E	6626	±498	E	7881	±564	E	6485	±527
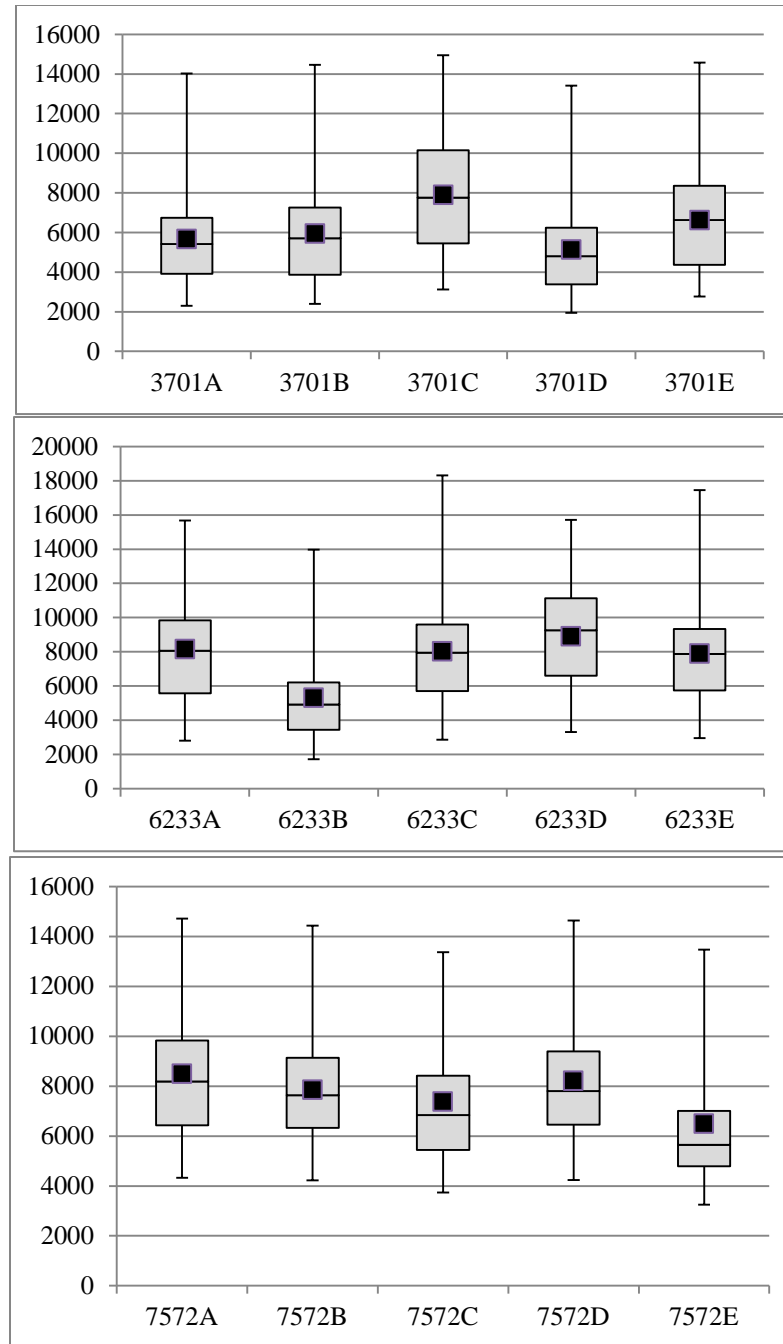
Figure 14 Box and whisker plots of the peak height data. The square represents the location of the average peak height for each punch location.

Table 14 Results of nested ANOVA testing for peak height. There was not a significant difference between any of the punches within each individual (p-value = 0.421), or between all fifteen punches (p-value = 0.874).

ANOVA

Source of Variation		Sum of Squares	Degrees of Freedom	Mean Square	F	P-value
Model	Hypothesis	159.862	1	159.862		
	Error	0.059	10.136	0.006	27319.745	0.000
	Hypothesis	0.007	4	0.002		
Person (Replicate)	Error	0.059	10.136	0.006	0.296	0.874
	Hypothesis	0.059	10	0.006		
Error	Error	1.024	180	0.006	1.029	0.421

3.5.3   Heterozygote Peak Height Ratios

Average heterozygote ratios and standard error were calculated for all 15 punches (Table 15). Figure 15 shows box and whisker plots for heterozygote peak height ratio for each of the five punches from each of the three samples. ANOVA showed that there was no significant difference found in the peak heights across all fifteen punches (Table 16).

Table 15 Results from the peak height ratio comparison for the fifteen edge punches. Average peak height ratio and standard error for each sample is given.

3701	Avg. Peak Height Ratio	Std. Error	6233	Avg. Peak Height Ratio	Std. Error	7572	Avg. Peak Height Ratio	Std. Error
A	0.91	±0.10	A	0.92	±0.01	A	0.92	±0.01
B	0.87	±0.03	B	0.93	±0.01	B	0.92	±0.01
C	0.87	±0.04	C	0.93	±0.01	C	0.93	±0.01
D	0.92	±0.01	D	0.92	±0.01	D	0.93	±0.01
E	0.89	±0.04	E	0.92	±0.01	E	0.90	±0.01
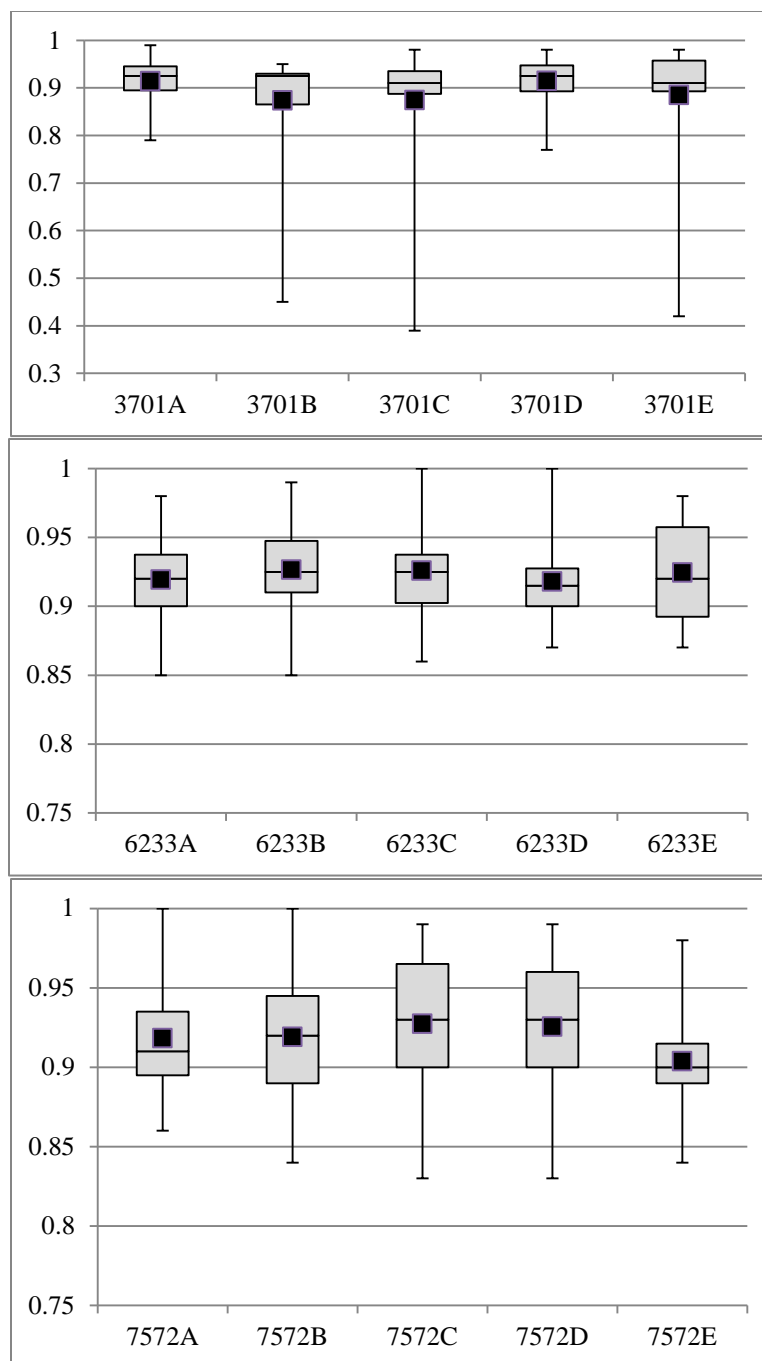
Figure 15 Box and whisker plots of the heterozygote peak height ratio data. The square represents the location of the average heterozygote peak height ratio for each punch location. The samples with imbalanced peak height ratios are easily visible on the plot for 3701B, C and E.

Table 16 Results of ANOVA testing for heterozygote peak height ratio. There was not a significant difference between any of the fifteen punches (significance > 0.05).

ANOVA

Source of Variation	Sum of Squares	Degrees of Freedom	Mean Square	F	P-value
Replicate	3459117.816	4	867279.454	.491	0.743
Error	17664089.382	10	1766408.938		
Total	21133207.198	14			

An imbalanced heterozygote peak ratio (ratio of less than or equal to 0.7) was observed three times within these 15 edge punch sample amplifications, and all three instances were from the same FTA™ card: one locus with a ratio of 0.45 in sample 3701B, one locus with a ratio of 0.39 in 3701C, and one locus with a ratio of 0.42 in sample 3701E. These imbalanced ratios are clearly visible in Figure 15. The other 12 samples did not contain any loci with a peak height ratio of less than 0.7. This shows that while one of the samples contained a few loci with imbalanced ratios, a comparison of the average peak height ratios between all the samples still showed that there was not a significant difference in profile quality in terms of overall peak height ratio.

CHAPTER 4. DISCUSSION

The center punch location had the highest percentage of partial profiles and allelic dropout, and was the only punch location to have an issue with concordance. However, there was no significant difference between the punch locations in terms of average peak heights, heterozygote peak height imbalance ratios, and presence of -A. The halfway punch location had the lowest average heterozygote peak height ratios, and the highest percentage of overall failed reactions. Overall, the edge punch location produced the highest quality and most reliable profile, although the differences between the three locations are very slight.

Though the quantity of DNA for each punch was not determined, as the punch would then be unavailable for STR amplification, given the observed profiles, the likely culprit to the reductions in profile qualities is an increase in DNA concentration. The quantity of DNA amplified was often so high that it led to numerous electrophoretic anomalies and problems in genotype interpretation. A seemingly simple solution to this would be to perform extraction and quantitation prior to amplification, despite the manufacturer's recommendation that a disc can be added directly to the amplification reaction tube. This seems to be the approach taken by most crime laboratories to avoid the problem of unknown DNA quantity [27, 40].

Some analytical issues were encountered in this study when trying to compare heterozygote ratios across punch locations, due to the high amounts of –A present at some loci. Because the peak heights of the –A peaks were higher than the true allele peaks in some locations, the heterozygote ratios were calculated by the analysis software program based on the –A peak heights instead of the true allele peak heights. Whenever a high –A peak with a smaller associated true allele peak was present, the true allele

peaks were therefore called as having a heterozygote ratio of less than 1.0. This may have skewed the heterozygote ratio data towards a smaller number on some samples relative to what would have been observed if the –A peaks had not been present. However, this could not be avoided without altering the parameters of the study to account for those occasions when extremely high –A peaks were present, and therefore the peak height ratios relative to their –A peaks were left in the calculations. Any future studies involving peak height imbalance with FTA™ cards may want to take this issue into account.

CHAPTER 5. CONCLUSIONS

Overall, the quality of profile obtained in this study was poor. The presence of minus A, pull-up, allelic drop-in and other issues, likely due to too much DNA present in the samples, led to profiles that were not easily interpreted and would likely not be acceptable to analysts in real-life crime laboratory situations. These samples would probably have been re-amplified due to the poor overall quality of profiles obtained. Also, samples adjacent to the original samples that contained allelic drop-in and dropout were re-amplified and these issues did not reoccur. This may show that the use of FTA™ cards as recommended by the manufacturer is unreliable for analysis of reference samples, as profiles obtained in this study were inconsistent between runs. As a result of similarly observed issues, most crime laboratories currently using FTA™ paper take advantage of its long-term storage capabilities, but do not directly add the disc to the amplification reaction [27, 40]. Based on new technologies being developed, it is obvious this has been an issue for some time in crime labs using FTA™ paper. The commercial STR kit manufacturers have been developing new, more robust STR kits to deal with this influx of PCR inhibitors and high concentrations of DNA, not just from FTA™ paper, but also from other forensic samples. For example, Applied Biosystems has a newly developed kit, the Identifiler® Direct PCR amplification kit, which allows analysts to place directly into the PCR reaction unwashed FTA™ card discs or any other piece of evidence (i.e. a cutting from a swab or a piece of clothing). This kit claims to be able to amplify STR loci from unwashed FTA™ card punches [5].

The conclusion of this study was that the edge punch location seemed to have the fewest problems in regards to quality, although the difference in profile quality between the three punch locations overall was not very significant. The center punch location had

the most partial profiles, which adversely affects the statistical analysis that is able to be performed when comparing two profiles, such as an evidentiary sample and a suspect, as the discriminatory power of a profile decreases with the decreasing number of loci. The center punch location also exhibited he largest incidence of allelic dropout, which affects forensic sample comparisons. Because FTA™ paper is mainly used for the analysis and storage of samples that contribute to the offender database, if allelic dropout leading to false homozygosity goes undetected in the analysis of an offender's profile, an incorrect profile will be uploaded into the database. However, in the case of CODIS searches, a difference of one allele would not be enough exclude a suspect because CODIS database searches have what is known as a "moderate" stringency setting [41]. Due to differences in primers between commercial STR kits, the possibility of a null allele occurring with use of one kit but not in another exists, which can lead to differences of one allele between profiles. Therefore, a "moderate" match occurs when all the alleles from one sample are present in the other, even if there are extras in the second [41]. For example, an allele call of homozygous 11, 11 would also be considered a moderate match to a heterozygous 11, 12.

The halfway punch location showed the lowest peak height ratios, and had the highest number of imbalanced peaks, but did not have a significantly lower imbalance ratio. Also, the issue of peak height imbalance is not as dire as the presence of allelic dropout, because if an analyst sees peak height imbalance and is unsure of whether a peak is a true peak, the sample may be reanalyzed, but if the peak has dropped out completely, an analyst may never know.

A comparison of profile quality between edge punches from three randomly selected individuals was undertaken to determine whether the differences in profile quality observed in the 150 sample study were truly due to punch location or simply because of variability between all punches. The results of this experiment showed that there was not a significant difference in profile quality when comparing only edge punches. These results showed that the differences observed between punch locations, although slight, do seem to be true differences.

REFERENCES

REFERENCES

1.	Divall, G.B., *The application of electrophoretic techniques in the field of criminology.* Electrophoresis, 1985. **6**(6): p. 249-258.

2.	Bell, S., B. Fisher, and R. Shaler, *Encyclopedia of Forensic Science*2008: Facts on File, Inc.

3.	Jeffreys, A.J., V. Wilson, and S.L. Thein, *Hypervariable 'minisatellite' regions in human DNA.* Nature, 1985. **314**(6006): p. 67-73.

4.	Tautz, D., *Notes on the definition and nomenclature of tandemly repetitive DNA sequences.* EXS, 1993. **67**: p. 21-8.

5.	Wang, D.Y., et al., *Development and validation of the AmpFlSTR(R) Identifiler(R) Direct PCR Amplification Kit: a multiplex assay for the direct amplification of single-source samples.* J Forensic Sci, 2011. **56**(4): p. 835-45.

6.	Butler, J.M., et al., *Forensic DNA typing by capillary electrophoresis using the ABI Prism 310 and 3100 genetic analyzers for STR analysis.* Electrophoresis, 2004. **25**(10-11): p. 1397-412.

7.	Gill, P., *Role of short tandem repeat DNA in forensic casework in the UK--past, present, and future perspectives.* Biotechniques, 2002. **32**(2): p. 366-8, 370, 372, passim.

8.	Lee, H.C., et al., *DNA typing in forensic science. I. Theory and background.* Am J Forensic Med Pathol, 1994. **15**(4): p. 269-82.

9.	*AmpFlSTR® Identifiler® Plus PCR Amplification Kit User's Guide*, Applied Biosystems.

10.	*DNA Analyst Training*. November 2, 2011]; President's DNA Initiative - DNA Analysts training website]. Available from: http://www.nfstc.org/pdi/.

11.   Walsh, P.S., H.A. Erlich, and R. Higuchi, *Preferential PCR amplification of alleles: mechanisms and solutions.* PCR Methods Appl, 1992. **1**(4): p. 241-50.

12.   Mullis, K., et al., *Specific enzymatic amplification of DNA in vitro: the polymerase chain reaction.* Cold Spring Harb Symp Quant Biol, 1986. **51 Pt 1**: p. 263-73.

13.   Budowle, B., et al., *Source Attribution of a Forensic DNA Profile.* Forensic Science Communications, 2000. **2**(3).

14.   Wilson, I.G., *Inhibition and facilitation of nucleic acid amplification.* Appl Environ Microbiol, 1997. **63**(10): p. 3741-51.

15.   Akane, A., et al., *Identification of the heme compound copurified with deoxyribonucleic acid (DNA) from bloodstains, a major inhibitor of polymerase chain reaction (PCR) amplification.* J Forensic Sci, 1994. **39**(2): p. 362-72.

16.   de Franchis, R., et al., *A potent inhibitor of Taq polymerase copurifies with human genomic DNA.* Nucleic Acids Res, 1988. **16**(21): p. 10355.

17.   Radstrom, P., et al., *Pre-PCR processing: strategies to generate PCR-compatible samples.* Mol Biotechnol, 2004. **26**(2): p. 133-46.

18.   Comey, C.T., et al., *DNA Extraction Strategies for Amplified Fragment Length Polymorphism Analysis* Journal of Forensic Sciences, 1994. **39**(5): p. 16.

19.   Burgoyne, L., et al. in *The Fifth International Symposium on Human Identification*. 1994. Madison, WI: Promega Corporation.

20.   Smith, L.M. and L.A. Burgoyne, *Collecting, archiving and processing DNA from wildlife samples using FTA databasing paper.* BMC Ecol, 2004. **4**: p. 4.

21.   *Whatman™ FTA™ for blood DNA*. 2010. **Data file 51641**.

22.   Burgoyne, L.A., *Solid Medium and Method for DNA Storage*, U.S.P. Office, Editor 1996: United States.

23.   Kline, M. *DNA Stability Studies*. in *Forensics @ NIST*. 2010. Gaithersburg, MD.

24.   Whatman®. *FTA™ Nucleic Acid Collection, Storage and Purification*. November 2, 2011]; Available from: http://www.whatman.com/FTANucleicAcidCollectionStorageandPurification.aspx.

25.   *Comparative analysis of FTA™ and NucleoSave™ cards*. 2010. **Application note 28-9822-24 AA**.

26.   Pezzoli, N., et al., *Quantification of mixed chimerism by real time PCR on whole blood-impregnated FTA cards.* Leuk Res, 2007. **31**(9): p. 1175-83.

27.   Picard, C. and S. Baneshwar, *An evaluation of FTA® card methods for genotyping reference samples*, 2011: Journal of Forensic Sciences (Under Review).

28.   Picard, C., 2012.

29.   *SWGDAM Interpretation Guidelines for Autosomal STR Typing by Forensic DNA Testing Laboratories*. 2010.

30.   Clark, J.M., *Novel non-templated nucleotide addition reactions catalyzed by procaryotic and eucaryotic DNA polymerases.* Nucleic Acids Res, 1988. **16**(20): p. 9677-86.

31.   Magnuson, V.L., et al., *Substrate nucleotide-determined non-templated addition of adenine by Taq DNA polymerase: implications for PCR-based genotyping and cloning.* Biotechniques, 1996. **21**(4): p. 700-9.

32.   Hauge, X.Y. and M. Litt, *A study of the origin of 'shadow bands' seen when typing dinucleotide repeat polymorphisms by the PCR.* Hum Mol Genet, 1993. **2**(4): p. 411-5.

33.   Gill, P., R. Sparkes, and C. Kimpton, *Development of guidelines to designate alleles using an STR multiplex system.* Forensic Sci Int, 1997. **89**(3): p. 185-97.

34.   Fregeau, C.J. and R.M. Fourney, *DNA typing with fluorescently tagged short tandem repeats: a sensitive and accurate approach to human identification.* Biotechniques, 1993. **15**(1): p. 100-19.

35.   *Revised Validation Guidelines*. 2003.

36.   Aranda, X., et al. *Alkaline Extraction of DNA from FTA® Paper Spotted with Buccal Epithelial Cells and Whole Blood*. in *15th International Symposium on Human Identification*. 2004.

37.   *Cross-Contamination Study: Carryover does not occur during punching and processing of FTA™ or CloneSaver™ Cards*. 2010. **Application Note 51621**.

38. Butler, J.M. and C.R. Hill. *ABI 3500 Studies*. in *Forensics @ NIST*. 2010. Gaithersburg, MD.

39. Taberlet, P., et al., *Reliable genotyping of samples with very low DNA quantities using PCR.* Nucleic Acids Res, 1996. **24**(16): p. 3189-94.

40. Sobieralski, C., Indiana State Police, *Personal Communication*, 2011.

41. Crouch, K., *Indiana State Police CODIS Section Supervisor*, 2012.

APPENDIX

Sample Name	Peak Height	Height Ratio	Marker	Allele	Profile Characteristics
CENTER					
008C	4678	1	D8S1179	14	Minus A, Imbalance
	4288	0.92	D8S1179	15	
	4195	1	D21S11	30	
	3788	0.9	D21S11	34.2	
	2414	1	D7S820	12	
	2111	0.87	D7S820	13	
	2784	1	CSF1PO	10	
	2714	0.97	CSF1PO	12	
	4639	1	D3S1358	15	
	4541	0.98	D3S1358	18	
	6408	0.99	TH01	6	
	6450	1	TH01	9.3	
	6615	1	D13S317	8	
	5610	0.85	D13S317	12	
	13093	1	D16S539	12	
	3473	1	D2S1338	20	
	3064	0.88	D2S1338	24	
	5123	1	D19S433	13	
	4609	0.9	D19S433	14	
	10656	1	vWA	17	
	10430	1	TPOX	8	
	4034	1	D18S51	12	
	2548	0.63	D18S51	22	
	6155	1	AMEL	X	
	6124	0.99	AMEL	Y	
	9592	1	D5S818	11	
	3783	1	FGA	19	
	3439	0.91	FGA	20	
062C	13092	1	D8S1179	14	Minus A
	6642	1	D21S11	29	
	6447	0.97	D21S11	31.2	
	2324	1	D7S820	10	
	2084	0.9	D7S820	12	
	3657	1	CSF1PO	11	
	3406	0.93	CSF1PO	12	
	6688	1	D3S1358	14	
	6054	0.91	D3S1358	15	
	11461	1	TH01	6	
	11063	0.97	TH01	9.3	

	12538	1	D13S317	11	
	17080	1	D16S539	11	
	4766	1	D2S1338	18	
	4408	0.92	D2S1338	19	
	12128	1	D19S433	15	
	9375	1	vWA	16	
	8413	0.9	vWA	17	
	8056	1	TPOX	8	
	7867	0.98	TPOX	10	
	3162	1	D18S51	16	
	2715	0.86	D18S51	20	
	11624	1	AMEL	X	
	11664	1	AMEL	Y	
	10813	1	D5S818	12	
	2574	1	FGA	23	
	2325	0.9	FGA	24	
088C	4991	1	D8S1179	13	Minus A
	4693	0.94	D8S1179	14	
	7930	1	D21S11	32.2	
	4030	1	D7S820	12	
	2437	1	CSF1PO	10	
	2242	0.92	CSF1PO	13	
	7366	1	D3S1358	15	
	5431	0.99	TH01	7	
	5474	1	TH01	9.3	
	5783	1	D13S317	8	
	5070	0.88	D13S317	13	
	7050	1	D16S539	9	
	6729	0.95	D16S539	10	
	3124	1	D2S1338	20	
	2953	0.95	D2S1338	23	
	5159	1	D19S433	13	
	4838	0.94	D19S433	14	
	5025	1	vWA	15	
	4824	0.96	vWA	18	
	9334	1	TPOX	8	
	2773	1	D18S51	15	
	2544	0.92	D18S51	18	
	11526	1	AMEL	X	
	4750	1	D5S818	11	
	4642	0.98	D5S818	13	
	4614	1	FGA	24	
127C	16694	1	D8S1179	13	Minus A
	9526	1	D21S11	30	
	8792	0.92	D21S11	30.2	

	4524	1	D7S820	8	
	4071	0.9	D7S820	12	
	5861	1	CSF1PO	11	
	5263	0.9	CSF1PO	14	
	10859	1	D3S1358	15	
	10003	0.92	D3S1358	18	
	14978	1	TH01	6	
	14417	0.96	TH01	7	
	12804	1	D13S317	8	
	11740	0.92	D13S317	11	
	15608	1	D16S539	11	
	8230	1	D2S1338	17	
	7457	0.91	D2S1338	19	
	12181	1	D19S433	12	
	10672	0.88	D19S433	13	
	13431	1	vWA	16	
	13189	0.98	vWA	17	
	14681	1	TPOX	8	
	11128	1	D18S51	14	
	12370	1	AMEL	X	
	10933	1	D5S818	11	
	9846	0.9	D5S818	12	
	5731	1	FGA	21.2	
	5460	0.95	FGA	22	
144C	6504	1	D8S1179	11	Minus A
	5864	0.9	D8S1179	14	
	5418	0.99	D21S11	28	
	5476	1	D21S11	30	
	3034	1	D7S820	10	
	2751	0.91	D7S820	12	
	3445	1	CSF1PO	10	
	3332	0.97	CSF1PO	12	
	6057	1	D3S1358	16	
	5271	0.87	D3S1358	19	
	7567	0.98	TH01	6	
	7707	1	TH01	9.3	
	7892	0.95	D13S317	9	
	8316	1	D13S317	10	
	9071	1	D16S539	12	
	8749	0.96	D16S539	13	
	5068	1	D2S1338	19	
	4266	0.84	D2S1338	25	
	7075	1	D19S433	13	
	6436	0.91	D19S433	14	
	13922	1	vWA	15	
	6572	1	TPOX	8	

	6285	0.96	TPOX	9
	4224	1	D18S51	16
	4187	0.99	D18S51	18
	7300	0.99	AMEL	X
	7368	1	AMEL	Y
	6776	1	D5S818	11
	6137	0.91	D5S818	13
	4205	1	FGA	20
	3895	0.93	FGA	21
146C	13783	1	D8S1179	14 Minus A
	8866	1	D21S11	28
	7468	0.84	D21S11	32.2
	4027	1	D7S820	11
	3605	0.9	D7S820	12
	4459	1	CSF1PO	10
	4213	0.94	CSF1PO	12
	8207	1	D3S1358	15
	7868	0.96	D3S1358	17
	11557	1	TH01	6
	11261	0.97	TH01	9.3
	16134	1	D13S317	11
	14121	1	D16S539	11
	6438	1	D2S1338	19
	5761	0.89	D2S1338	23
	10583	1	D19S433	13
	9753	0.92	D19S433	14
	10462	1	vWA	15
	9549	0.91	vWA	18
	8897	1	TPOX	10
	8503	0.96	TPOX	11
	11516	1	D18S51	14
	13360	1	AMEL	X
	9952	1	D5S818	11
	9072	0.91	D5S818	12
	4951	1	FGA	21
	4252	0.86	FGA	24
2145C	7852	1	D8S1179	12 Minus A
	7528	0.96	D8S1179	13
	5930	0.97	D21S11	30
	6135	1	D21S11	31.2
	4008	1	D7S820	9
	3758	0.94	D7S820	10
	5269	1	CSF1PO	10
	4959	0.94	CSF1PO	11
	9537	1	D3S1358	14

	8927	0.94	D3S1358	15
	8803	0.97	TH01	6
	9051	1	TH01	8
	8924	1	D13S317	8
	7971	0.89	D13S317	12
	10145	1	D16S539	9
	9196	0.91	D16S539	12
	5483	1	D2S1338	17
	4136	0.75	D2S1338	25
	7184	1	D19S433	13
	5892	0.82	D19S433	14
	12428	1	vWA	17
	10640	0.86	vWA	18
	8421	1	TPOX	8
	8224	0.98	TPOX	11
	13532	1	D18S51	14
	13846	1	AMEL	X
	7158	1	D5S818	11
	7069	0.99	D5S818	12
	4860	1	FGA	22
	4524	0.93	FGA	23
220C	12309	1	D8S1179	13 Minus A, Imbalance
	11497	0.93	D8S1179	14
	10994	1	D21S11	30
	10271	0.93	D21S11	31.2
	6255	1	D7S820	8
	5896	0.94	D7S820	10
	6923	1	CSF1PO	9
	6509	0.94	CSF1PO	12
	11158	1	D3S1358	14
	10072	0.9	D3S1358	17
	13737	1	TH01	6
	13592	0.99	TH01	9.3
	13246	1	D13S317	11
	11410	0.86	D13S317	12
	14748	1	D16S539	9
	14232	0.97	D16S539	12
	8527	1	D2S1338	21
	8240	0.97	D2S1338	24
	3630	0.34	D19S433	14
	10685	1	D19S433	15
	12523	1	vWA	17
	12172	0.97	vWA	19
	14677	1	TPOX	8
	9217	1	D18S51	12
	7662	0.83	D18S51	18

	13162	1	AMEL	X	
	11636	0.99	D5S818	11	
	11789	1	D5S818	12	
	7686	1	FGA	21	
	6797	0.88	FGA	24	
247C	9459	1	D8S1179	10	Minus A
	9277	0.98	D8S1179	12	
	7514	1	D21S11	31	
	7326	0.97	D21S11	32.2	
	7651	1	D7S820	11	
	4164	1	CSF1PO	12	
	3762	0.9	CSF1PO	14	
	8986	1	D3S1358	17	
	8229	0.92	D3S1358	18	
	11694	1	TH01	6	
	11562	0.99	TH01	8	
	11817	1	D13S317	10	
	11240	0.95	D13S317	11	
	12514	1	D16S539	11	
	11345	0.91	D16S539	13	
	7274	1	D2S1338	17	
	6375	0.88	D2S1338	19	
	9959	1	D19S433	13	
	9235	0.93	D19S433	14	
	13995	1	vWA	16	
	9219	1	TPOX	8	
	8812	0.96	TPOX	9	
	6692	1	D18S51	11	
	4915	0.73	D18S51	19	
	12766	1	AMEL	X	
	10499	1	D5S818	9	
	9638	0.92	D5S818	11	
	5881	1	FGA	20	
	4624	0.79	FGA	25	
2518C	11452	1	D8S1179	10	Minus A
	10555	0.92	D8S1179	11	
	8246	1	D21S11	29	
	7996	0.97	D21S11	31.2	
	9378	1	D7S820	10	
	6050	1	CSF1PO	11	
	5787	0.96	CSF1PO	13	
	14450	1	D3S1358	18	
	12582	1	TH01	6	
	12197	0.97	TH01	9.3	
	13195	1	D13S317	8	

	12291	0.93	D13S317	11	
	12857	1	D16S539	11	
	7632	1	D2S1338	22	
	7193	0.94	D2S1338	24	
	10732	1	D19S433	13	
	10112	0.94	D19S433	15	
	12794	1	vWA	17	
	12063	0.94	vWA	18	
	9502	1	TPOX	8	
	9423	0.99	TPOX	11	
	8768	1	D18S51	15	
	7838	0.89	D18S51	16	
	12960	1	AMEL	X	
	12991	1	D5S818	11	
	6368	1	FGA	23	
	5868	0.92	FGA	26	
297C	14243	1	D8S1179	13	Minus A, Imbalance
	14178	1	D8S1179	14	
	13308	1	D21S11	31.2	
	12406	0.93	D21S11	32.2	
	10476	1	D7S820	11	
	12466	1	CSF1PO	10	
	13775	1	D3S1358	14	
	10487	0.76	D3S1358	19	
	14178	0.94	TH01	7	
	15015	1	TH01	8.3	
	14489	0.99	D13S317	8	
	14650	1	D13S317	11	
	14873	1	D16S539	9	
	14842	1	D16S539	13	
	9896	1	D2S1338	17	
	7957	0.8	D2S1338	24	
	13653	1	D19S433	13	
	4998	0.37	D19S433	14	
	13839	0.97	vWA	18	
	14217	1	vWA	19	
	14376	1	TPOX	8	
	13084	0.91	TPOX	11	
	7895	1	D18S51	14	
	6171	0.78	D18S51	17	
	10829	0.95	AMEL	X	
	11375	1	AMEL	Y	
	12889	1	D5S818	11	
	12270	0.95	D5S818	12	
	7850	1	FGA	20	
	7213	0.92	FGA	21	

3104C	6457	1	D8S1179	13	Minus A
	5885	0.91	D8S1179	14	
	5246	1	D21S11	28	
	5051	0.96	D21S11	30	
	5180	1	D7S820	10	
	6771	1	CSF1PO	10	
	6201	1	D3S1358	17	
	5587	0.9	D3S1358	18	
	13499	1	TH01	9.3	
	7808	1	D13S317	8	
	7252	0.93	D13S317	11	
	8405	1	D16S539	12	
	7765	0.92	D16S539	13	
	4033	1	D2S1338	24	
	3505	0.87	D2S1338	25	
	7075	1	D19S433	13	
	6808	0.96	D19S433	15	
	8381	1	vWA	14	
	7402	0.88	vWA	19	
	6181	1	TPOX	11	
	5770	0.93	TPOX	12	
	4911	1	D18S51	13	
	4207	0.86	D18S51	17	
	7496	0.93	AMEL	X	
	8051	1	AMEL	Y	
	11369	1	D5S818	13	
	3482	1	FGA	23	
	3241	0.93	FGA	25	
311C	14720	1	D8S1179	12	Minus A
	8436	1	D21S11	28	
	7969	0.94	D21S11	29	
	3262	1	D7S820	10	
	2958	0.91	D7S820	13	
	4800	1	CSF1PO	10	
	4363	0.91	CSF1PO	11	
	9800	1	D3S1358	11	
	8689	0.89	D3S1358	15	
	13648	1	TH01	6	
	12245	0.9	TH01	9.3	
	9991	1	D13S317	8	
	8846	0.89	D13S317	11	
	10947	1	D16S539	13	
	9994	0.91	D16S539	15	
	5594	1	D2S1338	19	
	4532	0.81	D2S1338	26	

	9933	0.79	D19S433	12	
	8911	0.71	D19S433	14	
	12189	1	vWA	15	
	11044	0.91	vWA	17	
	10264	1	TPOX	8	
	9479	0.92	TPOX	11	
	9959	1	D18S51	15	
	2874	1	AMEL	X	
	8120	1	D5S818	12	
	7395	0.91	D5S818	13	
	4443	1	FGA	20	
	3702	0.83	FGA	24	
312AC	12387	1	D8S1179	10	Minus A
	10295	0.83	D8S1179	14	
	10774	1	D21S11	30	
	9863	0.92	D21S11	31	
	3604	1	D7S820	10	
	3579	0.99	D7S820	12	
	10057	1	CSF1PO	12	
	9448	1	D3S1358	14	
	8816	0.93	D3S1358	16	
	14456	1	TH01	6	
	14458	1	TH01	9	
	11862	1	D13S317	8	
	10975	0.93	D13S317	9	
	18023	1	D16S539	11	
	7780	1	D2S1338	18	
	7039	0.9	D2S1338	22	
	9444	1	D19S433	15	
	8863	0.94	D19S433	16.2	
	13448	1	vWA	16	
	12055	0.9	vWA	18	
	12092	1	TPOX	8	
	11232	0.93	TPOX	11	
	5847	1	D18S51	12	
	5530	0.95	D18S51	13	
	10120	0.86	AMEL	X	
	11764	1	AMEL	Y	
	9175	1	D5S818	12	
	8327	0.91	D5S818	13	
	4597	1	FGA	20	
	4201	0.91	FGA	21	
312BC	15645	1	D8S1179	12	Minus A, Partial Profile, Imba
	14000	1	D21S11	28	
	13431	0.96	D21S11	31.2	

7245	1	D7S820	9	
6635	0.92	D7S820	12	
8501	1	CSF1PO	11	
8011	0.94	CSF1PO	12	
18152	1	D3S1358	14	
14678	1	TH01	6	
14552	0.99	TH01	8	
14785	1	D13S317	9	
14814	1	D13S317	11	
18198	1	D16S539	12	
10414	1	D2S1338	23	
9603	0.92	D2S1338	25	
14689	1	vWA	14	
13558	0.92	vWA	16	
14089	1	TPOX	9	
11189	0.79	TPOX	11	
10607	1	D18S51	14	
9266	0.87	D18S51	18	
4415	1	AMEL	X	
14179	1	D5S818	11	
9624	0.68	D5S818	12	
9416	1	FGA	19	
8760	0.93	FGA	21	
333C	11745	1	D8S1179	10 Minus A
	11330	0.96	D8S1179	12
	10669	1	D21S11	27
	10158	0.95	D21S11	29
	9167	1	D7S820	12
	6569	1	CSF1PO	12
	6191	0.94	CSF1PO	13
	12364	1	D3S1358	15
	11755	0.95	D3S1358	17
	19853	1	TH01	9.3
	14633	1	D13S317	8
	13201	0.9	D13S317	13
	15478	1	D16S539	8
	14125	0.91	D16S539	12
	9806	1	D2S1338	17
	7884	0.8	D2S1338	25
	10934	0.78	D19S433	14
	10018	0.71	D19S433	16.2
	11131	0.81	vWA	14
	13822	1	vWA	17
	16187	1	TPOX	8
	8688	1	D18S51	12
	7335	0.84	D18S51	16

	5691	1	AMEL	X
	11522	1	D5S818	12
	11051	0.96	D5S818	13
	6270	1	FGA	23
	5853	0.93	FGA	26
338C	14379	1	D8S1179	13 Minus A
	7309	1	D21S11	29
	6758	0.92	D21S11	31
	3980	1	D7S820	9
	3961	1	D7S820	10
	4295	1	CSF1PO	11
	4072	0.95	CSF1PO	13
	11638	1	D3S1358	16
	9527	0.98	TH01	7
	9760	1	TH01	9.3
	10165	1	D13S317	12
	9277	0.91	D13S317	13
	11895	1	D16S539	11
	11011	0.93	D16S539	12
	5525	1	D2S1338	24
	5016	0.91	D2S1338	25
	9091	1	D19S433	14
	8316	0.91	D19S433	15
	14810	1	vWA	16
	8737	1	TPOX	8
	8178	0.94	TPOX	11
	6416	1	D18S51	12
	5108	0.8	D18S51	17
	14286	1	AMEL	X
	13450	1	D5S818	12
	4989	1	FGA	20
	4577	0.92	FGA	22
3701C	6297	1	D8S1179	11 Imbalance
	5647	0.9	D8S1179	14
	5179	1	D21S11	28
	4922	0.95	D21S11	29
	3662	1	D7S820	8
	3617	0.99	D7S820	10
	4540	1	CSF1PO	11
	4333	0.95	CSF1PO	12
	7446	1	D3S1358	17
	6970	0.94	D3S1358	18
	7179	1	TH01	6
	6757	0.94	TH01	9.3
	11731	1	D13S317	11

	8307	0.99	D16S539	11	
	8367	1	D16S539	13	
	5557	1	D2S1338	24	
	5160	0.93	D2S1338	25	
	14057	1	D19S433	12	
	8201	1	vWA	14	
	7847	0.96	vWA	16	
	5884	0.96	TPOX	8	
	6125	1	TPOX	11	
	7256	1	D18S51	15	
	6473	0.89	D18S51	16	
	6149	1	AMEL	X	
	2747	0.45	AMEL	Y	
	6563	0.96	D5S818	11	
	6829	1	D5S818	12	
	5009	1	FGA	19	
	4596	0.92	FGA	25	
3805C	9872	1	D8S1179	12	Minus A, Allelic Dropout, Imb
	8970	0.91	D8S1179	13	
	7613	1	D21S11	28	
	7190	0.94	D21S11	31	
	4313	1	D7S820	9	
	4252	0.99	D7S820	11	
	5727	1	CSF1PO	11	
	5194	0.91	CSF1PO	15	
	9636	1	D3S1358	14	
	8716	0.9	D3S1358	16	
	17313	1	TH01	9.3	
	11019	1	D13S317	12	
	9791	0.89	D13S317	13	
	13505	1	D16S539	10	
	13325	0.99	D16S539	12	
	6849	1	D2S1338	22	
	6409	0.94	D2S1338	24	
	13853	1	D19S433	12	
	9014	0.65	D19S433	14	
	12421	1	vWA	17	
	11353	0.91	vWA	18	
	9800	1	TPOX	8	
	9559	0.98	TPOX	9	
	8914	1	D18S51	14	
	7922	0.89	D18S51	15	
	10552	1	AMEL	X	
	10655	1	D5S818	11	
	5871	1	FGA	22	
	5273	0.9	FGA	23	

399C	13316	1	D8S1179	11 Minus A
	11910	0.89	D8S1179	14
	12168	1	D21S11	28
	10125	0.83	D21S11	33.2
	9278	1	D7S820	10
	10636	1	CSF1PO	12
	14872	1	D3S1358	16
	14400	1	TH01	7
	14152	0.98	TH01	8
	13606	1	D13S317	12
	11847	0.87	D13S317	14
	14808	1	D16S539	11
	14432	0.97	D16S539	12
	9009	1	D2S1338	18
	8680	0.96	D2S1338	19
	12487	0.9	D19S433	14
	11175	0.81	D19S433	15.2
	13488	1	vWA	17
	12417	0.92	vWA	18
	11095	1	TPOX	8
	10438	0.94	TPOX	11
	12737	1	D18S51	16
	8714	1	AMEL	X
	14181	1	D5S818	11
	6629	1	FGA	19
	5356	0.81	FGA	24
417C	14129	1	D8S1179	13 Minus A
	7402	1	D21S11	29
	7166	0.97	D21S11	30
	4402	1	D7S820	8
	4176	0.95	D7S820	10
	5313	1	CSF1PO	10
	4911	0.92	CSF1PO	12
	15611	1	D3S1358	15
	11751	1	TH01	6
	11571	0.98	TH01	9
	11953	1	D13S317	8
	11885	0.99	D13S317	11
	13685	1	D16S539	11
	12507	0.91	D16S539	12
	8215	1	D2S1338	17
	7841	0.95	D2S1338	19
	8434	1	D19S433	14
	7990	0.95	D19S433	15.2
	11374	1	vWA	14

	9636	0.85	vWA	19	
	9618	1	TPOX	8	
	9309	0.97	TPOX	11	
	7984	1	D18S51	14	
	7064	0.88	D18S51	15	
	10222	1	AMEL	X	
	10142	0.99	AMEL	Y	
	9649	1	D5S818	12	
	8799	0.91	D5S818	13	
	6241	1	FGA	22	
	5782	0.93	FGA	23	
420C	10885	1	D8S1179	13	
	10322	0.95	D8S1179	14	
	8859	1	D21S11	31.2	
	8159	0.92	D21S11	33.2	
	6090	1	D7S820	9	
	5613	0.92	D7S820	12	
	6748	1	CSF1PO	12	
	6310	0.94	CSF1PO	14	
	12269	0.87	D3S1358	14	
	14048	1	D3S1358	16	
	13942	1	TH01	6	
	13702	0.98	TH01	8	
	19526	1	D13S317	12	
	14275	1	D16S539	11	
	14059	0.98	D16S539	13	
	14558	1	D2S1338	19	
	14485	1	D19S433	15	
	14550	1	vWA	19	
	14207	0.98	vWA	20	
	13926	1	TPOX	8	
	16233	1	D18S51	16	
	11096	0.94	AMEL	X	
	11766	1	AMEL	Y	
	11557	1	D5S818	11	
	7411	1	FGA	21	
	6486	0.88	FGA	25	
4375C	10665	1	D8S1179	11	Minus A
	9643	0.9	D8S1179	14	
	10011	1	D21S11	28	
	9176	0.92	D21S11	29	
	4048	1	D7S820	7	
	3345	0.83	D7S820	12	
	4954	1	CSF1PO	11	
	4640	0.94	CSF1PO	12	

10313	1	D3S1358	15	
9175	0.89	D3S1358	16	
12529	1	TH01	7	
11618	0.93	TH01	9.3	
13291	1	D13S317	8	
11969	0.9	D13S317	12	
11753	0.88	D16S539	12	
13316	1	D16S539	13	
7263	1	D2S1338	17	
6092	0.84	D2S1338	23	
12405	1	D19S433	13	
12415	1	D19S433	13.2	
12902	1	vWA	17	
11613	0.9	vWA	18	
9074	1	TPOX	9	
9063	1	TPOX	11	
5470	1	D18S51	12	
4745	0.87	D18S51	20	
13114	1	AMEL	X	
12206	1	D5S818	11	
9228	1	FGA	23	

444C	8352	1	D8S1179	12	Minus A
	8129	0.97	D8S1179	13	
	7678	1	D21S11	29	
	7500	0.98	D21S11	30	
	4161	1	D7S820	8	
	3704	0.89	D7S820	11	
	4616	1	CSF1PO	10	
	4291	0.93	CSF1PO	11	
	7314	1	D3S1358	15	
	6806	0.93	D3S1358	16	
	14744	1	TH01	9.3	
	10136	1	D13S317	9	
	8828	0.87	D13S317	12	
	10606	1	D16S539	11	
	9966	0.94	D16S539	13	
	5861	1	D2S1338	18	
	4632	0.79	D2S1338	26	
	8067	1	D19S433	13	
	7472	0.93	D19S433	14	
	12281	1	vWA	18	
	7620	1	TPOX	8	
	7134	0.94	TPOX	11	
	5619	1	D18S51	12	
	5056	0.9	D18S51	16	
	11336	1	AMEL	X	

	8619	1	D5S818	12
	7821	0.91	D5S818	13
	4969	1	FGA	23
	4507	0.91	FGA	24
550C	11531	1	D8S1179	13 Minus A
	10510	0.91	D8S1179	14
	10068	1	D21S11	28
	9484	0.94	D21S11	30
	6229	1	D7S820	7
	5859	0.94	D7S820	10
	6934	1	CSF1PO	11
	6338	0.91	CSF1PO	13
	12152	1	D3S1358	15
	11592	0.95	D3S1358	17
	12122	0.85	TH01	6
	14316	1	TH01	7
	14351	1	D13S317	10
	12169	0.85	D13S317	12
	14427	1	D16S539	11
	14411	1	D16S539	12
	10007	1	D2S1338	19
	9231	0.92	D2S1338	21
	11465	1	D19S433	15.2
	10174	0.89	D19S433	16.2
	14252	1	vWA	14
	13665	0.96	vWA	18
	12871	1	TPOX	9
	12271	0.95	TPOX	11
	9900	1	D18S51	14
	9361	0.95	D18S51	16
	11884	1	AMEL	X
	11860	1	AMEL	Y
	15027	1	D5S818	11
	9125	1	FGA	19
	8098	0.89	FGA	20
565C	14636	1	D8S1179	10 Minus A, Allelic Drop-In, Imba
	14222	0.97	D8S1179	12
	20162	1	D21S11	29
	7430	0.99	D7S820	11
	7512	1	D7S820	12
	9046	1	CSF1PO	9
	8204	0.91	CSF1PO	12
	14363	1	D3S1358	14
	14055	0.98	D3S1358	17
	19710	1	TH01	9.3

	21103	1	D13S317	12
	19501	1	D16S539	11
	14756	0.76	D16S539	13
	13589	1	D2S1338	17
	11393	0.84	D2S1338	22
	15003	1	D19S433	13
	16280	1	vWA	14
	14816	0.91	vWA	20
	14007	1	TPOX	8
	9050	1	D18S51	18
	7973	0.88	D18S51	21
	12175	1	AMEL	X
	7015	0.58	AMEL	Y
	11532	1	D5S818	11
	11010	0.95	D5S818	12
	12575	1	FGA	21
589C	15924	1	D8S1179	13 Minus A, Imbalance
	10145	1	D21S11	30
	9730	0.96	D21S11	31.2
	5026	1	D7S820	10
	4830	0.96	D7S820	12
	5975	1	CSF1PO	10
	5420	0.91	CSF1PO	13
	11462	1	D3S1358	14
	10735	0.94	D3S1358	16
	18355	1	TH01	9.3
	13555	1	D13S317	11
	12468	0.92	D13S317	13
	14620	1	D16S539	9
	14096	0.96	D16S539	11
	8901	1	D2S1338	17
	7061	0.79	D2S1338	24
	10692	1	D19S433	14.2
	2540	0.24	D19S433	16
	18482	1	vWA	16
	16086	1	TPOX	8
	14761	1	D18S51	12
	14899	1	AMEL	X
	13352	1	D5S818	12
	6865	1	FGA	21
	5542	0.81	FGA	26
6080C	7724	0.78	D8S1179	9 Minus A
	7070	0.71	D8S1179	13
	7737	1	D21S11	28
	7097	0.92	D21S11	30

	4485	1	D7S820	8
	6316	1	CSF1PO	12
	5726	0.75	D3S1358	15
	4969	0.65	D3S1358	17
	14425	1	TH01	9.3
	7954	1	D13S317	11
	7527	0.95	D13S317	12
	16717	1	D16S539	9
	5945	1	D2S1338	17
	4857	0.82	D2S1338	24
	9606	1	D19S433	13
	8942	0.93	D19S433	14
	8564	0.85	vWA	17
	8079	0.8	vWA	19
	6829	1	TPOX	9
	6126	0.9	TPOX	11
	3871	1	D18S51	14
	3443	0.89	D18S51	16
	12368	1	AMEL	X
	6757	1	D5S818	11
	6271	0.93	D5S818	13
	3031	1	FGA	20
	2475	0.82	FGA	23
6233C	13553	1	D8S1179	10 Minus A, Partial Profile
	11976	0.88	D8S1179	15
	11698	1	D21S11	27
	11063	0.95	D21S11	29
	4905	1	D7S820	9
	4481	0.91	D7S820	12
	8252	1	CSF1PO	12
	8009	0.97	CSF1PO	13
	10671	1	D3S1358	16
	9367	0.88	D3S1358	17
	11761	1	D13S317	10
	10776	0.92	D13S317	12
	20342	1	D16S539	11
	9074	1	D2S1338	19
	8375	0.92	D2S1338	20
	18817	1	D19S433	14
	14234	1	TPOX	8
	13946	0.98	TPOX	11
	8916	1	D18S51	12
	8135	0.91	D18S51	14
	11700	0.95	AMEL	X
	12278	1	AMEL	Y
	10129	1	D5S818	10

	9246	0.91	D5S818	11
	4601	1	FGA	20
	4088	0.89	FGA	22
651C	12808	1	D8S1179	10	Minus A, Allelic Dropout
	11174	0.87	D8S1179	15
	10448	1	D21S11	29
	8942	0.86	D21S11	32.2
	4159	1	D7S820	10
	3790	0.91	D7S820	12
	9078	1	CSF1PO	12
	10588	1	D3S1358	14
	9244	0.87	D3S1358	17
	13609	1	TH01	8
	13272	0.98	TH01	9
	10817	1	D13S317	12
	20359	1	D16S539	11
	6262	1	D2S1338	20
	5895	0.94	D2S1338	22
	11054	1	D19S433	13
	9650	0.87	D19S433	15.2
	14713	0.98	vWA	17
	17790	1	TPOX	8
	5166	1	D18S51	16
	3861	0.75	D18S51	22
	14383	1	AMEL	X
	11919	1	D5S818	11
	10793	0.91	D5S818	12
	9079	1	FGA	25
709C	14275	1	D8S1179	10	Minus A, Imbalance
	13905	0.97	D8S1179	13
	12926	1	D21S11	28
	2724	0.21	D21S11	32.2
	7278	1	D7S820	8
	7029	0.97	D7S820	11
	8002	1	CSF1PO	11
	7345	0.92	CSF1PO	12
	13674	1	D3S1358	17
	13196	0.97	D3S1358	18
	14805	1	TH01	6
	14538	0.98	TH01	7
	12537	1	D13S317	8
	14834	1	D16S539	8
	14419	0.97	D16S539	13
	11579	1	D2S1338	17
	9239	0.8	D2S1338	24

	12549	0.89	D19S433	14	
	14692	1	vWA	14	
	14236	0.97	vWA	17	
	12936	1	TPOX	8	
	10433	1	D18S51	13	
	9478	0.91	D18S51	16	
	8741	1	AMEL	X	
	9799	0.76	D5S818	10	
	12963	1	D5S818	11	
	9164	1	FGA	20	
	7635	0.83	FGA	24.2	
735C	7344	1	D8S1179	12	Minus A
	6761	0.92	D8S1179	13	
	5798	1	D21S11	29	
	5306	0.92	D21S11	32.2	
	6875	1	D7S820	10	
	8911	1	CSF1PO	11	
	15108	1	D3S1358	15	
	10369	1	TH01	8	
	10298	0.99	TH01	9.3	
	9960	1	D13S317	11	
	9420	0.95	D13S317	12	
	11712	1	D16S539	11	
	10773	0.92	D16S539	12	
	7058	1	D2S1338	19	
	6140	0.87	D2S1338	24	
	7805	1	D19S433	13	
	7170	0.92	D19S433	14	
	8988	1	vWA	17	
	8475	0.94	vWA	18	
	7934	1	TPOX	8	
	7543	0.95	TPOX	11	
	5516	1	D18S51	18	
	4972	0.9	D18S51	22	
	8976	1	AMEL	X	
	8936	1	AMEL	Y	
	7560	0.94	D5S818	11	
	8023	1	D5S818	13	
	4786	1	FGA	22.2	
	4719	0.99	FGA	24	
746C	10541	1	D8S1179	11	Minus A, Imbalance
	9360	0.89	D8S1179	13	
	8343	1	D21S11	30	
	8112	0.97	D21S11	31.2	
	5195	1	D7S820	8	

5178	1	D7S820	10	
6466	1	CSF1PO	11	
5945	0.92	CSF1PO	12	
11720	1	D3S1358	14	
11278	0.96	D3S1358	15	
12120	1	TH01	6	
13241	1	D13S317	9	
13226	1	D13S317	10	
14081	1	D16S539	9	
13342	0.95	D16S539	13	
8461	1	D2S1338	19	
7140	0.84	D2S1338	25	
9289	1	D19S433	14.2	
4028	0.43	D19S433	15	
12346	1	vWA	18	
10676	0.86	vWA	19	
14834	1	TPOX	8	
8070	1	D18S51	15	
7384	0.91	D18S51	18	
11817	1	AMEL	X	
11736	0.99	AMEL	Y	
11305	0.99	D5S818	11	
11422	1	D5S818	12	
6747	1	FGA	24	
6236	0.92	FGA	25	
7485C	3523	1	D8S1179	8 Minus A
	3097	0.88	D8S1179	13
	2707	1	D21S11	31.2
	2418	0.89	D21S11	32.2
	1582	1	D7S820	8
	1344	0.85	D7S820	12
	1622	0.95	CSF1PO	10
	1711	1	CSF1PO	12
	3013	1	D3S1358	15
	2947	0.98	D3S1358	17
	3126	1	TH01	6
	3017	0.97	TH01	9.3
	4147	1	D13S317	12
	3752	0.9	D13S317	13
	7787	1	D16S539	12
	2751	1	D2S1338	14
	1939	0.7	D2S1338	26
	3729	1	D19S433	12
	3413	0.92	D19S433	13
	3629	1	vWA	16
	3533	0.97	vWA	19

	2785	0.97	TPOX	8
	2876	1	TPOX	10
	2769	1	D18S51	13
	2566	0.93	D18S51	14
	3463	0.96	AMEL	X
	3615	1	AMEL	Y
	3467	1	D5S818	12
	3232	0.93	D5S818	13
	4045	1	FGA	24
7572C	6015	1	D8S1179	10 Minus A
	5482	0.91	D8S1179	14
	4891	1	D21S11	28
	4705	0.96	D21S11	30
	5741	1	D7S820	10
	3755	1	CSF1PO	10
	3581	0.95	CSF1PO	12
	6350	1	D3S1358	17
	5727	0.9	D3S1358	18
	6510	1	TH01	7
	6374	0.98	TH01	9.3
	11256	1	D13S317	11
	8820	1	D16S539	12
	8329	0.94	D16S539	13
	5272	1	D2S1338	17
	4443	0.84	D2S1338	24
	6999	1	D19S433	14
	6278	0.9	D19S433	15
	7263	1	vWA	15
	7000	0.96	vWA	16
	10732	1	TPOX	8
	6033	1	D18S51	10
	5272	0.87	D18S51	14
	11802	1	AMEL	X
	11520	1	D5S818	12
	4115	1	FGA	22
	3941	0.96	FGA	25
7758C	9050	0.83	D8S1179	10 Minus A
	7968	0.73	D8S1179	14
	8352	1	D21S11	28
	7820	0.94	D21S11	30
	2694	1	D7S820	9
	2692	1	D7S820	13
	4102	1	CSF1PO	10
	3884	0.95	CSF1PO	12
	9709	0.86	D3S1358	15

	9758	0.99	TH01	7	
	9850	1	TH01	9.3	
	7951	1	D13S317	11	
	7608	0.96	D13S317	14	
	13272	1	D16S539	9	
	12059	0.91	D16S539	12	
	7748	1	D2S1338	17	
	5892	0.76	D2S1338	24	
	9899	1	D19S433	14	
	9184	0.93	D19S433	16	
	10068	0.96	vWA	16	
	9259	0.88	vWA	19	
	10371	0.97	TPOX	8	
	4457	1	D18S51	15	
	3929	0.88	D18S51	17	
	10615	1	AMEL	X	
	7636	1	D5S818	11	
	7075	0.93	D5S818	12	
	3293	1	FGA	23	
	2994	0.91	FGA	24	
777C	9872	1	D8S1179	8	Minus A, Imbalance
	8779	0.89	D8S1179	15	
	8538	1	D21S11	29	
	7630	0.89	D21S11	32.2	
	3897	1	D7S820	10	
	3780	0.97	D7S820	13	
	10167	1	CSF1PO	10	
	10309	1	D3S1358	14	
	9462	0.92	D3S1358	15	
	12977	1	TH01	6	
	12478	0.96	TH01	9.3	
	12208	1	D13S317	8	
	11123	0.91	D13S317	11	
	13673	1	D16S539	9	
	12203	0.89	D16S539	12	
	6664	1	D2S1338	20	
	6115	0.92	D2S1338	23	
	10123	1	D19S433	13	
	2276	0.22	D19S433	15	
	11890	1	vWA	16	
	11172	0.94	vWA	18	
	10504	1	TPOX	9	
	9892	0.94	TPOX	11	
	7553	1	D18S51	13	
	7052	0.93	D18S51	14	
	13598	1	AMEL	X	

	13644	1	D5S818	9	
	5793	1	FGA	21	
	4816	0.83	FGA	25	
802C	14108	1	D8S1179	10	Minus A
	13166	0.93	D8S1179	11	
	12036	1	D21S11	28	
	10698	0.89	D21S11	31	
	4691	1	D7S820	10	
	4261	0.91	D7S820	12	
	10920	1	CSF1PO	12	
	12209	1	D3S1358	15	
	11088	0.91	D3S1358	16	
	14536	0.98	TH01	6	
	14908	1	TH01	9.3	
	14438	1	D13S317	10	
	13958	0.97	D13S317	11	
	15064	1	D16S539	10	
	15125	1	D16S539	11	
	8788	1	D2S1338	18	
	7567	0.86	D2S1338	23	
	13075	1	D19S433	14	
	12051	0.92	D19S433	15.2	
	13582	0.57	vWA	16	
	12118	1	TPOX	10	
	11486	0.95	TPOX	11	
	6139	1	D18S51	16	
	5589	0.91	D18S51	18	
	11658	1	AMEL	X	
	11510	0.99	AMEL	Y	
	12018	1	D5S818	9	
	11898	0.99	D5S818	11	
	6636	1	FGA	20	
	6043	0.91	FGA	22	
8339C	577	1	D21S11	30	Minus A, Partial Profile
	694	1	D3S1358	15	
	644	0.93	D3S1358	17	
	535	1	TH01	6	
	507	0.95	TH01	7	
	868	1	D13S317	11	
	556	1	D16S539	11	
	556	1	D16S539	12	
	1269	1	D19S433	13	
	572	1	vWA	16	
	1255	1	AMEL	X	
	501	1	D5S818	11	

	575	1	FGA	21	
9066C	12566	1	D8S1179	11	Minus A, Allelic Dropout
	11529	0.92	D8S1179	13	
	10045	1	D21S11	28	
	9661	0.96	D21S11	30	
	5359	1	D7S820	9	
	3727	0.7	D7S820	11	
	13109	1	CSF1PO	11	
	11614	1	D3S1358	17	
	10229	0.88	D3S1358	18	
	11288	0.79	TH01	7	
	14278	1	TH01	9.3	
	11567	0.86	D13S317	8	
	13410	1	D13S317	13	
	15615	1	D16S539	11	
	9321	1	D2S1338	20	
	8202	0.88	D2S1338	21	
	14754	1	D19S433	12	
	12446	0.84	D19S433	15	
	14209	1	vWA	18	
	13222	0.93	vWA	19	
	11937	1	TPOX	9	
	9868	1	D18S51	12	
	8280	0.84	D18S51	16	
	12828	1	AMEL	X	
	11727	1	D5S818	10	
	11204	0.96	D5S818	13	
	6659	1	FGA	23	
	5789	0.87	FGA	26	
931C	10718	1	D8S1179	11	Minus A
	9218	0.86	D8S1179	15	
	8383	1	D21S11	28	
	7608	0.91	D21S11	30	
	4856	1	D7S820	8	
	4669	0.96	D7S820	10	
	6161	1	CSF1PO	12	
	5398	0.88	CSF1PO	13	
	17575	1	D3S1358	15	
	13230	1	TH01	8	
	12637	0.96	TH01	9.3	
	12461	1	D13S317	9	
	11800	0.95	D13S317	11	
	14290	1	D16S539	8	
	13500	0.94	D16S539	12	
	8278	1	D2S1338	20	

	6982	0.84	D2S1338	24
	16184	1	D19S433	13
	11353	1	vWA	15
	10596	0.93	vWA	18
	9774	1	TPOX	8
	9821	1	TPOX	10
	7723	1	D18S51	14
	6397	0.83	D18S51	19
	12170	1	AMEL	X
	11241	0.92	AMEL	Y
	10022	0.98	D5S818	11
	10214	1	D5S818	13
	7336	1	FGA	19
	6363	0.87	FGA	24
940C	8501	1	D8S1179	14
	8100	0.95	D8S1179	15
	12394	1	D21S11	30
	4371	1	D7S820	8
	3929	0.9	D7S820	11
	5658	1	CSF1PO	11
	5270	0.93	CSF1PO	12
	10597	1	D3S1358	14
	10070	0.95	D3S1358	15
	10819	1	TH01	6
	10474	0.97	TH01	9
	10779	1	D13S317	10
	10344	0.96	D13S317	11
	19729	1	D16S539	9
	6966	1	D2S1338	19
	6224	0.89	D2S1338	22
	8156	1	D19S433	13
	8065	0.99	D19S433	13.2
	9756	1	vWA	16
	9417	0.97	vWA	19
	8562	1	TPOX	9
	8337	0.97	TPOX	11
	7209	1	D18S51	14
	6691	0.93	D18S51	17
	14707	1	AMEL	X
	8502	1	D5S818	12
	8046	0.95	D5S818	13
	11338	1	FGA	22
9439C	10447	1	D8S1179	14 Minus A
	9765	0.93	D8S1179	15
	14512	1	D21S11	30

4822	1	D7S820	8	
3484	0.72	D7S820	11	
6062	1	CSF1PO	10	
5496	0.91	CSF1PO	12	
14784	1	D3S1358	16	
11587	0.99	TH01	7	
11690	1	TH01	9.3	
13754	1	D13S317	11	
13384	0.97	D13S317	12	
14204	1	D16S539	11	
7769	1	D2S1338	19	
7577	0.98	D2S1338	22	
11008	1	D19S433	15	
10137	0.92	D19S433	17.2	
13532	1	vWA	14	
12562	0.93	vWA	18	
10218	1	TPOX	8	
9728	0.95	TPOX	9	
8768	1	D18S51	12	
7635	0.87	D18S51	16	
11948	1	AMEL	X	
11990	1	AMEL	Y	
11622	1	D5S818	12	
11178	0.96	D5S818	13	
7050	1	FGA	21	
6288	0.89	FGA	23	

9899C	14683	1	D8S1179	9 Minus A, Imbalance
	14076	0.96	D8S1179	15
	21072	1	D21S11	28
	5986	1	D7S820	11
	2061	0.34	D7S820	12
	14086	1	CSF1PO	12
	17880	1	D3S1358	18
	21526	1	TH01	9.3
	14264	1	D13S317	12
	13842	0.97	D13S317	13
	14649	1	D16S539	10
	14204	0.97	D16S539	12
	9165	1	D2S1338	17
	7511	0.82	D2S1338	22
	13528	0.92	D19S433	12
	12429	0.84	D19S433	13.2
	12155	0.72	vWA	17
	16802	1	vWA	18
	19493	1	TPOX	11
	7983	1	D18S51	19

6948	0.87	D18S51	20	
4654	1	AMEL	X	
12567	1	D5S818	9	
11188	0.89	D5S818	11	
6933	1	FGA	20	
5837	0.84	FGA	24	
CaseyC	8644	1	D8S1179	10 Imbalance
8408	0.97	D8S1179	12	
4203	1	D21S11	28	
3854	0.92	D21S11	31.2	
2021	1	D7S820	8	
1863	0.92	D7S820	11	
2004	1	CSF1PO	10	
1886	0.94	CSF1PO	11	
18032	1	D3S1358	14	
6563	0.99	TH01	6	
6655	1	TH01	8	
6143	1	D13S317	9	
5687	0.93	D13S317	11	
4892	1	D16S539	11	
4712	0.96	D16S539	12	
2010	1	D2S1338	20	
1899	0.94	D2S1338	25	
3596	0.53	D19S433	14	
6756	1	D19S433	16	
13707	1	vWA	18	
3977	1	TPOX	9	
3735	0.94	TPOX	11	
3486	1	D18S51	10	
3122	0.9	D18S51	14	
10755	1	AMEL	X	
8992	1	D5S818	12	
8130	0.9	D5S818	13	
3915	1	FGA	20	
3753	0.96	FGA	21	
ChristiC	15178	1	D8S1179	14 Imbalance
6881	1	D21S11	28	
6113	0.89	D21S11	30	
4502	1	D7S820	8	
3870	0.86	D7S820	12	
4274	1	CSF1PO	10	
3916	0.92	CSF1PO	11	
12290	0.97	D3S1358	14	
12624	1	D3S1358	16	
14461	1	TH01	6	

15818	1	D13S317	11
9486	1	D16S539	11
9140	0.96	D16S539	12
4697	1	D2S1338	23
3821	0.81	D2S1338	24
10621	1	D19S433	15
2550	0.24	D19S433	16
11642	1	vWA	14
10656	0.92	vWA	18
6371	0.93	TPOX	8
6870	1	TPOX	9
13613	1	D18S51	12
14205	1	AMEL	X
11229	1	D5S818	11
10670	0.95	D5S818	12
6492	1	FGA	20
6285	0.97	FGA	23
JDWC	6252	1	D8S1179	10
5383	0.86	D8S1179	14
2678	1	D21S11	30
2607	0.97	D21S11	31
1303	1	D7S820	10
1286	0.99	D7S820	12
2523	1	CSF1PO	12
8033	1	D3S1358	14
7192	0.9	D3S1358	16
5048	1	TH01	6
4129	0.82	TH01	9
5016	1	D13S317	8
4598	0.92	D13S317	9
7106	1	D16S539	11
1904	1	D2S1338	18
1582	0.83	D2S1338	22
4900	1	D19S433	15
4826	0.98	D19S433	16.2
5481	1	vWA	16
5024	0.92	vWA	18
3048	1	TPOX	8
2787	0.91	TPOX	11
2544	1	D18S51	12
2274	0.89	D18S51	13
6513	1	AMEL	X
6395	0.98	AMEL	Y
6262	1	D5S818	12
4817	0.77	D5S818	13
3015	1	FGA	20

	2625	0.87	FGA	21	
LouieC	5032	1	D8S1179	12	
	4253	0.85	D8S1179	13	
	5014	1	D21S11	29	
	1246	0.99	D7S820	10	
	1261	1	D7S820	12	
	2577	1	CSF1PO	10	
	5839	1	D3S1358	15	
	5557	0.95	D3S1358	18	
	7535	1	TH01	9.3	
	6914	1	D13S317	12	
	6035	1	D16S539	12	
	1423	1	D2S1338	23	
	1227	0.86	D2S1338	24	
	9550	1	D19S433	14	
	4933	1	vWA	15	
	4550	0.92	vWA	18	
	3009	0.96	TPOX	7	
	3124	1	TPOX	8	
	2097	1	D18S51	12	
	1934	0.92	D18S51	14	
	10050	1	AMEL	X	
	7568	1	D5S818	12	
	2323	1	FGA	22	
	1997	0.86	FGA	23	
HALFWAY 008H	7075	1	D8S1179	14	Minus A, Imbalance
	6499	0.92	D8S1179	15	
	6533	1	D21S11	30	
	5883	0.9	D21S11	34.2	
	3842	1	D7S820	12	
	3419	0.89	D7S820	13	
	4493	1	CSF1PO	10	
	4249	0.95	CSF1PO	12	
	8775	1	D3S1358	15	
	8324	0.95	D3S1358	18	
	11090	1	TH01	6	
	10543	0.95	TH01	9.3	
	11443	1	D13S317	8	
	10115	0.88	D13S317	12	
	19416	1	D16S539	12	
	6351	1	D2S1338	20	
	5707	0.9	D2S1338	24	
	8858	1	D19S433	13	
	7923	0.89	D19S433	14	

	14502	1	vWA	17
	14333	1	TPOX	8
	6895	1	D18S51	12
	4651	0.67	D18S51	22
	9723	0.96	AMEL	X
	10107	1	AMEL	Y
	13541	1	D5S818	11
	6104	1	FGA	19
	5745	0.94	FGA	20
062H	12990	1	D8S1179	14 Minus A, Imbalance
	5666	1	D21S11	29
	5372	0.95	D21S11	31.2
	2680	1	D7S820	10
	2428	0.91	D7S820	12
	3772	1	CSF1PO	11
	3472	0.92	CSF1PO	12
	7517	1	D3S1358	14
	4212	0.56	D3S1358	15
	10135	1	TH01	6
	9628	0.95	TH01	9.3
	13761	1	D13S317	11
	14856	1	D16S539	11
	4997	1	D2S1338	18
	4437	0.89	D2S1338	19
	10895	1	D19S433	15
	8631	1	vWA	16
	7922	0.92	vWA	17
	7735	1	TPOX	8
	7176	0.93	TPOX	10
	3901	1	D18S51	16
	3259	0.84	D18S51	20
	10126	1	AMEL	X
	10144	1	AMEL	Y
	12152	1	D5S818	12
	3535	1	FGA	23
	3265	0.92	FGA	24
088H	8826	1	D8S1179	13 Minus A
	7963	0.9	D8S1179	14
	13902	1	D21S11	32.2
	7263	1	D7S820	12
	4368	1	CSF1PO	10
	4072	0.93	CSF1PO	13
	13869	1	D3S1358	15
	3347	0.32	TH01	6.3
	10530	1	TH01	7

	10482	1	TH01	9.3	
	11055	1	D13S317	8	
	9610	0.87	D13S317	13	
	13481	1	D16S539	9	
	12644	0.94	D16S539	10	
	6029	1	D2S1338	20	
	5692	0.94	D2S1338	23	
	9701	1	D19S433	13	
	8753	0.9	D19S433	14	
	9538	1	vWA	15	
	8908	0.93	vWA	18	
	14837	1	TPOX	8	
	5290	1	D18S51	15	
	4521	0.85	D18S51	18	
	11956	1	AMEL	X	
	8557	1	D5S818	11	
	8350	0.98	D5S818	13	
	8314	1	FGA	24	
127H	17673	1	D8S1179	13	Minus A
	9707	1	D21S11	30	
	9320	0.96	D21S11	30.2	
	4870	1	D7S820	8	
	4231	0.87	D7S820	12	
	5980	1	CSF1PO	11	
	5542	0.93	CSF1PO	14	
	12525	1	D3S1358	15	
	11241	0.9	D3S1358	18	
	14990	1	TH01	6	
	12997	0.87	TH01	7	
	13873	1	D13S317	8	
	12774	0.92	D13S317	11	
	18142	1	D16S539	11	
	8657	1	D2S1338	17	
	8119	0.94	D2S1338	19	
	12821	0.9	D19S433	12	
	13225	1	vWA	16	
	10823	0.82	vWA	17	
	20855	1	TPOX	8	
	11813	1	D18S51	14	
	5750	1	AMEL	X	
	11466	1	D5S818	11	
	11128	0.97	D5S818	12	
	6402	1	FGA	21.2	
	6377	1	FGA	22	
144H	10578	1	D8S1179	11	Minus A

	10024	0.95	D8S1179	14	
	9630	0.99	D21S11	28	
	9733	1	D21S11	30	
	4748	1	D7S820	10	
	4668	0.98	D7S820	12	
	5705	0.99	CSF1PO	10	
	5760	1	CSF1PO	12	
	9572	1	D3S1358	16	
	8157	0.85	D3S1358	19	
	3219	0.25	TH01	5.3	
	12709	0.97	TH01	6	
	13086	1	TH01	9.3	
	13661	0.99	D13S317	9	
	13810	1	D13S317	10	
	14368	1	D16S539	12	
	14017	0.98	D16S539	13	
	7800	1	D2S1338	19	
	6864	0.88	D2S1338	25	
	11922	1	D19S433	13	
	10673	0.9	D19S433	14	
	14958	1	vWA	15	
	10589	1	TPOX	8	
	10180	0.96	TPOX	9	
	6864	1	D18S51	16	
	6326	0.92	D18S51	18	
	11971	1	AMEL	X	
	11211	0.94	AMEL	Y	
	11253	1	D5S818	11	
	10115	0.9	D5S818	13	
	6817	1	FGA	20	
	6303	0.92	FGA	21	
146H	13451	1	D8S1179	14	Minus A
	7063	1	D21S11	28	
	6209	0.88	D21S11	32.2	
	3344	1	D7S820	11	
	3199	0.96	D7S820	12	
	4097	1	CSF1PO	10	
	3623	0.88	CSF1PO	12	
	5886	1	D3S1358	15	
	5666	0.96	D3S1358	17	
	2424	0.29	TH01	5.3	
	8408	1	TH01	6	
	8449	1	TH01	9.3	
	14459	1	D13S317	11	
	17577	1	D16S539	11	
	5293	1	D2S1338	19	

	5044	0.95	D2S1338	23	
	8051	1	D19S433	13	
	7245	0.9	D19S433	14	
	8292	1	vWA	15	
	7611	0.92	vWA	18	
	7371	1	TPOX	10	
	7311	0.99	TPOX	11	
	10595	1	D18S51	14	
	13111	1	AMEL	X	
	7273	1	D5S818	11	
	6503	0.89	D5S818	12	
	4062	1	FGA	21	
	3621	0.89	FGA	24	
220H	15135	1	D8S1179	13	Minus A
	14128	0.93	D8S1179	14	
	14173	0.95	D21S11	30	
	14868	1	D21S11	31.2	
	8602	1	D7S820	8	
	8202	0.95	D7S820	10	
	9497	1	CSF1PO	9	
	8855	0.93	CSF1PO	12	
	14500	1	D3S1358	14	
	13857	0.96	D3S1358	17	
	6891	0.37	TH01	5.3	
	17851	0.96	TH01	6	
	18538	1	TH01	9.3	
	19891	1	D13S317	11	
	16391	0.82	D13S317	12	
	16998	1	D16S539	9	
	14708	0.87	D16S539	12	
	11616	1	D2S1338	21	
	10707	0.92	D2S1338	24	
	14429	0.98	D19S433	15	
	15287	1	vWA	17	
	14379	0.94	vWA	19	
	17100	1	TPOX	8	
	12595	1	D18S51	12	
	9236	0.73	D18S51	18	
	4309	1	AMEL	X	
	11398	0.8	D5S818	11	
	14306	1	D5S818	12	
	9766	1	FGA	21	
	8506	0.87	FGA	24	
247H	10626	1	D8S1179	10	Minus A
	10554	0.99	D8S1179	12	

	9447	1	D21S11	31
	9227	0.98	D21S11	32.2
	9755	1	D7S820	11
	5376	1	CSF1PO	12
	4959	0.92	CSF1PO	14
	9506	1	D3S1358	17
	8473	0.89	D3S1358	18
	3059	0.24	TH01	5.3
	12973	1	TH01	6
	3103	0.24	TH01	7.3
	12930	1	TH01	8
	13294	1	D13S317	10
	12718	0.96	D13S317	11
	14023	1	D16S539	11
	13657	0.97	D16S539	13
	8424	1	D2S1338	17
	7925	0.94	D2S1338	19
	11593	1	D19S433	13
	10451	0.9	D19S433	14
	18406	1	vWA	16
	11111	1	TPOX	8
	10637	0.96	TPOX	9
	8622	1	D18S51	11
	6237	0.72	D18S51	19
	13523	1	AMEL	X
	10781	1	D5S818	9
	10288	0.95	D5S818	11
	6486	1	FGA	20
	5315	0.82	FGA	25
2518H	13876	1	D8S1179	10 Minus A
	12408	0.89	D8S1179	11
	10468	1	D21S11	29
	9928	0.95	D21S11	31.2
	11426	1	D7S820	10
	7829	1	CSF1PO	11
	7340	0.94	CSF1PO	13
	16301	1	D3S1358	18
	14737	1	TH01	6
	14203	0.96	TH01	9.3
	11730	0.84	D13S317	8
	13933	1	D13S317	11
	17771	1	D16S539	11
	8313	1	D2S1338	22
	7290	0.88	D2S1338	24
	11343	1	D19S433	13
	10811	0.95	D19S433	15

	16680	1	vWA	17
	14584	0.87	vWA	18
	14118	1	TPOX	8
	13962	0.99	TPOX	11
	11156	1	D18S51	15
	10380	0.93	D18S51	16
	13776	1	AMEL	X
	15172	1	D5S818	11
	6686	1	FGA	23
	5825	0.87	FGA	26
297H	13263	1	D8S1179	13 Minus A
	12180	0.92	D8S1179	14
	12354	1	D21S11	31.2
	11080	0.9	D21S11	32.2
	9262	1	D7S820	11
	11602	1	CSF1PO	10
	11268	1	D3S1358	14
	8636	0.76	D3S1358	19
	6770	0.46	TH01	6.3
	12066	0.82	TH01	7
	14649	1	TH01	8.3
	11658	0.85	D13S317	8
	13657	1	D13S317	11
	14765	1	D16S539	9
	11749	0.8	D16S539	13
	9305	1	D2S1338	17
	7493	0.81	D2S1338	24
	13844	1	D19S433	13
	4648	0.34	D19S433	14
	13887	1	vWA	18
	11858	0.85	vWA	19
	11502	1	TPOX	8
	10658	0.93	TPOX	11
	6275	1	D18S51	14
	5690	0.91	D18S51	17
	10474	0.91	AMEL	X
	11457	1	AMEL	Y
	11515	0.99	D5S818	11
	11673	1	D5S818	12
	6493	1	FGA	20
	5999	0.92	FGA	21
3104H	4548	1	D8S1179	13 Minus A, Imbalance
	4100	0.9	D8S1179	14
	3255	1	D21S11	28
	3067	0.94	D21S11	30

	2715	1	D7S820	10
	3728	1	CSF1PO	10
	3845	1	D3S1358	17
	3413	0.89	D3S1358	18
	10325	1	TH01	9.3
	5063	1	D13S317	8
	4184	0.83	D13S317	11
	4907	1	D16S539	12
	4373	0.89	D16S539	13
	2294	1	D2S1338	24
	2033	0.89	D2S1338	25
	4800	1	D19S433	13
	4264	0.89	D19S433	15
	6113	1	vWA	14
	4412	0.72	vWA	19
	3915	1	TPOX	11
	3473	0.89	TPOX	12
	2589	1	D18S51	13
	2217	0.86	D18S51	17
	7462	1	AMEL	X
	7406	0.99	AMEL	Y
	7016	1	D5S818	13
	2099	1	FGA	23
	1953	0.93	FGA	25
311H	13652	1	D8S1179	12 Minus A
	6344	1	D21S11	28
	6233	0.98	D21S11	29
	2254	1	D7S820	10
	2026	0.9	D7S820	13
	3366	1	CSF1PO	10
	3240	0.96	CSF1PO	11
	7875	1	D3S1358	11
	6655	0.85	D3S1358	15
	10916	1	TH01	6
	10125	0.93	TH01	9.3
	7922	1	D13S317	8
	6756	0.85	D13S317	11
	8601	1	D16S539	13
	7507	0.87	D16S539	15
	4169	1	D2S1338	19
	3331	0.8	D2S1338	26
	7267	1	D19S433	12
	6652	0.92	D19S433	14
	9050	1	vWA	15
	8272	0.91	vWA	17
	7346	1	TPOX	8

	7084	0.96	TPOX	11
	7005	1	D18S51	15
	12845	1	AMEL	X
	6503	1	D5S818	12
	5916	0.91	D5S818	13
	3490	1	FGA	20
	2843	0.81	FGA	24
312AH	13339	1	D8S1179	10 Minus A
	11984	0.9	D8S1179	14
	10948	1	D21S11	30
	9979	0.91	D21S11	31
	4771	1	D7S820	10
	4703	0.99	D7S820	12
	11903	1	CSF1PO	12
	13143	1	D3S1358	14
	11834	0.9	D3S1358	16
	14522	1	TH01	6
	14473	1	TH01	9
	14224	1	D13S317	8
	13938	0.98	D13S317	9
	19721	1	D16S539	11
	8722	1	D2S1338	18
	7722	0.89	D2S1338	22
	11191	1	D19S433	15
	10629	0.95	D19S433	16.2
	11645	0.85	vWA	16
	13703	1	vWA	18
	13419	1	TPOX	8
	12599	0.94	TPOX	11
	8390	1	D18S51	12
	7635	0.91	D18S51	13
	10420	0.87	AMEL	X
	11931	1	AMEL	Y
	11612	1	D5S818	12
	10570	0.91	D5S818	13
	6676	1	FGA	20
	6306	0.94	FGA	21
312BH	14169	1	D8S1179	12 Minus A, Imbalance
	7060	1	D21S11	28
	6610	0.94	D21S11	31.2
	4964	1	D7S820	9
	4795	0.97	D7S820	12
	5869	1	CSF1PO	11
	5517	0.94	CSF1PO	12
	14517	1	D3S1358	14

	9890	1	TH01	6
	9440	0.95	TH01	8
	11503	1	D13S317	9
	10824	0.94	D13S317	11
	19306	1	D16S539	12
	7082	1	D2S1338	23
	6605	0.93	D2S1338	25
	4212	0.55	D19S433	14
	7682	1	D19S433	15.2
	9549	1	vWA	14
	9099	0.95	vWA	16
	8279	1	TPOX	9
	7948	0.96	TPOX	11
	8246	1	D18S51	14
	7312	0.89	D18S51	18
	13356	1	AMEL	X
	10856	1	D5S818	11
	8787	0.81	D5S818	12
	6654	1	FGA	19
	6196	0.93	FGA	21
3258H	7486	1	D8S1179	10 Minus A
	6594	0.88	D8S1179	15
	5587	0.99	D21S11	29
	5658	1	D21S11	31.2
	3659	1	D7S820	9
	3347	0.91	D7S820	12
	4803	1	CSF1PO	10
	4534	0.94	CSF1PO	13
	7859	1	D3S1358	15
	7445	0.95	D3S1358	17
	9051	1	TH01	6
	8773	0.97	TH01	7
	9238	1	D13S317	9
	9151	0.99	D13S317	11
	17262	1	D16S539	13
	6700	1	D2S1338	19
	6149	0.92	D2S1338	20
	8470	1	D19S433	14
	6869	0.81	D19S433	15
	9111	1	vWA	15
	8520	0.94	vWA	18
	13630	1	TPOX	11
	7721	1	D18S51	13
	6933	0.9	D18S51	14
	7461	0.94	AMEL	X
	7958	1	AMEL	Y

	7751	0.99	D5S818	11	
	7855	1	D5S818	12	
	4948	1	FGA	21	
	4773	0.96	FGA	26	
333H	10381	1	D8S1179	10	Minus A
	9874	0.95	D8S1179	12	
	8777	1	D21S11	27	
	8272	0.94	D21S11	29	
	7342	1	D7S820	12	
	5438	1	CSF1PO	12	
	4937	0.91	CSF1PO	13	
	11158	1	D3S1358	15	
	10126	0.91	D3S1358	17	
	19292	1	TH01	9.3	
	13031	1	D13S317	8	
	10905	0.84	D13S317	13	
	14691	1	D16S539	8	
	13894	0.95	D16S539	12	
	8388	1	D2S1338	17	
	6374	0.76	D2S1338	25	
	10077	1	D19S433	14	
	8875	0.88	D19S433	16.2	
	13204	1	vWA	14	
	12110	0.92	vWA	17	
	14645	1	TPOX	8	
	7075	1	D18S51	12	
	6372	0.9	D18S51	16	
	15497	1	AMEL	X	
	10035	1	D5S818	12	
	9373	0.93	D5S818	13	
	5083	1	FGA	23	
	4873	0.96	FGA	26	
338H	14547	1	D8S1179	13	Minus A
	7371	1	D21S11	29	
	7178	0.97	D21S11	31	
	3577	0.98	D7S820	9	
	3640	1	D7S820	10	
	3981	1	CSF1PO	11	
	3692	0.93	CSF1PO	13	
	11134	1	D3S1358	16	
	3094	0.31	TH01	6.3	
	9975	1	TH01	7	
	9948	1	TH01	9.3	
	9372	1	D13S317	12	
	8573	0.91	D13S317	13	

	11730	1	D16S539	11	
	10889	0.93	D16S539	12	
	5315	1	D2S1338	24	
	4726	0.89	D2S1338	25	
	8590	1	D19S433	14	
	7743	0.9	D19S433	15	
	15173	1	vWA	16	
	8044	1	TPOX	8	
	7592	0.94	TPOX	11	
	5553	1	D18S51	12	
	4377	0.79	D18S51	17	
	12182	1	AMEL	X	
	13936	1	D5S818	12	
	4701	1	FGA	20	
	4336	0.92	FGA	22	
3701H	7256	1	D8S1179	11	Minus A, Imbalance
	6809	0.94	D8S1179	14	
	6367	1	D21S11	28	
	6109	0.96	D21S11	29	
	3354	1	D7S820	8	
	3229	0.96	D7S820	10	
	3879	1	CSF1PO	11	
	3707	0.96	CSF1PO	12	
	7022	1	D3S1358	17	
	6071	0.86	D3S1358	18	
	1649	0.21	TH01	5.3	
	7805	1	TH01	6	
	7585	0.97	TH01	9.3	
	13513	1	D13S317	11	
	9284	1	D16S539	11	
	8753	0.94	D16S539	13	
	4904	1	D2S1338	24	
	4355	0.89	D2S1338	25	
	13394	1	D19S433	12	
	8561	1	vWA	14	
	8121	0.95	vWA	16	
	6291	1	TPOX	8	
	6028	0.96	TPOX	11	
	5271	1	D18S51	15	
	4846	0.92	D18S51	16	
	8439	1	AMEL	X	
	1952	0.23	AMEL	Y	
	8061	1	D5S818	11	
	8088	1	D5S818	12	
	5150	1	FGA	19	
	4072	0.79	FGA	25	

3805H	12992	1	D8S1179	12	Imbalance
	12268	0.94	D8S1179	13	
	11602	1	D21S11	28	
	11356	0.98	D21S11	31	
	8090	1	D7S820	9	
	7330	0.91	D7S820	11	
	9420	1	CSF1PO	11	
	8738	0.93	CSF1PO	15	
	14752	1	D3S1358	14	
	13035	0.88	D3S1358	16	
	23580	1	TH01	9.3	
	14601	1	D13S317	12	
	14357	0.98	D13S317	13	
	14704	1	D16S539	10	
	14515	0.99	D16S539	12	
	10721	1	D2S1338	22	
	9937	0.93	D2S1338	24	
	14824	1	D19S433	12	
	6806	0.46	D19S433	14	
	14742	0.89	vWA	17	
	16618	1	vWA	18	
	13064	0.91	TPOX	8	
	14286	1	TPOX	9	
	13947	1	D18S51	14	
	13422	0.96	D18S51	15	
	11499	1	AMEL	X	
	4101	0.36	AMEL	Y	
	10943	1	D5S818	11	
	9606	1	FGA	22	
	8990	0.94	FGA	23	
399H	14031	1	D8S1179	11	Minus A
	12753	0.91	D8S1179	14	
	13214	1	D21S11	28	
	11063	0.84	D21S11	33.2	
	10000	1	D7S820	10	
	11725	1	CSF1PO	12	
	16585	1	D3S1358	16	
	6274	0.44	TH01	6.3	
	14419	1	TH01	7	
	6035	0.42	TH01	7.3	
	12287	0.85	TH01	8	
	14021	1	D13S317	12	
	12986	0.93	D13S317	14	
	15363	1	D16S539	11	
	14779	0.96	D16S539	12	

	9931	1	D2S1338	18
	8902	0.9	D2S1338	19
	13299	1	D19S433	14
	12452	0.94	D19S433	15.2
	13782	0.99	vWA	17
	13924	1	vWA	18
	12784	1	TPOX	8
	11678	0.91	TPOX	11
	13399	1	D18S51	16
	9432	1	AMEL	X
	13061	1	D5S818	11
	6987	1	FGA	19
	5445	0.78	FGA	24
417H	15695	1	D8S1179	13
	9512	1	D21S11	29
	9126	0.96	D21S11	30
	6926	1	D7S820	8
	6699	0.97	D7S820	10
	7164	1	CSF1PO	10
	6768	0.94	CSF1PO	12
	17556	1	D3S1358	15
	14288	1	TH01	6
	13776	0.96	TH01	9
	14441	1	D13S317	8
	14075	0.97	D13S317	11
	14373	1	D16S539	11
	14239	0.99	D16S539	12
	10020	1	D2S1338	17
	9236	0.92	D2S1338	19
	9495	1	D19S433	14
	9014	0.95	D19S433	15.2
	14541	1	vWA	14
	11610	0.8	vWA	19
	13469	1	TPOX	8
	13230	0.98	TPOX	11
	11461	1	D18S51	14
	10486	0.91	D18S51	15
	10665	0.96	AMEL	X
	11052	1	AMEL	Y
	10149	1	D5S818	12
	9287	0.92	D5S818	13
	8119	1	FGA	22
	7460	0.92	FGA	23
420H	5435	1	D8S1179	13 Minus A
	4928	0.91	D8S1179	14

	4336	1	D21S11	31.2
	4085	0.94	D21S11	33.2
	2768	1	D7S820	9
	2643	0.95	D7S820	12
	3244	1	CSF1PO	12
	3131	0.97	CSF1PO	14
	6914	1	D3S1358	14
	6866	0.99	D3S1358	16
	7659	1	TH01	6
	7316	0.96	TH01	8
	14025	1	D13S317	12
	7763	1	D16S539	11
	7796	1	D16S539	13
	9702	1	D2S1338	19
	11405	1	D19S433	15
	7563	1	vWA	19
	6841	0.9	vWA	20
	13331	1	TPOX	8
	9743	1	D18S51	16
	6671	1	AMEL	X
	6670	1	AMEL	Y
	10913	1	D5S818	11
	3944	1	FGA	21
	3387	0.86	FGA	25
4375H	6895	1	D8S1179	11 Minus A
	6409	0.93	D8S1179	14
	6490	1	D21S11	28
	5869	0.9	D21S11	29
	2493	1	D7S820	7
	2063	0.83	D7S820	12
	2966	1	CSF1PO	11
	2843	0.96	CSF1PO	12
	6202	0.92	D3S1358	15
	5552	0.82	D3S1358	16
	3191	0.43	TH01	6.3
	7475	1	TH01	7
	7366	0.99	TH01	9.3
	8032	1	D13S317	8
	6752	0.84	D13S317	12
	8745	1	D16S539	12
	7812	0.89	D16S539	13
	4198	1	D2S1338	17
	3387	0.81	D2S1338	23
	7974	1	D19S433	13
	7726	0.97	D19S433	13.2
	8242	1	vWA	17

	7571	0.92	vWA	18	
	5796	1	TPOX	9	
	5767	0.99	TPOX	11	
	4099	1	D18S51	12	
	2876	0.7	D18S51	20	
	10491	1	AMEL	X	
	11342	1	D5S818	11	
	5564	1	FGA	23	
444H	12460	1	D8S1179	12	Minus A, Imbalance
	11556	0.93	D8S1179	13	
	11273	1	D21S11	29	
	10643	0.94	D21S11	30	
	6031	1	D7S820	8	
	5641	0.94	D7S820	11	
	6291	1	CSF1PO	10	
	5842	0.93	CSF1PO	11	
	11688	1	D3S1358	15	
	6572	0.56	D3S1358	15.2	
	10842	0.93	D3S1358	16	
	12906	1	TH01	9.3	
	12064	0.9	D13S317	9	
	13456	1	D13S317	12	
	14587	1	D16S539	11	
	13506	0.93	D16S539	13	
	8827	1	D2S1338	18	
	7243	0.82	D2S1338	26	
	13187	1	D19S433	13	
	11951	0.91	D19S433	14	
	19129	1	vWA	18	
	11282	1	TPOX	8	
	11030	0.98	TPOX	11	
	3395	0.44	D18S51	12	
	7729	1	D18S51	16	
	14767	1	AMEL	X	
	11980	1	D5S818	12	
	11416	0.95	D5S818	13	
	7643	1	FGA	23	
	6987	0.91	FGA	24	
550H	10999	1	D8S1179	13	Minus A
	10083	0.92	D8S1179	14	
	10124	1	D21S11	28	
	9528	0.94	D21S11	30	
	5160	1	D7S820	7	
	4658	0.9	D7S820	10	
	5588	1	CSF1PO	11	

5258	0.94	CSF1PO	13	
11176	1	D3S1358	15	
10198	0.91	D3S1358	17	
14505	1	TH01	6	
14517	1	TH01	7	
13979	1	D13S317	10	
13291	0.95	D13S317	12	
14814	1	D16S539	11	
14559	0.98	D16S539	12	
8191	1	D2S1338	19	
7293	0.89	D2S1338	21	
10369	1	D19S433	15.2	
8916	0.86	D19S433	16.2	
11134	0.94	vWA	14	
11847	1	vWA	18	
10916	1	TPOX	9	
10502	0.96	TPOX	11	
7264	1	D18S51	14	
6722	0.93	D18S51	16	
12684	1	AMEL	X	
12656	1	AMEL	Y	
14213	1	D5S818	11	
7502	1	FGA	19	
6864	0.91	FGA	20	
565H	14405	1	D8S1179	10 Minus A
	14038	0.97	D8S1179	12
	11294	1	D21S11	29
	6380	0.99	D7S820	11
	6431	1	D7S820	12
	7635	1	CSF1PO	9
	6882	0.9	CSF1PO	12
	13745	1	D3S1358	14
	12226	0.89	D3S1358	17
	23379	1	TH01	9.3
	17155	1	D13S317	12
	14942	1	D16S539	11
	14968	1	D16S539	13
	11679	1	D2S1338	17
	9749	0.83	D2S1338	22
	13497	1	D19S433	13
	14689	1	vWA	14
	11251	0.77	vWA	20
	13115	0.98	TPOX	8
	7484	1	D18S51	18
	6473	0.86	D18S51	21
	10530	1	AMEL	X

	10461	0.99	AMEL	Y
	13198	1	D5S818	11
	12768	0.97	D5S818	12
	9282	1	FGA	21
589H	14519	1	D8S1179	13 Minus A
	7469	1	D21S11	30
	7050	0.94	D21S11	31.2
	3298	0.99	D7S820	10
	3319	1	D7S820	12
	3968	1	CSF1PO	10
	3639	0.92	CSF1PO	13
	8273	1	D3S1358	14
	7788	0.94	D3S1358	16
	14834	1	TH01	9.3
	9699	1	D13S317	11
	8842	0.91	D13S317	13
	12950	1	D16S539	9
	11965	0.92	D16S539	11
	6307	1	D2S1338	17
	5136	0.81	D2S1338	24
	8339	1	D19S433	14.2
	7797	0.94	D19S433	16
	14579	1	vWA	16
	12529	1	TPOX	8
	10987	1	D18S51	12
	12967	1	AMEL	X
	13463	1	D5S818	12
	4296	1	FGA	21
	3568	0.83	FGA	26
6080H	6109	0.83	D8S1179	9 Minus A
	5344	0.72	D8S1179	13
	5822	1	D21S11	28
	5587	0.96	D21S11	30
	3467	1	D7S820	8
	5004	1	CSF1PO	12
	3869	0.76	D3S1358	15
	3559	0.7	D3S1358	17
	12979	1	TH01	9.3
	5583	1	D13S317	11
	5382	0.96	D13S317	12
	14704	1	D16S539	9
	4389	1	D2S1338	17
	3549	0.81	D2S1338	24
	7429	1	D19S433	13
	6872	0.93	D19S433	14

	6745	0.88	vWA	17
	6538	0.85	vWA	19
	5288	1	TPOX	9
	5024	0.95	TPOX	11
	3031	1	D18S51	14
	2821	0.93	D18S51	16
	11151	1	AMEL	X
	4983	1	D5S818	11
	4702	0.94	D5S818	13
	2166	1	FGA	20
	1737	0.8	FGA	23
6233H	9745	0.73	D8S1179	10 Minus A
	8130	0.61	D8S1179	15
	9531	1	D21S11	27
	9248	0.97	D21S11	29
	2814	1	D7S820	9
	2454	0.87	D7S820	12
	4211	1	CSF1PO	12
	3734	0.89	CSF1PO	13
	6626	0.75	D3S1358	16
	5806	0.66	D3S1358	17
	5739	0.51	TH01	8.3
	10759	0.96	TH01	9
	11211	1	TH01	9.3
	9492	1	D13S317	10
	8694	0.92	D13S317	12
	14035	1	D16S539	11
	7752	1	D2S1338	19
	7034	0.91	D2S1338	20
	16576	1	D19S433	14
	11236	0.83	vWA	17
	10557	0.78	vWA	18
	7944	1	TPOX	8
	7854	0.99	TPOX	11
	5131	1	D18S51	12
	4625	0.9	D18S51	14
	11580	0.99	AMEL	X
	11639	1	AMEL	Y
	8596	1	D5S818	10
	7804	0.91	D5S818	11
	3521	1	FGA	20
	3239	0.92	FGA	22
651H	14607	1	D8S1179	10 Minus A, Stutter, Partial Profi
	14199	0.97	D8S1179	15
	11961	1	D21S11	29

10327	0.86	D21S11	32.2
4289	1	D7S820	10
4016	0.94	D7S820	12
8384	1	CSF1PO	12
14476	1	D3S1358	14
13623	0.94	D3S1358	17
14616	1	TH01	8
4473	0.31	TH01	8.3
14589	1	TH01	9
14644	1	D13S317	11
13617	0.93	D13S317	12
20176	1	D16S539	11
6226	1	D2S1338	20
5642	0.91	D2S1338	22
14724	1	D19S433	13
16943	1	TPOX	8
5373	1	D18S51	16
3730	0.69	D18S51	22
8373	1	AMEL	X
14281	1	D5S818	11
10969	0.77	D5S818	12
11376	1	FGA	25

709H	13798	1	D8S1179	10
	12609	0.91	D8S1179	13
	10751	1	D21S11	28
	8789	0.82	D21S11	32.2
	6772	1	D7S820	8
	6466	0.95	D7S820	11
	7776	1	CSF1PO	11
	7120	0.92	CSF1PO	12
	13142	0.9	D3S1358	17
	14592	1	D3S1358	18
	11875	0.98	TH01	6
	12107	1	TH01	7
	14941	1	D13S317	8
	15579	1	D16S539	8
	13915	0.89	D16S539	13
	9715	1	D2S1338	17
	7789	0.8	D2S1338	24
	15513	1	D19S433	14
	15389	1	vWA	14
	15031	0.98	vWA	17
	17096	1	TPOX	8
	10981	1	D18S51	13
	9417	0.86	D18S51	16
	17261	1	AMEL	X

	12274	1	D5S818	10	
	10982	0.89	D5S818	11	
	7735	1	FGA	20	
	6459	0.84	FGA	24.2	
735H	13640	1	D8S1179	12	Imbalance
	12854	0.94	D8S1179	13	
	10604	1	D21S11	29	
	10057	0.95	D21S11	32.2	
	13412	1	D7S820	10	
	14060	1	CSF1PO	11	
	18364	1	D3S1358	15	
	9131	0.62	TH01	8	
	14725	1	TH01	9.3	
	14353	1	D13S317	11	
	12178	0.85	D13S317	12	
	14508	1	D16S539	11	
	14489	1	D16S539	12	
	11235	1	D2S1338	19	
	9566	0.85	D2S1338	24	
	13305	1	D19S433	13	
	13024	0.98	D19S433	14	
	14763	1	vWA	17	
	14735	1	vWA	18	
	14530	1	TPOX	8	
	14243	0.98	TPOX	11	
	10571	1	D18S51	18	
	8959	0.85	D18S51	22	
	12493	1	AMEL	X	
	11048	0.88	AMEL	Y	
	10973	0.95	D5S818	11	
	11603	1	D5S818	13	
	7278	1	FGA	22.2	
	6990	0.96	FGA	24	
746H	8869	1	D8S1179	11	Minus A
	8020	0.9	D8S1179	13	
	6888	1	D21S11	30	
	6604	0.96	D21S11	31.2	
	4948	1	D7S820	8	
	4569	0.92	D7S820	10	
	5917	1	CSF1PO	11	
	5438	0.92	CSF1PO	12	
	10649	1	D3S1358	14	
	10063	0.94	D3S1358	15	
	18807	1	TH01	6	
	11547	1	D13S317	9	

	11417	0.99	D13S317	10	
	12622	1	D16S539	9	
	11382	0.9	D16S539	13	
	7585	1	D2S1338	19	
	6435	0.85	D2S1338	25	
	7706	1	D19S433	14.2	
	6272	0.81	D19S433	15	
	10443	1	vWA	18	
	9748	0.93	vWA	19	
	14645	1	TPOX	8	
	7764	1	D18S51	15	
	7162	0.92	D18S51	18	
	9665	1	AMEL	X	
	9553	0.99	AMEL	Y	
	9758	0.95	D5S818	11	
	10262	1	D5S818	12	
	6505	1	FGA	24	
	5929	0.91	FGA	25	
7485H	7409	1	D8S1179	8	Minus A, Imbalance
	7209	0.97	D8S1179	13	
	6199	1	D21S11	31.2	
	5475	0.88	D21S11	32.2	
	3920	1	D7S820	8	
	1105	0.28	D7S820	12	
	4948	1	CSF1PO	10	
	4485	0.91	CSF1PO	12	
	7846	0.99	D3S1358	15	
	7945	1	D3S1358	17	
	8009	0.98	TH01	6	
	8163	1	TH01	9.3	
	9924	1	D13S317	12	
	9186	0.93	D13S317	13	
	14843	1	D16S539	12	
	7483	1	D2S1338	14	
	5401	0.72	D2S1338	26	
	9456	1	D19S433	12	
	8201	0.87	D19S433	13	
	8519	1	vWA	16	
	8236	0.97	vWA	19	
	6670	0.97	TPOX	8	
	6860	1	TPOX	10	
	7978	1	D18S51	13	
	7403	0.93	D18S51	14	
	7605	0.98	AMEL	X	
	7773	1	AMEL	Y	
	8413	1	D5S818	12	

	7420	0.88	D5S818	13	
	10295	1	FGA	24	
7572H	7458	1	D8S1179	10	Minus A
	7100	0.95	D8S1179	14	
	6130	1	D21S11	28	
	5879	0.96	D21S11	30	
	7424	1	D7S820	10	
	4843	1	CSF1PO	10	
	4538	0.94	CSF1PO	12	
	8038	1	D3S1358	17	
	7263	0.9	D3S1358	18	
	7931	1	TH01	7	
	7669	0.97	TH01	9.3	
	13604	1	D13S317	11	
	10507	1	D16S539	12	
	9869	0.94	D16S539	13	
	6262	1	D2S1338	17	
	5376	0.86	D2S1338	24	
	8429	1	D19S433	14	
	7497	0.89	D19S433	15	
	9127	1	vWA	15	
	8396	0.92	vWA	16	
	13464	1	TPOX	8	
	7239	1	D18S51	10	
	6665	0.92	D18S51	14	
	13052	1	AMEL	X	
	12739	1	D5S818	12	
	5126	1	FGA	22	
	4696	0.92	FGA	25	
7758H	10109	0.76	D8S1179	10	Minus A, Allelic Dropout, Imb
	8710	0.65	D8S1179	14	
	9460	1	D21S11	28	
	9376	0.99	D21S11	30	
	2943	1	D7S820	9	
	2771	0.94	D7S820	13	
	4314	1	CSF1PO	10	
	4041	0.94	CSF1PO	12	
	10676	0.79	D3S1358	15	
	5156	0.45	TH01	6.3	
	11440	1	TH01	7	
	9118	1	D13S317	11	
	8040	0.88	D13S317	14	
	13909	1	D16S539	9	
	13622	0.98	D16S539	12	
	8208	1	D2S1338	17	

	6380	0.78	D2S1338	24
	11073	1	D19S433	14
	10490	0.95	D19S433	16
	10820	0.6	vWA	16
	18036	1	vWA	19
	14270	1	TPOX	8
	4720	1	D18S51	15
	4285	0.91	D18S51	17
	12608	1	AMEL	X
	8752	1	D5S818	11
	7977	0.91	D5S818	12
	3447	1	FGA	23
	3178	0.92	FGA	24
777H	6115	1	D8S1179	8 Minus A
	5438	0.89	D8S1179	15
	4911	1	D21S11	29
	4624	0.94	D21S11	32.2
	2948	1	D7S820	10
	2850	0.97	D7S820	13
	7426	1	CSF1PO	10
	6582	1	D3S1358	14
	6222	0.95	D3S1358	15
	6881	1	TH01	6
	6667	0.97	TH01	9.3
	7818	1	D13S317	8
	7324	0.94	D13S317	11
	8655	1	D16S539	9
	8006	0.93	D16S539	12
	4700	1	D2S1338	20
	4315	0.92	D2S1338	23
	5870	1	D19S433	13
	5517	0.94	D19S433	15
	6950	1	vWA	16
	6476	0.93	vWA	18
	6018	1	TPOX	9
	5761	0.96	TPOX	11
	6065	1	D18S51	13
	5469	0.9	D18S51	14
	12265	1	AMEL	X
	12106	1	D5S818	9
	4446	1	FGA	21
	3941	0.89	FGA	25
9066H	11609	1	D8S1179	11 Minus A, Imbalance
	11379	0.98	D8S1179	13
	10164	1	D21S11	28

	9469	0.93	D21S11	30	
	4830	1	D7S820	9	
	1337	0.28	D7S820	11	
	12247	1	CSF1PO	11	
	11323	1	D3S1358	17	
	9834	0.87	D3S1358	18	
	14002	1	TH01	7	
	13928	0.99	TH01	9.3	
	13982	1	D13S317	8	
	12211	0.87	D13S317	13	
	17336	1	D16S539	11	
	8858	1	D2S1338	20	
	7686	0.87	D2S1338	21	
	14930	1	D19S433	12	
	11845	0.79	D19S433	15	
	13615	1	vWA	18	
	13274	0.97	vWA	19	
	17663	1	TPOX	9	
	8401	1	D18S51	12	
	7185	0.86	D18S51	16	
	13244	1	AMEL	X	
	7390	0.56	AMEL	Y	
	11779	1	D5S818	10	
	10966	0.93	D5S818	13	
	5904	1	FGA	23	
	5392	0.91	FGA	26	
931H	8546	1	D8S1179	11	Minus A
	7619	0.89	D8S1179	15	
	6573	1	D21S11	28	
	6405	0.97	D21S11	30	
	3872	1	D7S820	8	
	3693	0.95	D7S820	10	
	4572	1	CSF1PO	12	
	4141	0.91	CSF1PO	13	
	14981	1	D3S1358	15	
	10462	0.93	TH01	8	
	11208	1	TH01	9.3	
	10889	1	D13S317	9	
	9935	0.91	D13S317	11	
	13018	1	D16S539	8	
	11159	0.86	D16S539	12	
	6524	1	D2S1338	20	
	5627	0.86	D2S1338	24	
	13502	1	D19S433	13	
	10005	1	vWA	15	
	9574	0.96	vWA	18	

	8793	1	TPOX	8
	8018	0.91	TPOX	10
	6478	1	D18S51	14
	5284	0.82	D18S51	19
	10858	1	AMEL	X
	10665	0.98	AMEL	Y
	8656	1	D5S818	11
	8225	0.95	D5S818	13
	5838	1	FGA	19
	5042	0.86	FGA	24
940H	7049	1	D8S1179	14 Minus A
	6617	0.94	D8S1179	15
	10880	1	D21S11	30
	3848	1	D7S820	8
	3383	0.88	D7S820	11
	4837	1	CSF1PO	11
	4385	0.91	CSF1PO	12
	9344	1	D3S1358	14
	8288	0.89	D3S1358	15
	9335	1	TH01	6
	9133	0.98	TH01	9
	9628	1	D13S317	10
	8863	0.92	D13S317	11
	14962	1	D16S539	9
	6449	1	D2S1338	19
	5859	0.91	D2S1338	22
	7188	1	D19S433	13
	7011	0.98	D19S433	13.2
	8604	1	vWA	16
	8310	0.97	vWA	19
	7948	1	TPOX	9
	7918	1	TPOX	11
	6479	1	D18S51	14
	5771	0.89	D18S51	17
	13131	1	AMEL	X
	7580	1	D5S818	12
	6874	0.91	D5S818	13
	9886	1	FGA	22
9439H	9667	1	D8S1179	14 Minus A
	9034	0.93	D8S1179	15
	13174	1	D21S11	30
	4170	1	D7S820	8
	3873	0.93	D7S820	11
	4944	1	CSF1PO	10
	4589	0.93	CSF1PO	12

	13209	0.97	D3S1358	16
	3040	0.27	TH01	6.3
	11249	1	TH01	7
	11068	0.98	TH01	9.3
	13326	1	D13S317	11
	11862	0.89	D13S317	12
	20262	1	D16S539	11
	6790	1	D2S1338	19
	6492	0.96	D2S1338	22
	9686	1	D19S433	15
	8729	0.9	D19S433	17.2
	12248	1	vWA	14
	10478	0.86	vWA	18
	8943	1	TPOX	8
	8399	0.94	TPOX	9
	6871	1	D18S51	12
	5807	0.85	D18S51	16
	12023	1	AMEL	X
	11894	0.99	AMEL	Y
	10700	1	D5S818	12
	9873	0.92	D5S818	13
	5926	1	FGA	21
	5441	0.92	FGA	23
9899H	12307	1	D8S1179	9 Minus A
	9561	0.78	D8S1179	15
	15160	1	D21S11	28
	3886	1	D7S820	11
	3610	0.93	D7S820	12
	9694	1	CSF1PO	12
	12457	0.9	D3S1358	18
	12281	1	TH01	9.3
	11939	1	D13S317	12
	10645	0.89	D13S317	13
	14480	1	D16S539	10
	13883	0.96	D16S539	12
	7643	1	D2S1338	17
	6822	0.89	D2S1338	22
	13252	0.95	D19S433	12
	10429	0.84	vWA	17
	12370	1	vWA	18
	15559	1	TPOX	11
	5491	1	D18S51	19
	4917	0.9	D18S51	20
	7929	1	AMEL	X
	11090	1	D5S818	9
	9849	0.89	D5S818	11

	5294	1	FGA	20
	4193	0.79	FGA	24
CaseyH	4357	1	D8S1179	10
	3979	0.91	D8S1179	12
	1772	0.98	D21S11	28
	1806	1	D21S11	31.2
	813	0.97	D7S820	8
	836	1	D7S820	11
	1000	1	CSF1PO	10
	991	0.99	CSF1PO	11
	11940	1	D3S1358	14
	3752	1	TH01	6
	3205	0.85	TH01	8
	3103	1	D13S317	9
	2938	0.95	D13S317	11
	2429	1	D16S539	11
	2409	0.99	D16S539	12
	1074	1	D2S1338	20
	952	0.89	D2S1338	25
	3651	0.97	D19S433	14
	3754	1	D19S433	16
	7038	1	vWA	18
	2330	1	TPOX	9
	2037	0.87	TPOX	11
	1541	1	D18S51	10
	1465	0.95	D18S51	14
	9699	1	AMEL	X
	4687	1	D5S818	12
	4132	0.88	D5S818	13
	2025	1	FGA	20
	1891	0.93	FGA	21
ChristiH	13418	1	D8S1179	14	Minus A, Allelic Dropout
	8458	1	D21S11	28
	7886	0.93	D21S11	30
	4458	1	D7S820	8
	3814	0.86	D7S820	12
	4773	1	CSF1PO	10
	4236	0.89	CSF1PO	11
	13915	1	D3S1358	14
	13977	1	D3S1358	16
	14896	1	TH01	6
	14855	1	D13S317	11
	11073	1	D16S539	11
	10168	0.92	D16S539	12
	5170	1	D2S1338	23

	4748	0.92	D2S1338	24
	11500	1	D19S433	15
	13586	1	vWA	14
	10852	0.8	vWA	18
	8453	1	TPOX	8
	7898	0.93	TPOX	9
	14246	1	D18S51	12
	10960	1	AMEL	X
	13643	1	D5S818	11
	11840	0.87	D5S818	12
	8090	1	FGA	20
	7038	0.87	FGA	23
JDWH	9657	1	D8S1179	10
	7603	0.79	D8S1179	14
	4766	1	D21S11	30
	4148	0.87	D21S11	31
	2462	1	D7S820	10
	2429	0.99	D7S820	12
	4549	1	CSF1PO	12
	10506	1	D3S1358	14
	10487	1	D3S1358	16
	6928	1	TH01	6
	6816	0.98	TH01	9
	7588	1	D13S317	8
	7305	0.96	D13S317	9
	11314	1	D16S539	11
	2839	1	D2S1338	18
	2728	0.96	D2S1338	22
	7913	1	D19S433	15
	7133	0.9	D19S433	16.2
	8134	1	vWA	16
	8054	0.99	vWA	18
	4971	1	TPOX	8
	4458	0.9	TPOX	11
	4346	1	D18S51	12
	3966	0.91	D18S51	13
	9093	1	AMEL	X
	8429	0.93	AMEL	Y
	10137	1	D5S818	12
	7549	0.74	D5S818	13
	4739	1	FGA	20
	4295	0.91	FGA	21
LouieH	2971	1	D8S1179	12
	2599	0.87	D8S1179	13
	2770	1	D21S11	29

768	1	D7S820	10	
669	0.87	D7S820	12	
1443	1	CSF1PO	10	
3715	1	D3S1358	15	
3371	0.91	D3S1358	18	
4592	1	TH01	9.3	
3817	1	D13S317	12	
3450	1	D16S539	12	
907	1	D2S1338	23	
702	0.77	D2S1338	24	
5229	1	D19S433	14	
2908	1	vWA	15	
2703	0.93	vWA	18	
1853	1	TPOX	7	
1554	0.84	TPOX	8	
1304	1	D18S51	12	
1292	0.99	D18S51	14	
6256	1	AMEL	X	
5062	1	D5S818	12	
1360	1	FGA	22	
1193	0.88	FGA	23	

EDGE
008E

6306	1	D8S1179	14	Minus A
6015	0.95	D8S1179	15	
5985	1	D21S11	30	
5644	0.94	D21S11	34.2	
4397	1	D7S820	12	
3764	0.86	D7S820	13	
4492	1	CSF1PO	10	
4337	0.97	CSF1PO	12	
8487	1	D3S1358	15	
7878	0.93	D3S1358	18	
8818	1	TH01	6	
8664	0.98	TH01	9.3	
10806	1	D13S317	8	
9650	0.89	D13S317	12	
14758	1	D16S539	12	
6449	1	D2S1338	20	
5613	0.87	D2S1338	24	
6472	1	D19S433	13	
6087	0.94	D19S433	14	
14791	1	vWA	17	
14327	1	TPOX	8	
7389	1	D18S51	12	
5537	0.75	D18S51	22	
7942	1	AMEL	X	

	6740	0.85	AMEL	Y	
	11738	1	D5S818	11	
	6114	1	FGA	19	
	5823	0.95	FGA	20	
062E	14222	1	D8S1179	14	Minus A
	10571	1	D21S11	29	
	10227	0.97	D21S11	31.2	
	4755	1	D7S820	10	
	4507	0.95	D7S820	12	
	6758	1	CSF1PO	11	
	5953	0.88	CSF1PO	12	
	13828	0.97	D3S1358	14	
	14220	1	D3S1358	15	
	14769	0.99	TH01	6	
	14978	1	TH01	9.3	
	20844	1	D13S317	11	
	20419	1	D16S539	11	
	9100	1	D2S1338	18	
	8274	0.91	D2S1338	19	
	9928	1	D19S433	15	
	14930	1	vWA	16	
	14112	0.95	vWA	17	
	13835	1	TPOX	8	
	13341	0.96	TPOX	10	
	6593	1	D18S51	16	
	5564	0.84	D18S51	20	
	10715	0.88	AMEL	X	
	12211	1	AMEL	Y	
	13209	1	D5S818	12	
	6443	1	FGA	23	
	5691	0.88	FGA	24	
088E	7655	1	D8S1179	13	Minus A
	7092	0.93	D8S1179	14	
	12630	1	D21S11	32.2	
	8148	1	D7S820	12	
	4676	1	CSF1PO	10	
	4016	0.86	CSF1PO	13	
	13722	1	D3S1358	15	
	8288	0.97	TH01	7	
	8532	1	TH01	9.3	
	10685	1	D13S317	8	
	9694	0.91	D13S317	13	
	12357	1	D16S539	9	
	11252	0.91	D16S539	10	
	6059	1	D2S1338	20	

	5423	0.9	D2S1338	23	
	7875	1	D19S433	13	
	7332	0.93	D19S433	14	
	7995	0.97	vWA	15	
	8214	1	vWA	18	
	11700	1	TPOX	8	
	6043	1	D18S51	15	
	5452	0.9	D18S51	18	
	12883	1	AMEL	X	
	7934	0.92	D5S818	11	
	8591	1	D5S818	13	
	9841	1	FGA	24	
127E	14200	1	D8S1179	13	Minus A
	8420	1	D21S11	30	
	7662	0.91	D21S11	30.2	
	3984	1	D7S820	8	
	3521	0.88	D7S820	12	
	4911	1	CSF1PO	11	
	4405	0.9	CSF1PO	14	
	9592	1	D3S1358	15	
	8656	0.9	D3S1358	18	
	13713	1	TH01	6	
	13715	1	TH01	7	
	12274	1	D13S317	8	
	10626	0.87	D13S317	11	
	18060	1	D16S539	11	
	7090	1	D2S1338	17	
	6541	0.92	D2S1338	19	
	10940	1	D19S433	12	
	9836	0.9	D19S433	13	
	12966	1	vWA	16	
	11468	0.88	vWA	17	
	15517	1	TPOX	8	
	12310	1	D18S51	14	
	12404	1	AMEL	X	
	9873	1	D5S818	11	
	8889	0.9	D5S818	12	
	5181	1	FGA	21.2	
	4858	0.94	FGA	22	
144E	8592	1	D8S1179	11	Minus A, Imbalance
	7787	0.91	D8S1179	14	
	7428	1	D21S11	28	
	7372	0.99	D21S11	30	
	4305	1	D7S820	10	
	4012	0.93	D7S820	12	

4986	1	CSF1PO	10
4810	0.96	CSF1PO	12
8346	1	D3S1358	16
7209	0.86	D3S1358	19
2145	0.22	TH01	6
9890	1	TH01	9.3
11266	1	D13S317	9
11098	0.99	D13S317	10
12210	1	D16S539	12
11750	0.96	D16S539	13
6472	1	D2S1338	19
5565	0.86	D2S1338	25
8862	1	D19S433	13
8329	0.94	D19S433	14
14549	1	vWA	15
8260	1	TPOX	8
8140	0.99	TPOX	9
6159	1	D18S51	16
5733	0.93	D18S51	18
9493	0.98	AMEL	X
9685	1	AMEL	Y
9631	1	D5S818	11
8538	0.89	D5S818	13
6237	1	FGA	20
5650	0.91	FGA	21

146E	11193	1	D8S1179	14 Minus A
	5560	1	D21S11	28
	5160	0.93	D21S11	32.2
	3612	1	D7S820	11
	3197	0.89	D7S820	12
	3891	1	CSF1PO	10
	3681	0.95	CSF1PO	12
	5642	1	D3S1358	15
	5389	0.96	D3S1358	17
	5982	0.94	TH01	6
	6334	1	TH01	9.3
	12081	1	D13S317	11
	13345	1	D16S539	11
	5125	1	D2S1338	19
	4568	0.89	D2S1338	23
	6309	1	D19S433	13
	5824	0.92	D19S433	14
	6820	1	vWA	15
	6359	0.93	vWA	18
	5610	1	TPOX	10
	5510	0.98	TPOX	11

	11324	1	D18S51	14
	12125	1	AMEL	X
	6732	1	D5S818	11
	6301	0.94	D5S818	12
	4511	1	FGA	21
	4235	0.94	FGA	24
2145E	14657	1	D8S1179	12 Minus A, Imbalance
	14402	0.98	D8S1179	13
	12861	1	D21S11	30
	12637	0.98	D21S11	31.2
	7859	1	D7S820	9
	7190	0.91	D7S820	10
	10013	1	CSF1PO	10
	9476	0.95	CSF1PO	11
	17280	1	D3S1358	14
	14891	0.86	D3S1358	15
	14836	1	TH01	6
	12215	0.82	TH01	8
	14922	1	D13S317	8
	14605	0.98	D13S317	12
	17476	1	D16S539	9
	14808	0.85	D16S539	12
	11065	1	D2S1338	17
	8615	0.78	D2S1338	25
	12669	0.84	D19S433	13
	3968	0.26	D19S433	14
	13077	0.72	vWA	17
	18285	1	vWA	18
	14158	0.95	TPOX	8
	14932	1	TPOX	11
	14707	1	D18S51	14
	7456	1	AMEL	X
	12944	1	D5S818	11
	12404	0.96	D5S818	12
	9217	1	FGA	22
	8493	0.92	FGA	23
220E	14308	1	D8S1179	13 Minus A
	14058	0.98	D8S1179	14
	14024	1	D21S11	30
	13377	0.95	D21S11	31.2
	7968	1	D7S820	8
	7416	0.93	D7S820	10
	8417	1	CSF1PO	9
	7919	0.94	CSF1PO	12
	13682	1	D3S1358	14

	9400	0.69	D3S1358	16.2
	12186	0.89	D3S1358	17
	14770	1	TH01	6
	14601	0.99	TH01	9.3
	13335	0.92	D13S317	11
	14519	1	D13S317	12
	19297	1	D16S539	9
	14674	0.76	D16S539	12
	10195	1	D2S1338	21
	9729	0.95	D2S1338	24
	11001	0.78	D19S433	14
	10684	0.75	D19S433	15
	12476	0.89	vWA	17
	13958	1	vWA	19
	16433	1	TPOX	8
	10970	1	D18S51	12
	8428	0.77	D18S51	18
	8215	1	AMEL	X
	13290	1	D5S818	11
	13119	0.99	D5S818	12
	9359	1	FGA	21
	8294	0.89	FGA	24
247E	8596	1	D8S1179	10 Minus A, Imbalance
	8110	0.94	D8S1179	12
	7262	1	D21S11	31
	6891	0.95	D21S11	32.2
	6568	1	D7S820	11
	3701	1	CSF1PO	12
	3464	0.94	CSF1PO	14
	6607	1	D3S1358	17
	6092	0.92	D3S1358	18
	9085	1	TH01	6
	8901	0.98	TH01	8
	9813	1	D13S317	10
	8890	0.91	D13S317	11
	10327	1	D16S539	11
	9863	0.96	D16S539	13
	5832	1	D2S1338	17
	5261	0.9	D2S1338	19
	8017	1	D19S433	13
	7449	0.93	D19S433	14
	14891	1	vWA	16
	7669	1	TPOX	8
	6994	0.91	TPOX	9
	5559	1	D18S51	11
	3835	0.69	D18S51	19

	12834	1	AMEL	X
	8836	1	D5S818	9
	7959	0.9	D5S818	11
	4664	1	FGA	20
	3868	0.83	FGA	25
2518E	9543	1	D8S1179	10 Minus A
	8608	0.9	D8S1179	11
	6866	1	D21S11	29
	6733	0.98	D21S11	31.2
	7419	1	D7S820	10
	4914	1	CSF1PO	11
	4401	0.9	CSF1PO	13
	14036	1	D3S1358	18
	10932	1	TH01	6
	10358	0.95	TH01	9.3
	10477	1	D13S317	8
	9607	0.92	D13S317	11
	18860	1	D16S539	11
	5740	1	D2S1338	22
	5303	0.92	D2S1338	24
	9373	1	D19S433	13
	8818	0.94	D19S433	15
	11539	1	vWA	17
	10214	0.89	vWA	18
	9141	1	TPOX	8
	8674	0.95	TPOX	11
	7192	1	D18S51	15
	6388	0.89	D18S51	16
	12943	1	AMEL	X
	13506	1	D5S818	11
	4737	1	FGA	23
	4275	0.9	FGA	26
297E	13417	1	D8S1179	13 Minus A, Imbalance
	12221	0.91	D8S1179	14
	13116	1	D21S11	31.2
	11640	0.89	D21S11	32.2
	9914	1	D7S820	11
	12779	1	CSF1PO	10
	11746	0.98	D3S1358	14
	8654	0.72	D3S1358	19
	11460	0.98	TH01	7
	11671	1	TH01	8.3
	14486	1	D13S317	8
	13999	0.97	D13S317	11
	11644	0.8	D16S539	9

	14588	1	D16S539	13	
	10092	1	D2S1338	17	
	8206	0.81	D2S1338	24	
	14371	1	D19S433	13	
	8048	0.56	D19S433	14	
	13645	1	vWA	18	
	13199	0.97	vWA	19	
	12759	1	TPOX	8	
	11564	0.91	TPOX	11	
	7697	1	D18S51	14	
	6543	0.85	D18S51	17	
	13750	1	AMEL	X	
	11003	0.8	AMEL	Y	
	11671	1	D5S818	11	
	11659	1	D5S818	12	
	6845	1	FGA	20	
	6314	0.92	FGA	21	
3104E	10584	1	D8S1179	13	Minus A
	9125	0.86	D8S1179	14	
	8411	1	D21S11	28	
	8120	0.97	D21S11	30	
	7472	1	D7S820	10	
	9437	1	CSF1PO	10	
	9075	1	D3S1358	17	
	8063	0.89	D3S1358	18	
	17086	1	TH01	9.3	
	12318	1	D13S317	8	
	10902	0.89	D13S317	11	
	13327	1	D16S539	12	
	12299	0.92	D16S539	13	
	5937	1	D2S1338	24	
	5321	0.9	D2S1338	25	
	10825	1	D19S433	13	
	9833	0.91	D19S433	15	
	12291	1	vWA	14	
	10813	0.88	vWA	19	
	8903	1	TPOX	11	
	8175	0.92	TPOX	12	
	6018	1	D18S51	13	
	5297	0.88	D18S51	17	
	11877	1	AMEL	X	
	11395	0.96	AMEL	Y	
	14375	1	D5S818	13	
	4774	1	FGA	23	
	4432	0.93	FGA	25	

311E	17306	1	D8S1179	12	Minus A, Imbalance
	11093	1	D21S11	28	
	10802	0.97	D21S11	29	
	4397	1	D7S820	10	
	3966	0.9	D7S820	13	
	6453	1	CSF1PO	10	
	5879	0.91	CSF1PO	11	
	12430	0.93	D3S1358	11	
	13343	1	D3S1358	15	
	14987	1	TH01	6	
	14907	0.99	TH01	9.3	
	12409	0.87	D13S317	8	
	14259	1	D13S317	11	
	14396	0.99	D16S539	13	
	14471	1	D16S539	15	
	8301	1	D2S1338	19	
	6883	0.83	D2S1338	26	
	14130	0.95	D19S433	12	
	13555	0.91	D19S433	14	
	3551	0.3	vWA	15	
	11800	1	vWA	17	
	13880	1	TPOX	8	
	12856	0.93	TPOX	11	
	14034	1	D18S51	15	
	5723	1	AMEL	X	
	11267	1	D5S818	12	
	11060	0.98	D5S818	13	
	7090	1	FGA	20	
	5894	0.83	FGA	24	
312A	15000	1	D8S1179	10	Minus A
	14304	0.95	D8S1179	14	
	13037	1	D21S11	30	
	11662	0.89	D21S11	31	
	6455	1	D7S820	10	
	6283	0.97	D7S820	12	
	14201	1	CSF1PO	12	
	12208	0.98	D3S1358	14	
	12461	1	D3S1358	16	
	14574	0.83	TH01	6	
	17602	1	TH01	9	
	14622	0.98	D13S317	8	
	14890	1	D13S317	9	
	22760	1	D16S539	11	
	10621	1	D2S1338	18	
	9803	0.92	D2S1338	22	
	12916	1	D19S433	15	

	12349	0.96	D19S433	16.2
	14953	1	vWA	16
	14158	0.95	vWA	18
	14720	1	TPOX	8
	14318	0.97	TPOX	11
	11540	1	D18S51	12
	10609	0.92	D18S51	13
	11676	0.92	AMEL	X
	12719	1	AMEL	Y
	10709	0.95	D5S818	12
	11305	1	D5S818	13
	9213	1	FGA	20
	8474	0.92	FGA	21
312BE	13512	1	D8S1179	12 Minus A
	7540	1	D21S11	28
	7115	0.94	D21S11	31.2
	3536	1	D7S820	9
	3227	0.91	D7S820	12
	4029	1	CSF1PO	11
	3783	0.94	CSF1PO	12
	14186	1	D3S1358	14
	9314	1	TH01	6
	9230	0.99	TH01	8
	10125	1	D13S317	9
	9330	0.92	D13S317	11
	14527	1	D16S539	12
	5162	1	D2S1338	23
	4909	0.95	D2S1338	25
	4848	0.61	D19S433	14
	7896	1	D19S433	15.2
	9916	1	vWA	14
	9335	0.94	vWA	16
	7800	1	TPOX	9
	7213	0.92	TPOX	11
	5173	1	D18S51	14
	4472	0.86	D18S51	18
	11957	1	AMEL	X
	9084	1	D5S818	11
	8286	0.91	D5S818	12
	4765	1	FGA	19
	4437	0.93	FGA	21
3258E	7184	1	D8S1179	10 Minus A
	6288	0.88	D8S1179	15
	5693	1	D21S11	29
	5388	0.95	D21S11	31.2

	4046	1	D7S820	9
	3847	0.95	D7S820	12
	5348	1	CSF1PO	10
	5125	0.96	CSF1PO	13
	8320	1	D3S1358	15
	7777	0.93	D3S1358	17
	8789	1	TH01	6
	8296	0.94	TH01	7
	10008	1	D13S317	9
	9536	0.95	D13S317	11
	14913	1	D16S539	13
	7342	1	D2S1338	19
	6932	0.94	D2S1338	20
	8251	1	D19S433	14
	7070	0.86	D19S433	15
	9063	1	vWA	15
	8994	0.99	vWA	18
	14191	1	TPOX	11
	8318	1	D18S51	13
	7704	0.93	D18S51	14
	7115	0.93	AMEL	X
	7626	1	AMEL	Y
	7441	0.94	D5S818	11
	7938	1	D5S818	12
	5731	1	FGA	21
	5428	0.95	FGA	26
333E	13868	0.97	D8S1179	10 Minus A
	14346	1	D8S1179	12
	11914	1	D21S11	27
	11201	0.94	D21S11	29
	10792	1	D7S820	12
	7228	1	CSF1PO	12
	6629	0.92	CSF1PO	13
	14892	0.99	D3S1358	15
	15042	1	D3S1358	17
	14372	1	TH01	9.3
	14494	1	D13S317	8
	13036	0.9	D13S317	13
	14994	1	D16S539	8
	13107	0.87	D16S539	12
	9501	1	D2S1338	17
	7177	0.76	D2S1338	25
	11423	0.84	D19S433	14
	10364	0.76	D19S433	16.2
	13280	1	vWA	14
	11778	0.89	vWA	17

	15608	1	TPOX	8	
	10881	1	D18S51	12	
	8988	0.83	D18S51	16	
	6322	1	AMEL	X	
	11719	1	D5S818	12	
	11372	0.97	D5S818	13	
	6375	1	FGA	23	
	5677	0.89	FGA	26	
338E	16495	1	D8S1179	13	Minus A, Stutter
	13785	1	D21S11	29	
	13043	0.95	D21S11	31	
	7046	1	D7S820	9	
	6984	0.99	D7S820	10	
	7441	1	CSF1PO	11	
	7072	0.95	CSF1PO	13	
	14645	1	D3S1358	16	
	14462	0.98	TH01	7	
	14741	1	TH01	9.3	
	14681	0.99	D13S317	12	
	14890	1	D13S317	13	
	18480	1	D16S539	11	
	14863	0.8	D16S539	12	
	10333	1	D2S1338	24	
	8612	0.83	D2S1338	25	
	13430	0.89	D19S433	14	
	14259	0.95	D19S433	15	
	13665	0.91	vWA	16	
	14271	1	TPOX	8	
	14115	0.99	TPOX	11	
	10951	1	D18S51	12	
	8756	0.8	D18S51	17	
	7879	1	AMEL	X	
	6097	0.92	D5S818	12	
	9310	1	FGA	20	
	8473	0.91	FGA	22	
3664E	11665	1	D8S1179	11	Minus A
	10150	0.87	D8S1179	15	
	10251	1	D21S11	33.2	
	5403	1	D7S820	8	
	5010	0.93	D7S820	11	
	6509	1	CSF1PO	10	
	5944	0.91	CSF1PO	12	
	15197	1	D3S1358	15	
	13207	1	TH01	6	
	13194	1	TH01	9.3	

	14113	1	D13S317	8
	13777	0.98	D13S317	9
	12302	0.85	D16S539	9
	14446	1	D16S539	13
	8476	1	D2S1338	20
	7964	0.94	D2S1338	23
	11739	1	D19S433	14
	10985	0.94	D19S433	16
	15116	1	vWA	15
	10747	1	TPOX	8
	10462	0.97	TPOX	11
	8921	1	D18S51	12
	8870	0.99	D18S51	14
	12006	1	AMEL	X
	11620	0.97	AMEL	Y
	13848	1	D5S818	12
	7412	1	FGA	20
	6372	0.86	FGA	24
3701E	7286	1	D8S1179	11 Minus A, Imbalance
	6814	0.94	D8S1179	14
	6384	1	D21S11	28
	6145	0.96	D21S11	29
	3361	1	D7S820	8
	3139	0.93	D7S820	10
	4084	1	CSF1PO	11
	3831	0.94	CSF1PO	12
	7613	1	D3S1358	17
	6718	0.88	D3S1358	18
	8228	1	TH01	6
	8029	0.98	TH01	9.3
	14657	1	D13S317	11
	9886	1	D16S539	11
	9453	0.96	D16S539	13
	5401	1	D2S1338	24
	4636	0.86	D2S1338	25
	14756	1	D19S433	12
	9044	1	vWA	14
	8588	0.95	vWA	16
	6724	1	TPOX	8
	6326	0.94	TPOX	11
	6137	1	D18S51	15
	5440	0.89	D18S51	16
	8571	1	AMEL	X
	2085	0.24	AMEL	Y
	8292	1	D5S818	11
	7971	0.96	D5S818	12

	5169	1	FGA	19	
	4158	0.8	FGA	25	
3805E	9802	1	D8S1179	12	Minus A, Allelic Dropout
	8593	0.88	D8S1179	13	
	7655	1	D21S11	28	
	7355	0.96	D21S11	31	
	4613	1	D7S820	9	
	4340	0.94	D7S820	11	
	5537	1	CSF1PO	11	
	5381	0.97	CSF1PO	15	
	10085	1	D3S1358	14	
	9455	0.94	D3S1358	16	
	17088	1	TH01	9.3	
	12143	1	D13S317	12	
	11134	0.92	D13S317	13	
	13730	0.98	D16S539	10	
	13986	1	D16S539	12	
	7178	1	D2S1338	22	
	6740	0.94	D2S1338	24	
	13468	1	D19S433	12	
	11907	1	vWA	17	
	11399	0.96	vWA	18	
	9935	1	TPOX	8	
	9443	0.95	TPOX	9	
	8956	1	D18S51	14	
	8233	0.92	D18S51	15	
	10791	1	AMEL	X	
	11699	1	D5S818	11	
	6759	1	FGA	22	
	6092	0.9	FGA	23	
399E	14232	1	D8S1179	11	Minus A
	13794	0.97	D8S1179	14	
	14200	1	D21S11	28	
	12528	0.88	D21S11	33.2	
	11636	1	D7S820	10	
	13370	1	CSF1PO	12	
	17091	0.92	D3S1358	16	
	14834	1	TH01	7	
	14210	0.96	TH01	8	
	12237	0.88	D13S317	12	
	13939	1	D13S317	14	
	17503	1	D16S539	11	
	14683	0.84	D16S539	12	
	10554	1	D2S1338	18	
	10108	0.96	D2S1338	19	

	14147	0.97	D19S433	14	
	12994	0.89	D19S433	15.2	
	14962	1	vWA	17	
	14087	0.94	vWA	18	
	13473	1	TPOX	8	
	13358	0.99	TPOX	11	
	14679	1	D18S51	16	
	5482	1	AMEL	X	
	8733	1	D5S818	11	
	7900	1	FGA	19	
	6526	0.83	FGA	24	
417E	10759	1	D8S1179	13	Minus A
	5426	1	D21S11	29	
	5100	0.94	D21S11	30	
	3627	1	D7S820	8	
	3553	0.98	D7S820	10	
	4176	1	CSF1PO	10	
	3751	0.9	CSF1PO	12	
	12516	1	D3S1358	15	
	8242	1	TH01	6	
	7783	0.94	TH01	9	
	9853	1	D13S317	8	
	8715	0.88	D13S317	11	
	9691	1	D16S539	11	
	8934	0.92	D16S539	12	
	6290	1	D2S1338	17	
	6099	0.97	D2S1338	19	
	6028	1	D19S433	14	
	5851	0.97	D19S433	15.2	
	8431	1	vWA	14	
	7625	0.9	vWA	19	
	6678	1	TPOX	8	
	6311	0.95	TPOX	11	
	6635	1	D18S51	14	
	6185	0.93	D18S51	15	
	7307	0.99	AMEL	X	
	7359	1	AMEL	Y	
	7247	1	D5S818	12	
	6801	0.94	D5S818	13	
	5367	1	FGA	22	
	4763	0.89	FGA	23	
420E	4680	1	D8S1179	13	Minus A
	4288	0.92	D8S1179	14	
	3718	1	D21S11	31.2	
	3472	0.93	D21S11	33.2	

	2274	1	D7S820	9
	2134	0.94	D7S820	12
	2624	1	CSF1PO	12
	2341	0.89	CSF1PO	14
	4892	1	D3S1358	14
	4809	0.98	D3S1358	16
	5536	1	TH01	6
	5428	0.98	TH01	8
	10781	1	D13S317	12
	6410	1	D16S539	11
	5938	0.93	D16S539	13
	7130	1	D2S1338	19
	8260	1	D19S433	15
	5473	1	vWA	19
	4998	0.91	vWA	20
	9439	1	TPOX	8
	7063	1	D18S51	16
	5559	0.97	AMEL	X
	5727	1	AMEL	Y
	9491	1	D5S818	11
	3172	1	FGA	21
	2879	0.91	FGA	25
4375E	5126	1	D8S1179	11 Minus A
	4649	0.91	D8S1179	14
	4651	1	D21S11	28
	4259	0.92	D21S11	29
	1877	1	D7S820	7
	1618	0.86	D7S820	12
	2334	1	CSF1PO	11
	2146	0.92	CSF1PO	12
	4470	0.95	D3S1358	15
	3912	0.83	D3S1358	16
	5583	1	TH01	7
	5537	0.99	TH01	9.3
	5631	1	D13S317	8
	4873	0.87	D13S317	12
	6432	1	D16S539	12
	5949	0.92	D16S539	13
	3146	1	D2S1338	17
	2710	0.86	D2S1338	23
	5500	1	D19S433	13
	5360	0.97	D19S433	13.2
	5799	1	vWA	17
	5213	0.9	vWA	18
	4216	0.99	TPOX	9
	4274	1	TPOX	11

	2898	1	D18S51	12
	2110	0.73	D18S51	20
	12188	1	AMEL	X
	9467	1	D5S818	11
	4345	1	FGA	23
444E	12517	1	D8S1179	12 Minus A, Partial Profile, Imba
	11892	0.95	D8S1179	13
	12433	1	D21S11	29
	11874	0.96	D21S11	30
	6358	1	D7S820	8
	5584	0.88	D7S820	11
	6734	1	CSF1PO	10
	6421	0.95	CSF1PO	11
	11019	1	D3S1358	15
	9984	0.91	D3S1358	16
	12270	0.88	D13S317	9
	13901	1	D13S317	12
	14737	1	D16S539	11
	14106	0.96	D16S539	13
	9648	1	D2S1338	18
	7472	0.77	D2S1338	26
	12384	1	D19S433	13
	11158	0.9	D19S433	14
	11028	1	TPOX	8
	10775	0.98	TPOX	11
	3392	0.46	D18S51	12
	7346	1	D18S51	16
	12575	1	AMEL	X
	11800	1	D5S818	12
	11538	0.98	D5S818	13
	7539	1	FGA	23
	6468	0.86	FGA	24
550E	11054	1	D8S1179	13 Minus A
	10198	0.92	D8S1179	14
	10160	1	D21S11	28
	9481	0.93	D21S11	30
	5260	1	D7S820	7
	4916	0.93	D7S820	10
	5805	1	CSF1PO	11
	5339	0.92	CSF1PO	13
	10680	1	D3S1358	15
	9559	0.9	D3S1358	17
	12300	0.89	TH01	6
	13860	1	TH01	7
	14038	1	D13S317	10

	13040	0.93	D13S317	12	
	13097	1	D16S539	11	
	12234	0.93	D16S539	12	
	8166	1	D2S1338	19	
	7514	0.92	D2S1338	21	
	10834	1	D19S433	15.2	
	9684	0.89	D19S433	16.2	
	13227	1	vWA	14	
	11998	0.91	vWA	18	
	11177	1	TPOX	9	
	10813	0.97	TPOX	11	
	7938	1	D18S51	14	
	7146	0.9	D18S51	16	
	12449	0.98	AMEL	X	
	12644	1	AMEL	Y	
	14898	1	D5S818	11	
	7238	1	FGA	19	
	6586	0.91	FGA	20	
565E	8144	0.99	D8S1179	10	
	8192	1	D8S1179	12	
	12830	1	D21S11	29	
	4077	1	D7S820	11	
	3930	0.96	D7S820	12	
	5071	1	CSF1PO	9	
	4628	0.91	CSF1PO	12	
	9469	1	D3S1358	14	
	8781	0.93	D3S1358	17	
	14676	1	TH01	9.3	
	14615	1	D13S317	12	
	9748	1	D16S539	11	
	8951	0.92	D16S539	13	
	6100	1	D2S1338	17	
	5258	0.86	D2S1338	22	
	13799	1	D19S433	13	
	13153	1	vWA	14	
	11365	0.86	vWA	20	
	14555	1	TPOX	8	
	5926	1	D18S51	18	
	5496	0.93	D18S51	21	
	8912	0.98	AMEL	X	
	9082	1	AMEL	Y	
	7211	1	D5S818	11	
	7082	0.98	D5S818	12	
	9647	1	FGA	21	
589E	14533	1	D8S1179	13	Minus A, Imbalance

7916	1	D21S11	30	
7905	1	D21S11	31.2	
4567	0.93	D7S820	10	
4897	1	D7S820	12	
5686	1	CSF1PO	10	
5111	0.9	CSF1PO	13	
8982	1	D3S1358	14	
8626	0.96	D3S1358	16	
16797	1	TH01	9.3	
11283	1	D13S317	11	
11004	0.98	D13S317	13	
13994	1	D16S539	9	
12424	0.89	D16S539	11	
7904	1	D2S1338	17	
6449	0.82	D2S1338	24	
8786	1	D19S433	14.2	
2099	0.24	D19S433	16	
14741	1	vWA	16	
14476	1	TPOX	8	
14622	1	D18S51	12	
11531	1	AMEL	X	
14441	1	D5S818	12	
6297	1	FGA	21	
5340	0.85	FGA	26	
6080E	12023	1	D8S1179	9 Minus A
	11822	0.98	D8S1179	13
	10761	1	D21S11	28
	10166	0.94	D21S11	30
	8618	1	D7S820	8
	12126	1	CSF1PO	12
	10144	1	D3S1358	15
	9372	0.92	D3S1358	17
	22254	1	TH01	9.3
	11369	1	D13S317	11
	11034	0.97	D13S317	12
	20962	1	D16S539	9
	8217	1	D2S1338	17
	6673	0.81	D2S1338	24
	10769	1	D19S433	13
	9788	0.91	D19S433	14
	14557	1	vWA	17
	12592	0.87	vWA	19
	13046	0.98	TPOX	9
	13277	1	TPOX	11
	6927	1	D18S51	14
	6420	0.93	D18S51	16

	16152	1	AMEL	X	
	9175	1	D5S818	11	
	8667	0.94	D5S818	13	
	4432	1	FGA	20	
	3864	0.87	FGA	23	
6233E	6798	0.7	D8S1179	10	Minus A, Partial Profile
	5457	0.56	D8S1179	15	
	5445	1	D21S11	27	
	4687	0.86	D21S11	29	
	1282	1	D7S820	9	
	1210	0.94	D7S820	12	
	4336	0.74	D3S1358	16	
	4255	0.73	D3S1358	17	
	6823	1	TH01	9	
	6764	0.99	TH01	9.3	
	4686	1	D13S317	10	
	4401	0.94	D13S317	12	
	14895	1	D16S539	11	
	4121	1	D2S1338	19	
	4030	0.98	D2S1338	20	
	14549	1	D19S433	14	
	6590	0.76	vWA	17	
	6745	0.78	vWA	18	
	4309	1	TPOX	8	
	4207	0.98	TPOX	11	
	2423	1	D18S51	12	
	2189	0.9	D18S51	14	
	9800	1	AMEL	X	
	8786	0.9	AMEL	Y	
	6101	1	D5S818	10	
	5492	0.9	D5S818	11	
	1954	1	FGA	20	
	1741	0.89	FGA	22	
651E	14725	1	D8S1179	10	Minus A
	14330	0.97	D8S1179	15	
	13903	1	D21S11	29	
	12664	0.91	D21S11	32.2	
	5745	1	D7S820	10	
	5424	0.94	D7S820	12	
	12541	1	CSF1PO	12	
	14546	1	D3S1358	14	
	13569	0.93	D3S1358	17	
	15153	1	TH01	8	
	14880	0.98	TH01	9	
	14660	1	D13S317	11	

	12995	0.89	D13S317	12
	16892	1	D16S539	11
	9250	1	D2S1338	20
	8483	0.92	D2S1338	22
	11342	0.8	D19S433	13
	14065	1	D19S433	15.2
	14047	0.67	vWA	17
	14642	1	TPOX	8
	7018	1	D18S51	16
	5186	0.74	D18S51	22
	7981	1	AMEL	X
	9847	0.96	D5S818	11
	10272	1	D5S818	12
	11711	1	FGA	25
709E	14417	1	D8S1179	10 Minus A
	14472	1	D8S1179	13
	13997	1	D21S11	28
	11591	0.83	D21S11	32.2
	8049	1	D7S820	8
	7734	0.96	D7S820	11
	8800	1	CSF1PO	11
	8064	0.92	CSF1PO	12
	14656	1	D3S1358	17
	14232	0.97	D3S1358	18
	16566	1	TH01	6
	15452	0.93	TH01	7
	11079	1	D13S317	8
	12720	0.76	D16S539	8
	16753	1	D16S539	13
	12680	1	D2S1338	17
	10428	0.82	D2S1338	24
	14846	0.98	D19S433	14
	14697	1	vWA	14
	14558	0.99	vWA	17
	17381	1	TPOX	8
	11265	1	D18S51	13
	10176	0.9	D18S51	16
	5883	1	AMEL	X
	12643	1	D5S818	10
	9718	0.77	D5S818	11
	11132	1	FGA	20
	8781	0.79	FGA	24.2
735E	8312	1	D8S1179	12 Minus A
	7439	0.89	D8S1179	13
	6342	1	D21S11	29

	5642	0.89	D21S11	32.2
	6994	1	D7S820	10
	9100	1	CSF1PO	11
	14932	1	D3S1358	15
	10254	1	TH01	8
	10300	1	TH01	9.3
	10583	1	D13S317	11
	9792	0.93	D13S317	12
	11815	1	D16S539	11
	10673	0.9	D16S539	12
	6666	1	D2S1338	19
	5804	0.87	D2S1338	24
	8969	1	D19S433	13
	8289	0.92	D19S433	14
	10659	1	vWA	17
	9466	0.89	vWA	18
	9123	1	TPOX	8
	8573	0.94	TPOX	11
	6171	1	D18S51	18
	5252	0.85	D18S51	22
	9292	1	AMEL	X
	9270	1	AMEL	Y
	7954	0.97	D5S818	11
	8164	1	D5S818	13
	4665	1	FGA	22.2
	4280	0.92	FGA	24
746E	6544	1	D8S1179	11 Minus A
	5969	0.91	D8S1179	13
	5015	1	D21S11	30
	4999	1	D21S11	31.2
	3691	1	D7S820	8
	3536	0.96	D7S820	10
	4374	1	CSF1PO	11
	4023	0.92	CSF1PO	12
	8550	1	D3S1358	14
	8052	0.94	D3S1358	15
	14615	1	TH01	6
	9820	1	D13S317	9
	9255	0.94	D13S317	10
	9526	1	D16S539	9
	9242	0.97	D16S539	13
	6039	1	D2S1338	19
	5136	0.85	D2S1338	25
	6600	1	D19S433	14.2
	6403	0.97	D19S433	15
	8401	1	vWA	18

	7796	0.93	vWA	19	
	14009	1	TPOX	8	
	6462	1	D18S51	15	
	5879	0.91	D18S51	18	
	7702	1	AMEL	X	
	7646	0.99	AMEL	Y	
	7509	0.95	D5S818	11	
	7894	1	D5S818	12	
	5085	1	FGA	24	
	4577	0.9	FGA	25	
7485E	6005	1	D8S1179	8	Minus A, Imbalance
	5412	0.9	D8S1179	13	
	4767	1	D21S11	31.2	
	4492	0.94	D21S11	32.2	
	2677	1	D7S820	8	
	2491	0.93	D7S820	12	
	3217	1	CSF1PO	10	
	3129	0.97	CSF1PO	12	
	5837	1	D3S1358	15	
	5445	0.93	D3S1358	17	
	6393	1	TH01	6	
	6040	0.94	TH01	9.3	
	7537	1	D13S317	12	
	7226	0.96	D13S317	13	
	14107	1	D16S539	12	
	5252	1	D2S1338	14	
	3622	0.69	D2S1338	26	
	6680	1	D19S433	12	
	6369	0.95	D19S433	13	
	6346	1	vWA	16	
	6059	0.95	vWA	19	
	5308	1	TPOX	8	
	5135	0.97	TPOX	10	
	4825	1	D18S51	13	
	4476	0.93	D18S51	14	
	6863	1	AMEL	X	
	6890	1	AMEL	Y	
	6617	1	D5S818	12	
	6027	0.91	D5S818	13	
	7105	1	FGA	24	
7572E	9604	1	D8S1179	10	Minus A
	8782	0.91	D8S1179	14	
	7868	1	D21S11	28	
	7789	0.99	D21S11	30	
	8352	1	D7S820	10	

	5445	1	CSF1PO	10
	5031	0.92	CSF1PO	12
	9522	1	D3S1358	17
	8606	0.9	D3S1358	18
	10074	0.99	TH01	7
	10227	1	TH01	9.3
	13601	1	D13S317	11
	12949	1	D16S539	12
	12376	0.96	D16S539	13
	7501	1	D2S1338	17
	6286	0.84	D2S1338	24
	10682	1	D19S433	14
	9598	0.9	D19S433	15
	11408	1	vWA	15
	10783	0.95	vWA	16
	13177	1	TPOX	8
	8338	1	D18S51	10
	7215	0.87	D18S51	14
	13604	1	AMEL	X
	13051	1	D5S818	12
	6312	1	FGA	22
	5670	0.9	FGA	25
7758E	6965	0.74	D8S1179	10 Minus A
	5879	0.62	D8S1179	14
	6606	1	D21S11	28
	6378	0.97	D21S11	30
	1991	1	D7S820	9
	1977	0.99	D7S820	13
	3017	1	CSF1PO	10
	2750	0.91	CSF1PO	12
	7514	0.77	D3S1358	15
	7911	0.99	TH01	7
	7985	1	TH01	9.3
	6112	1	D13S317	11
	5749	0.94	D13S317	14
	10135	1	D16S539	9
	9337	0.92	D16S539	12
	5412	1	D2S1338	17
	4345	0.8	D2S1338	24
	7486	1	D19S433	14
	7026	0.94	D19S433	16
	7373	0.86	vWA	16
	7032	0.82	vWA	19
	10952	1	TPOX	8
	2980	1	D18S51	15
	2815	0.94	D18S51	17

	9485	1	AMEL	X
	6161	1	D5S818	11
	5651	0.92	D5S818	12
	2458	1	FGA	23
	2207	0.9	FGA	24
777E	6732	1	D8S1179	8
	5839	0.87	D8S1179	15
	5176	1	D21S11	29
	5090	0.98	D21S11	32.2
	3908	1	D7S820	10
	3769	0.96	D7S820	13
	8734	1	CSF1PO	10
	8391	1	D3S1358	14
	7860	0.94	D3S1358	15
	6918	1	TH01	6
	6782	0.98	TH01	9.3
	9871	1	D13S317	8
	9472	0.96	D13S317	11
	8720	1	D16S539	9
	8689	1	D16S539	12
	5744	1	D2S1338	20
	5727	1	D2S1338	23
	6836	1	D19S433	13
	6514	0.95	D19S433	15
	8646	1	vWA	16
	8439	0.98	vWA	18
	6403	1	TPOX	9
	6104	0.95	TPOX	11
	7358	1	D18S51	13
	6844	0.93	D18S51	14
	12079	1	AMEL	X
	13679	1	D5S818	9
	5382	1	FGA	21
	5037	0.94	FGA	25
802E	14366	1	D8S1179	10 Minus A
	13527	0.94	D8S1179	11
	12314	1	D21S11	28
	10827	0.88	D21S11	31
	5485	1	D7S820	10
	5035	0.92	D7S820	12
	11163	1	CSF1PO	12
	12583	1	D3S1358	15
	11493	0.91	D3S1358	16
	11842	1	TH01	6
	11074	0.94	TH01	9.3

14475	1	D13S317	10	
11314	0.78	D13S317	11	
14536	0.99	D16S539	10	
14742	1	D16S539	11	
8493	1	D2S1338	18	
7389	0.87	D2S1338	23	
12798	1	D19S433	14	
11871	0.93	D19S433	15.2	
14835	1	vWA	16	
11774	1	TPOX	10	
11215	0.95	TPOX	11	
7178	1	D18S51	16	
6676	0.93	D18S51	18	
11396	0.95	AMEL	X	
12025	1	AMEL	Y	
13012	1	D5S818	9	
11413	0.88	D5S818	11	
7808	1	FGA	20	
7262	0.93	FGA	22	

9066E	10201	1	D8S1179	11 Minus A, Imbalance
	9797	0.96	D8S1179	13
	8960	1	D21S11	28
	7918	0.88	D21S11	30
	4335	1	D7S820	9
	3527	0.81	D7S820	11
	9972	1	CSF1PO	11
	9807	1	D3S1358	17
	8577	0.87	D3S1358	18
	13028	1	TH01	7
	12746	0.98	TH01	9.3
	12891	1	D13S317	8
	10871	0.84	D13S317	13
	20025	1	D16S539	11
	7446	1	D2S1338	20
	6867	0.92	D2S1338	21
	14804	1	D19S433	12
	10640	0.72	D19S433	15
	12627	1	vWA	18
	11349	0.9	vWA	19
	14695	1	TPOX	9
	7672	1	D18S51	12
	6214	0.81	D18S51	16
	11712	1	AMEL	X
	4482	0.38	AMEL	Y
	10416	1	D5S818	10
	9434	0.91	D5S818	13

	5036	1	FGA	23	
	4663	0.93	FGA	26	
940E	5412	1	D8S1179	14	
	5245	0.97	D8S1179	15	
	8034	1	D21S11	30	
	3063	1	D7S820	8	
	2997	0.98	D7S820	11	
	3622	1	CSF1PO	11	
	3387	0.94	CSF1PO	12	
	6713	1	D3S1358	14	
	6415	0.96	D3S1358	15	
	5911	1	TH01	6	
	5741	0.97	TH01	9	
	7123	1	D13S317	10	
	6606	0.93	D13S317	11	
	14256	1	D16S539	9	
	4830	1	D2S1338	19	
	4284	0.89	D2S1338	22	
	5592	1	D19S433	13	
	5477	0.98	D19S433	13.2	
	6954	1	vWA	16	
	6735	0.97	vWA	19	
	5844	1	TPOX	9	
	5711	0.98	TPOX	11	
	5538	1	D18S51	14	
	5048	0.91	D18S51	17	
	10019	1	AMEL	X	
	5644	1	D5S818	12	
	4927	0.87	D5S818	13	
	7526	1	FGA	22	
9439E	7773	1	D8S1179	14	Minus A
	7256	0.93	D8S1179	15	
	12646	1	D21S11	30	
	4664	0.99	D7S820	8	
	4693	1	D7S820	11	
	5338	1	CSF1PO	10	
	5024	0.94	CSF1PO	12	
	12716	1	D3S1358	16	
	8804	1	TH01	7	
	8705	0.99	TH01	9.3	
	10677	1	D13S317	11	
	10092	0.95	D13S317	12	
	14840	1	D16S539	11	
	7113	1	D2S1338	19	
	7048	0.99	D2S1338	22	

	8308	1	D19S433	15
	7604	0.92	D19S433	17.2
	10323	1	vWA	14
	9665	0.94	vWA	18
	7640	1	TPOX	8
	7651	1	TPOX	9
	8669	1	D18S51	12
	7408	0.85	D18S51	16
	7780	0.93	AMEL	X
	8350	1	AMEL	Y
	8370	0.96	D5S818	12
	8685	1	D5S818	13
	6090	1	FGA	21
	5897	0.97	FGA	23
9899E	14056	1	D8S1179	9 Minus A, Imbalance
	12236	0.87	D8S1179	15
	20565	1	D21S11	28
	5050	1	D7S820	11
	1579	0.31	D7S820	12
	12196	1	CSF1PO	12
	15814	1	D3S1358	18
	21713	1	TH01	9.3
	11039	0.83	D13S317	12
	13348	1	D13S317	13
	15536	1	D16S539	10
	14791	0.95	D16S539	12
	10132	1	D2S1338	17
	8886	0.88	D2S1338	22
	14182	0.98	D19S433	12
	14314	0.99	D19S433	13.2
	14504	1	vWA	17
	14337	0.99	vWA	18
	18532	1	TPOX	11
	7313	1	D18S51	19
	6510	0.89	D18S51	20
	8785	1	AMEL	X
	11290	0.99	D5S818	9
	11400	1	D5S818	11
	6960	1	FGA	20
	5821	0.84	FGA	24
CaseyE	8072	1	D8S1179	10 Imbalance
	7703	0.95	D8S1179	12
	4608	1	D21S11	28
	4571	0.99	D21S11	31.2
	3023	1	D7S820	8

2648	0.88	D7S820	11
3038	0.95	CSF1PO	10
3192	1	CSF1PO	11
14516	1	D3S1358	14
7870	1	TH01	6
7217	0.92	TH01	8
7600	1	D13S317	9
7033	0.93	D13S317	11
6677	1	D16S539	11
6502	0.97	D16S539	12
3390	1	D2S1338	20
3221	0.95	D2S1338	25
1746	0.24	D19S433	14
7366	1	D19S433	16
14272	1	vWA	18
6053	1	TPOX	9
5754	0.95	TPOX	11
5392	1	D18S51	10
4459	0.83	D18S51	14
13320	1	AMEL	X
8225	1	D5S818	12
7637	0.93	D5S818	13
4406	1	FGA	20
4142	0.94	FGA	21
ChristiE 1140	1	D8S1179	14
930	0.9	D3S1358	14
1036	1	D3S1358	16
1388	1	TH01	6
1218	1	D13S317	11
572	1	D16S539	11
815	1	D19S433	15
749	0.92	D19S433	16
814	1	vWA	14
714	0.88	vWA	18
716	1	D18S51	12
1558	1	AMEL	X
786	1	D5S818	11
615	0.78	D5S818	12
JDWE 8525	1	D8S1179	10 Imbalance
6200	0.73	D8S1179	14
4014	1	D21S11	30
3653	0.91	D21S11	31
2160	0.96	D7S820	10
2260	1	D7S820	12
4262	1	CSF1PO	12

9170	1	D3S1358	14
8553	0.93	D3S1358	16
6479	0.99	TH01	6
6536	1	TH01	9
6671	1	D13S317	8
6561	0.98	D13S317	9
10804	1	D16S539	11
3272	1	D2S1338	18
2819	0.86	D2S1338	22
6652	1	D19S433	15
6525	0.98	D19S433	16.2
7306	1	vWA	16
6836	0.94	vWA	18
4540	1	TPOX	8
4496	0.99	TPOX	11
3824	1	D18S51	12
3448	0.9	D18S51	13
7437	1	AMEL	X
7434	1	AMEL	Y
8977	1	D5S818	12
6231	0.69	D5S818	13
3601	0.94	FGA	20
3829	1	FGA	21

LouieE	2146	1	D8S1179	12
	1934	0.9	D8S1179	13
	2144	1	D21S11	29
	583	1	D7S820	10
	559	0.96	D7S820	12
	1378	1	CSF1PO	10
	2661	1	D3S1358	15
	2664	1	D3S1358	18
	3225	1	TH01	9.3
	3344	1	D13S317	12
	3129	1	D16S539	12
	863	1	D2S1338	23
	757	0.88	D2S1338	24
	4414	1	D19S433	14
	2346	1	vWA	15
	1852	0.79	vWA	18
	1380	1	TPOX	7
	1231	0.89	TPOX	8
	1208	1	D18S51	12
	958	0.79	D18S51	14
	4400	1	AMEL	X
	3576	1	D5S818	12
	1065	0.95	FGA	22

| | 1124 | 1 | FGA | 23 | |

ADDITIONAL EXPERIMENTS

3701a	5890	1	D8S1179	11	Minus A
	5223	0.89	D8S1179	14	
	5270	1	D21S11	28	
	4918	0.93	D21S11	29	
	2464	1	D7S820	8	
	2299	0.93	D7S820	10	
	3353	1	CSF1PO	11	
	3093	0.92	CSF1PO	12	
	5415	1	D3S1358	17	
	4772	0.88	D3S1358	18	
	7118	1	TH01	6	
	6828	0.96	TH01	9.3	
	12285	1	D13S317	11	
	7602	1	D16S539	11	
	7432	0.98	D16S539	13	
	4155	1	D2S1338	24	
	3802	0.92	D2S1338	25	
	14029	1	D19S433	12	
	6950	1	vWA	14	
	6450	0.93	vWA	16	
	5719	1	TPOX	8	
	5421	0.95	TPOX	11	
	4219	1	D18S51	15	
	3842	0.91	D18S51	16	
	7334	1	AMEL	X	
	6023	0.82	AMEL	Y	
	5971	1	D5S818	11	
	5882	0.99	D5S818	12	
	3626	1	FGA	19	
	2851	0.79	FGA	25	
3701b	6607	1	D8S1179	11	Minus A
	5705	0.86	D8S1179	14	
	5696	1	D21S11	28	
	5158	0.91	D21S11	29	
	2518	1	D7S820	8	
	2396	0.95	D7S820	10	
	3369	1	CSF1PO	11	
	3127	0.93	CSF1PO	12	
	5801	1	D3S1358	17	
	4997	0.86	D3S1358	18	
	7774	1	TH01	6	
	7382	0.95	TH01	9.3	
	13140	1	D13S317	11	

	8353	1	D16S539	11
	7759	0.93	D16S539	13
	4378	1	D2S1338	24
	3872	0.88	D2S1338	25
	14455	1	D19S433	12
	7394	1	vWA	14
	6862	0.93	vWA	16
	6151	1	TPOX	8
	5701	0.93	TPOX	11
	4138	1	D18S51	15
	3816	0.92	D18S51	16
	8553	1	AMEL	X
	3862	0.45	AMEL	Y
	6558	1	D5S818	11
	6147	0.94	D5S818	12
	3655	1	FGA	19
	2898	0.79	FGA	25
3701c	8603	1	D8S1179	11 Minus A
	7557	0.88	D8S1179	14
	7529	1	D21S11	28
	7061	0.94	D21S11	29
	3456	1	D7S820	8
	3129	0.91	D7S820	10
	4754	1	CSF1PO	11
	4329	0.91	CSF1PO	12
	7965	1	D3S1358	17
	7260	0.91	D3S1358	18
	10947	1	TH01	6
	10343	0.94	TH01	9.3
	14838	1	D13S317	11
	11893	1	D16S539	11
	10776	0.91	D16S539	13
	6217	1	D2S1338	24
	5674	0.91	D2S1338	25
	14949	1	D19S433	12
	10374	1	vWA	14
	9552	0.92	vWA	16
	8242	1	TPOX	8
	7987	0.97	TPOX	11
	6119	1	D18S51	15
	5381	0.88	D18S51	16
	11061	1	AMEL	X
	4266	0.39	AMEL	Y
	8880	1	D5S818	11
	8701	0.98	D5S818	12
	5010	1	FGA	19

	3943	0.79	FGA	25	

3701d					
	5078	1	D8S1179	11	Minus A
	4842	0.95	D8S1179	14	
	4671	1	D21S11	28	
	4570	0.98	D21S11	29	
	2100	1	D7S820	8	
	1946	0.93	D7S820	10	
	2831	1	CSF1PO	11	
	2603	0.92	CSF1PO	12	
	4763	1	D3S1358	17	
	4204	0.88	D3S1358	18	
	6465	1	TH01	6	
	6346	0.98	TH01	9.3	
	11295	1	D13S317	11	
	7014	1	D16S539	11	
	6791	0.97	D16S539	13	
	3741	1	D2S1338	24	
	3319	0.89	D2S1338	25	
	13413	1	D19S433	12	
	6298	1	vWA	14	
	5656	0.9	vWA	16	
	4991	1	TPOX	8	
	4689	0.94	TPOX	11	
	3568	1	D18S51	15	
	3222	0.9	D18S51	16	
	7077	1	AMEL	X	
	6067	0.86	AMEL	Y	
	5521	1	D5S818	11	
	5193	0.94	D5S818	12	
	3127	1	FGA	19	
	2401	0.77	FGA	25	

3701e					
	7469	1	D8S1179	11	Minus A
	6682	0.89	D8S1179	14	
	6340	1	D21S11	28	
	6202	0.98	D21S11	29	
	2819	1	D7S820	8	
	2769	0.98	D7S820	10	
	3835	1	CSF1PO	11	
	3642	0.95	CSF1PO	12	
	6824	1	D3S1358	17	
	6058	0.89	D3S1358	18	
	8923	1	TH01	6	
	8542	0.96	TH01	9.3	
	11847	1	D13S317	11	
	9507	1	D16S539	11	

	8679	0.91	D16S539	13	
	4830	1	D2S1338	24	
	4406	0.91	D2S1338	25	
	14580	1	D19S433	12	
	8690	1	vWA	14	
	7814	0.9	vWA	16	
	6849	1	TPOX	8	
	6561	0.96	TPOX	11	
	4818	1	D18S51	15	
	4363	0.91	D18S51	16	
	9642	1	AMEL	X	
	4071	0.42	AMEL	Y	
	7517	1	D5S818	11	
	7050	0.94	D5S818	12	
	4162	1	FGA	19	
	3290	0.79	FGA	25	
3805C_2	6117	1	D8S1179	12	Minus A
	5790	0.95	D8S1179	13	
	5039	1	D21S11	28	
	4584	0.91	D21S11	31	
	2532	1	D7S820	9	
	2361	0.93	D7S820	11	
	3250	1	CSF1PO	11	
	3027	0.93	CSF1PO	15	
	6205	1	D3S1358	14	
	5567	0.9	D3S1358	16	
	14101	1	TH01	9.3	
	7328	1	D13S317	12	
	6612	0.9	D13S317	13	
	8637	1	D16S539	10	
	8048	0.93	D16S539	12	
	4317	1	D2S1338	22	
	4230	0.98	D2S1338	24	
	7212	1	D19S433	12	
	6864	0.95	D19S433	14	
	7056	1	vWA	17	
	6591	0.93	vWA	18	
	6067	1	TPOX	8	
	6096	1	TPOX	9	
	4784	1	D18S51	14	
	4360	0.91	D18S51	15	
	7945	1	AMEL	X	
	7927	1	AMEL	Y	
	11717	1	D5S818	11	
	3764	1	FGA	22	
	3348	0.89	FGA	23	

3805E_2	6999	1	D8S1179	12 Minus A
	6315	0.9	D8S1179	13
	5932	1	D21S11	28
	5339	0.9	D21S11	31
	2372	1	D7S820	9
	2190	0.92	D7S820	11
	3213	1	CSF1PO	11
	2801	0.87	CSF1PO	15
	6274	1	D3S1358	14
	5546	0.88	D3S1358	16
	11713	1	TH01	9.3
	7095	1	D13S317	12
	6441	0.91	D13S317	13
	9254	1	D16S539	10
	8437	0.91	D16S539	12
	4188	1	D2S1338	22
	3812	0.91	D2S1338	24
	8415	1	D19S433	12
	7311	0.87	D19S433	14
	7533	1	vWA	17
	6835	0.91	vWA	18
	6336	1	TPOX	8
	6337	1	TPOX	9
	3961	1	D18S51	14
	3574	0.9	D18S51	15
	10084	1	AMEL	X
	2274	0.23	AMEL	Y
	11823	1	D5S818	11
	3325	1	FGA	22
	3079	0.93	FGA	23
565C_2	5833	1	D8S1179	10 Minus A
	5538	0.95	D8S1179	12
	8569	1	D21S11	29
	2001	1	D7S820	11
	1880	0.94	D7S820	12
	2700	1	CSF1PO	9
	2411	0.89	CSF1PO	12
	5519	1	D3S1358	14
	4923	0.89	D3S1358	17
	13740	1	TH01	9.3
	11227	1	D13S317	12
	6950	1	D16S539	11
	6440	0.93	D16S539	13
	3956	1	D2S1338	17
	3494	0.88	D2S1338	22

	12527	1	D19S433	13
	6452	1	vWA	14
	5394	0.84	vWA	20
	11303	1	TPOX	8
	2915	1	D18S51	18
	2606	0.89	D18S51	21
	7449	1	AMEL	X
	7416	1	AMEL	Y
	5781	1	D5S818	11
	5426	0.94	D5S818	12
	5891	1	FGA	21
6233a	9502	1	D8S1179	10 Minus A
	8097	0.85	D8S1179	15
	8042	1	D21S11	27
	7424	0.92	D21S11	29
	3108	1	D7S820	9
	2803	0.9	D7S820	12
	4289	1	CSF1PO	12
	3968	0.93	CSF1PO	13
	8028	1	D3S1358	16
	7102	0.88	D3S1358	17
	10969	1	TH01	9
	10713	0.98	TH01	9.3
	9892	1	D13S317	10
	9384	0.95	D13S317	12
	15679	1	D16S539	11
	6481	1	D2S1338	19
	5843	0.9	D2S1338	20
	14904	1	D19S433	14
	10632	1	vWA	17
	9681	0.91	vWA	18
	8717	1	TPOX	8
	7863	0.9	TPOX	11
	5492	1	D18S51	12
	5126	0.93	D18S51	14
	11949	1	AMEL	X
	11513	0.96	AMEL	Y
	9623	1	D5S818	10
	9011	0.94	D5S818	11
	4551	1	FGA	20
	4187	0.92	FGA	22
6233b	5814	1	D8S1179	10 Minus A
	4953	0.85	D8S1179	15
	4899	1	D21S11	27
	4645	0.95	D21S11	29

1905	1	D7S820	9	
1724	0.9	D7S820	12	
2564	1	CSF1PO	12	
2331	0.91	CSF1PO	13	
4833	1	D3S1358	16	
4422	0.91	D3S1358	17	
6606	0.97	TH01	9	
6831	1	TH01	9.3	
6308	1	D13S317	10	
5686	0.9	D13S317	12	
13964	1	D16S539	11	
3837	1	D2S1338	19	
3624	0.94	D2S1338	20	
11418	1	D19S433	14	
6300	1	vWA	17	
5965	0.95	vWA	18	
5195	1	TPOX	8	
4774	0.92	TPOX	11	
3395	1	D18S51	12	
3178	0.94	D18S51	14	
8633	0.99	AMEL	X	
8711	1	AMEL	Y	
5828	1	D5S818	10	
5285	0.91	D5S818	11	
2741	1	FGA	20	
2561	0.93	FGA	22	
6233c	9482	1	D8S1179	10 Minus A
	8154	0.86	D8S1179	15
	7527	1	D21S11	27
	7185	0.95	D21S11	29
	3117	1	D7S820	9
	2866	0.92	D7S820	12
	4198	1	CSF1PO	12
	3909	0.93	CSF1PO	13
	7734	1	D3S1358	16
	6968	0.9	D3S1358	17
	10412	1	TH01	9
	10361	1	TH01	9.3
	9638	1	D13S317	10
	8827	0.92	D13S317	12
	18306	1	D16S539	11
	6506	1	D2S1338	19
	5707	0.88	D2S1338	20
	13206	1	D19S433	14
	10157	1	vWA	17
	9416	0.93	vWA	18

	8170	1	TPOX	8
	7692	0.94	TPOX	11
	5706	1	D18S51	12
	5207	0.91	D18S51	14
	11883	1	AMEL	X
	11742	0.99	AMEL	Y
	9124	1	D5S818	10
	8453	0.93	D5S818	11
	4539	1	FGA	20
	4077	0.9	FGA	22
6233d	10867	1	D8S1179	10 Minus A
	9433	0.87	D8S1179	15
	8973	1	D21S11	27
	8047	0.9	D21S11	29
	3628	1	D7S820	9
	3318	0.91	D7S820	12
	4786	1	CSF1PO	12
	4456	0.93	CSF1PO	13
	8808	1	D3S1358	16
	7785	0.88	D3S1358	17
	11781	0.97	TH01	9
	12113	1	TH01	9.3
	11213	1	D13S317	10
	10353	0.92	D13S317	12
	12491	1	D16S539	11
	7517	1	D2S1338	19
	6674	0.89	D2S1338	20
	15718	1	D19S433	14
	12011	1	vWA	17
	10787	0.9	vWA	18
	9616	1	TPOX	8
	9087	0.94	TPOX	11
	6583	1	D18S51	12
	5925	0.9	D18S51	14
	12068	1	AMEL	X
	12037	1	AMEL	Y
	10753	1	D5S818	10
	9914	0.92	D5S818	11
	5152	1	FGA	20
	4743	0.92	FGA	22
6233e	9205	1	D8S1179	10 Minus A
	7970	0.87	D8S1179	15
	7325	1	D21S11	27
	6998	0.96	D21S11	29
	3226	1	D7S820	9

2965	0.92	D7S820	12	
4191	1	CSF1PO	12	
4061	0.97	CSF1PO	13	
7892	1	D3S1358	16	
6842	0.87	D3S1358	17	
9350	0.95	TH01	9	
9802	1	TH01	9.3	
9943	1	D13S317	10	
9157	0.92	D13S317	12	
17454	1	D16S539	11	
6455	1	D2S1338	19	
5742	0.89	D2S1338	20	
13046	1	D19S433	14	
10305	1	vWA	17	
9122	0.89	vWA	18	
7872	1	TPOX	8	
7081	0.9	TPOX	11	
5766	1	D18S51	12	
5300	0.92	D18S51	14	
11067	1	AMEL	X	
10866	0.98	AMEL	Y	
9323	1	D5S818	10	
8798	0.94	D5S818	11	
4740	1	FGA	20	
4559	0.96	FGA	22	
651C	8727	1	D8S1179	10 Minus A
	7314	0.84	D8S1179	15
	6414	1	D21S11	29
	5728	0.89	D21S11	32.2
	2314	1	D7S820	10
	2209	0.95	D7S820	12
	5757	1	CSF1PO	12
	8105	1	D3S1358	14
	7153	0.88	D3S1358	17
	10090	1	TH01	8
	9608	0.95	TH01	9
	8430	1	D13S317	11
	7602	0.9	D13S317	12
	14531	1	D16S539	11
	4473	1	D2S1338	20
	4037	0.9	D2S1338	22
	8779	1	D19S433	13
	7721	0.88	D19S433	15.2
	14221	1	vWA	17
	13923	1	TPOX	8
	3385	1	D18S51	16

	2503	0.74	D18S51	22
	11384	1	AMEL	X
	8255	1	D5S818	11
	7522	0.91	D5S818	12
	6059	1	FGA	25
7572a	8538	1	D8S1179	10 Minus A
	7746	0.91	D8S1179	14
	6539	1	D21S11	28
	6401	0.98	D21S11	30
	6689	1	D7S820	10
	4741	1	CSF1PO	10
	4326	0.91	CSF1PO	12
	8188	1	D3S1358	17
	7334	0.9	D3S1358	18
	9560	1	TH01	7
	9571	1	TH01	9.3
	13890	1	D13S317	11
	11265	1	D16S539	12
	10484	0.93	D16S539	13
	6448	1	D2S1338	17
	5608	0.87	D2S1338	24
	9050	1	D19S433	14
	8231	0.91	D19S433	15
	10089	1	vWA	15
	9492	0.94	vWA	16
	14530	1	TPOX	8
	7021	1	D18S51	10
	6068	0.86	D18S51	14
	14716	1	AMEL	X
	13328	1	D5S818	12
	4852	1	FGA	22
	4331	0.89	FGA	25
7572b	8435	1	D8S1179	10 Minus A
	7306	0.87	D8S1179	14
	6422	1	D21S11	28
	6240	0.97	D21S11	30
	6409	1	D7S820	10
	4446	1	CSF1PO	10
	4227	0.95	CSF1PO	12
	7641	1	D3S1358	17
	6944	0.91	D3S1358	18
	9160	1	TH01	7
	9120	1	TH01	9.3
	13372	1	D13S317	11
	10815	1	D16S539	12

	10184	0.94	D16S539	13
	6404	1	D2S1338	17
	5381	0.84	D2S1338	24
	8464	1	D19S433	14
	7872	0.93	D19S433	15
	9748	1	vWA	15
	8941	0.92	vWA	16
	14435	1	TPOX	8
	6713	1	D18S51	10
	5891	0.88	D18S51	14
	9753	1	AMEL	X
	8522	1	D5S818	12
	4689	1	FGA	22
	4222	0.9	FGA	25
7572c	7311	1	D8S1179	10 Minus A
	6543	0.89	D8S1179	14
	5379	0.99	D21S11	28
	5452	1	D21S11	30
	5671	1	D7S820	10
	3986	1	CSF1PO	10
	3740	0.94	CSF1PO	12
	6842	1	D3S1358	17
	6215	0.91	D3S1358	18
	8353	1	TH01	7
	8159	0.98	TH01	9.3
	12195	1	D13S317	11
	9885	1	D16S539	12
	9457	0.96	D16S539	13
	5791	1	D2S1338	17
	4812	0.83	D2S1338	24
	7721	1	D19S433	14
	7169	0.93	D19S433	15
	8486	1	vWA	15
	8193	0.97	vWA	16
	13361	1	TPOX	8
	6202	1	D18S51	10
	5434	0.88	D18S51	14
	13205	1	AMEL	X
	11672	1	D5S818	12
	4069	1	FGA	22
	3733	0.92	FGA	25
7572d	8588	1	D8S1179	10 Minus A
	7796	0.91	D8S1179	14
	6538	1	D21S11	28
	6373	0.97	D21S11	30

	6602	1	D7S820	10
	4379	1	CSF1PO	10
	4346	0.99	CSF1PO	12
	7981	1	D3S1358	17
	7233	0.91	D3S1358	18
	9201	1	TH01	7
	9092	0.99	TH01	9.3
	14640	1	D13S317	11
	11059	1	D16S539	12
	10233	0.93	D16S539	13
	6742	1	D2S1338	17
	5564	0.83	D2S1338	24
	8344	1	D19S433	14
	7792	0.93	D19S433	15
	9572	1	vWA	15
	9065	0.95	vWA	16
	14285	1	TPOX	8
	6936	1	D18S51	10
	6116	0.88	D18S51	14
	10970	1	AMEL	X
	13245	1	D5S818	12
	4749	1	FGA	22
	4241	0.89	FGA	25
7572e	6166	1	D8S1179	10 Minus A
	5516	0.89	D8S1179	14
	4975	1	D21S11	28
	4493	0.9	D21S11	30
	5093	1	D7S820	10
	3611	1	CSF1PO	10
	3245	0.9	CSF1PO	12
	6043	1	D3S1358	17
	5387	0.89	D3S1358	18
	6788	1	TH01	7
	6648	0.98	TH01	9.3
	13464	1	D13S317	11
	8312	1	D16S539	12
	7781	0.94	D16S539	13
	4936	1	D2S1338	17
	4348	0.88	D2S1338	24
	6170	1	D19S433	14
	5651	0.92	D19S433	15
	7235	1	vWA	15
	6551	0.91	vWA	16
	11573	1	TPOX	8
	5542	1	D18S51	10
	4649	0.84	D18S51	14

	12049	1	AMEL	X
	11576	1	D5S818	12
	3866	1	FGA	22
	3436	0.89	FGA	25
7758H_2	9056	1	D8S1179	10 Minus A
	7880	0.87	D8S1179	14
	7619	1	D21S11	28
	6895	0.9	D21S11	30
	3063	1	D7S820	9
	2872	0.94	D7S820	13
	4225	1	CSF1PO	10
	3786	0.9	CSF1PO	12
	12077	1	D3S1358	15
	11061	1	TH01	7
	11005	0.99	TH01	9.3
	8669	1	D13S317	11
	8054	0.93	D13S317	14
	12053	1	D16S539	9
	10840	0.9	D16S539	12
	6427	1	D2S1338	17
	5155	0.8	D2S1338	24
	9685	1	D19S433	14
	8460	0.87	D19S433	16
	9717	1	vWA	16
	8787	0.9	vWA	19
	14160	1	TPOX	8
	4637	1	D18S51	15
	4186	0.9	D18S51	17
	12744	1	AMEL	X
	8490	1	D5S818	11
	8051	0.95	D5S818	12
	3950	1	FGA	23
	3578	0.91	FGA	24
9066C_2	7847	1	D8S1179	11 Minus A
	7120	0.91	D8S1179	13
	6301	1	D21S11	28
	5984	0.95	D21S11	30
	3591	1	D7S820	9
	1210	0.34	D7S820	11
	9274	1	CSF1PO	11
	8264	1	D3S1358	17
	7306	0.88	D3S1358	18
	8831	0.96	TH01	7
	9164	1	TH01	9.3
	10451	1	D13S317	8

9041	0.87	D13S317	13	
14770	1	D16S539	11	
6636	1	D2S1338	20	
6096	0.92	D2S1338	21	
9546	1	D19S433	12	
8193	0.86	D19S433	15	
9042	1	vWA	18	
8475	0.94	vWA	19	
14153	1	TPOX	9	
7237	1	D18S51	12	
6580	0.91	D18S51	16	
9158	1	AMEL	X	
8731	0.95	AMEL	Y	
8083	0.98	D5S818	10	
8260	1	D5S818	13	
5193	1	FGA	23	
4663	0.9	FGA	26	
ChristiH_2	6618	1	D8S1179	14 Minus A
	2253	1	D21S11	28
	1972	0.88	D21S11	30
	1071	1	D7S820	8
	968	0.9	D7S820	12
	1212	0.98	CSF1PO	10
	1238	1	CSF1PO	11
	4785	1	D3S1358	14
	4446	0.93	D3S1358	16
	7111	1	TH01	6
	6199	1	D13S317	11
	3121	1	D16S539	11
	2888	0.93	D16S539	12
	1388	1	D2S1338	23
	1217	0.88	D2S1338	24
	3917	1	D19S433	15
	3376	0.86	D19S433	16
	3909	1	vWA	14
	3396	0.87	vWA	18
	2743	1	TPOX	8
	2341	0.85	TPOX	9
	4098	1	D18S51	12
	10106	1	AMEL	X
	4641	1	D5S818	11
	3553	0.77	D5S818	12
	2234	1	FGA	20
	1845	0.83	FGA	23